ISBN 978-82-326-1498-1 (printed version)
ISBN 978-82-326-1499-8 (electronic version)
ISSN 1503-8181

NTNU
Norwegian University of
Science and Technology

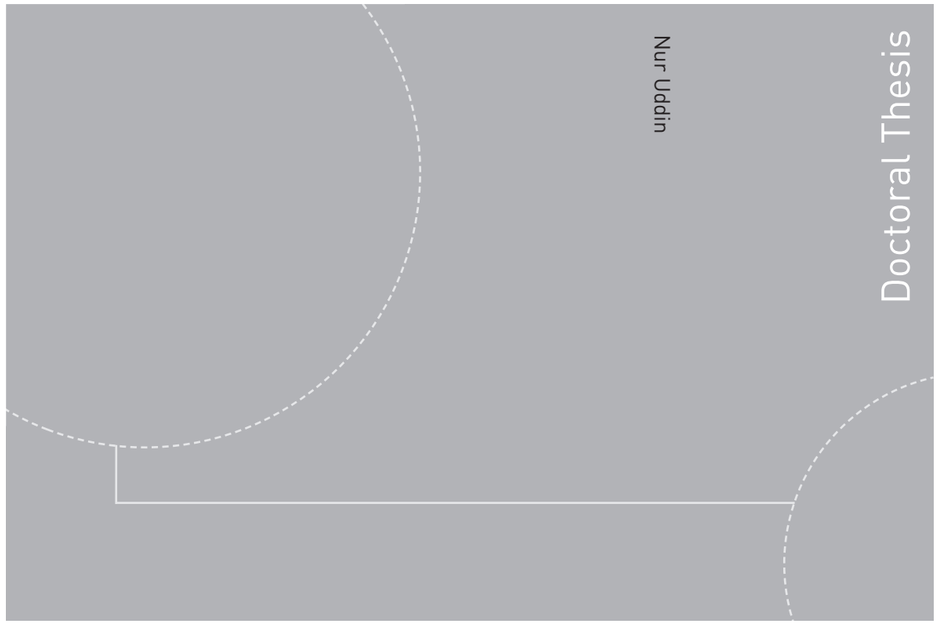

Doctoral theses at NTNU, 2016:80

Nur Uddin

Active Compressor Surge Control System Using Piston Actuation

Theory, Design, and Experiments

Doctoral theses at NTNU, 2016:80

NTNU

NTNU
Norwegian University of
Science and Technology
Faculty of Information Technology,
Mathematics and Electrical Engineering
Department of Engineering Cybernetics

NTNU
Norwegian University of
Science and Technology

Nur Uddin

Active Compressor Surge Control System Using Piston Actuation

Theory, Design, and Experiments

Thesis for the degree of Philosophiae Doctor

Trondheim, March 2016

Norwegian University of Science and Technology
Faculty of Information Technology,
Mathematics and Electrical Engineering
Department of Engineering Cybernetics

NTNU
Norwegian University of
Science and Technology

NTNU
Norwegian University of Science and Technology

Thesis for the degree of Philosophiae Doctor

Faculty of Information Technology,
Mathematics and Electrical Engineering
Department of Engineering Cybernetics

ISBN 978-82-326-1498-1 (printed version)
ISBN 978-82-326-1499-8 (electronic version)
ISSN 1503-8181

Doctoral theses at NTNU, 2016:80

Printed by Skipnes Kommunikasjon as

Alhamdulillah, this thesis is completed.
A dedication for my parents, my wife, my children, and all of my teachers.

Summary

This thesis presents a novel active compressor surge control system using piston actuation, and this system is called the piston-actuated active surge control system (PAASCS). This work addresses the development of PAASCS from the beginning to the experimental results, including system modeling, control design, system improvement, piston prototyping, laboratory test setup, system implementation, and experimental tests. The thesis is presented as a collection of papers, including seven conference papers and a journal paper.

The work began by developing a PAASCS model that is a modification of the Greitzer compressor model by including the effect of piston dynamics on the compression system. The resulting model was used in control design. Two control methods were initially applied in the control design. Applying the backstepping method proved that the closed-loop system was globally asymptotically stable (GAS), but the state feedback control law was too complicated and not practical to implement. Applying a linear control method to the linearized model resulted in a simple state feedback control law, but it only achieves locally asymptotic stability (Uddin and Gravdahl, 2011a).

The PAASCS performance was evaluated through simulations. Two problems were identified, and the solutions to these problems were presented. 1) The piston was drifting during the surge stabilization. The piston drift was solved by introducing integral control action to the PAASCS controller (Uddin and Gravdahl, 2011b). 2) There are possibilities for the piston to fail during the surge stabilization. Piston failures due to jamming and saturation were discussed. The simulation results showed that a piston failure results in a deep surge when the compressor operates in the stabilized surge area. A solution was presented by introducing a backup system that uses another surge control system. Two studies were performed that presented a blow-off system as a backup system for PAASCS (Uddin and Gravdahl, 2012a) and a surge avoidance system as a backup system for PAASCS (Uddin and Gravdahl, 2012c).

A novel approach to model a compression system from an energy flow perspective using bond graphs was presented. A compression system is modelled using bond graph. Energy flows among the components in the compression system are described in a bond graph model of the compression system. Two basic surge solutions were identified through analysing the bond graph model, and named the upstream energy injection and the downstream energy dissipation. The PAASCS is classified as downstream energy dissipation (Uddin and Gravdahl, 2012b, 2015).

Two novel state feedback control laws named the ϕ-control and the ψ-control derived using Lyapunov based control method are presented for the upstream energy injection and the downstream energy dissipation, respectively. Both control laws guarantee that the closed-loop system is GAS (Uddin and Gravdahl, 2016a).

A laboratory-scale compressor test rig was constructed to experimentally examine the PAASCS. The PAASCS was applying the ψ-control. The control algorithm was implemented in a Simulink

model and embedded in a dSpace system to construct a hardware-in-loop simulation of compressor surge stabilization. The experimental test results demonstrated that the PAASCS is able to stabilize surge and prove the concept of PAASCS (Uddin and Gravdahl, 2016b).

Contents

List of figures

List of tables

Preface

This thesis is submitted in partial fulfillment of the requirements for the degree of philosophiae doctor (PhD) at the Norwegian University of Science and Technology (NTNU).

I performed this work at Department of Engineering Cybernetics from July 2009 to May 2015 with a one year leave for working at a company. My supervisor was Professor Dr.ing. Jan Tommy Gravdahl and my co-supervisor was Associate Professor Dr.ing. Fredrik Dessen. This research was financed by a scholarship under the Siemens-NTNU Oil and Gas Offshore Project.

Acknowledgments

First and foremost, I would like to express my deep gratitude to my supervisor, Professor Dr.ing. Jan Tommy Gravdahl, for introducing me to compressor surge and nonlinear control. I have been fortune to have him as my supervisor, who has provided valuable advice, comments, motivations and inspirations for the research and preparing the publications. He has cared so much not only for my work but also for my life balance between work and family. I would like to thank my co-supervisor, Associate Professor Dr.ing. Fredrik Dessen, for the discussions on industrial compressor and the control system.

I would like to thank Siemens Oil and Gas Division for the financial support, technical meetings, and a field trip to see the compressor fabrication in Duisburg, Germany. I would like to thank Dr.ing. Anngjerd Pleym at Siemens and Dr. Morten Grønli at NTNU for managing the research collaboration between Siemens and NTNU.

The staff in the department are acknowledged for creating a very pleasant environment and for supports for my study and research. Special thanks to Per Inge Snildal and Terje Haugen for constructing the piston and the mechanical helps, Rune Mellingseter and Jonas Rotabakk for electrical installation on the piston, Torkel Hansen and Jan Leistad for the IT support, Stefano Brevik Bertelli for the technical advice, and Glenn Angell for the mechanical helps. Special thanks also to Unni Johansen, Tove Kristin Blomset Johnsen, Eva Amdahl, Bente Seem Lindquist, and Janne Karin Hagen for the administrative assistance during the study.

I would like to thank Rahmat Nur Adi Wijaya for his help when I arrived in Trondheim for an interview test to obtain the PhD position and then when I started the PhD program, and moreover, for sharing his knowledge about compressor surge.

I would like to thank my colleagues at the Technical Department of Mandala Airlines in Jakarta for sharing knowledge and practical experience, particularly on aircraft engines.

I would like to thank my officemate Anders Fougner for creating a very pleasant place to work and for the LaTeX help. I would like to thank all of my colleagues at the Department of Engineering Cybernetics for the friendship and the very good work environment. Sincere thanks are extended to Christian Holden, Arnfinn Aas Eielsen, and Christoph Backi.

I would like to thank the Indonesian students association in Trondheim (PPI Trondheim) and Indonesian communities in Trondheim as well as in Oslo and Akerhus for the supports, solidarity, cooperation and activities.

Finally, I would like to express my love and deepest gratitude to my mother, Siti Fatimah; my father, Muhammad Salim; my wife, Kiky; my daughter, Alisha; and my son, Fariz. Sincere thanks and appreciation are given to my big family in Indonesia for their supports and motivations.

Fornebu, March 2016

Nur Uddin

Chapter 1

Introduction

1.1 Background and Motivation

The operating area of dynamic compressors (centrifugal and axial compressors) is limited by a surge line at lower mass flows and by a stonewall at higher mass flows. The operating area of a compressor is commonly depicted by curves of the compressor pressure versus compressor mass flow for several compressor rotational speeds, and it is called a compressor map. When operating a compressor, crossing the surge line results in surge, and crossing the stonewall causes compressor choke. Compressor surge is an aerodynamic instability that is represented by an axisymmetric oscillation of mass flow and pressure increase (Gravdahl and Egeland, 1999). The surge is shown by reversal flow, pressure fluctuation, rapid temperature increase, and severe vibration in the compression system. These lead to compressor damage, particularly to the rotating parts, such as blades and bearings (Forsthoffer, 2005). Compressor choke is a condition in which the compressor cannot pump any more gas. This condition occurs when the gas velocity relative to the blade is equal to the speed of sound (Nisenfeld, 1982).

According to Forsthoffer (2005), a compressor can only operate in stonewall if the head (energy) required by the process system is low enough such that the compressor operates in the high-flow-rate region of the compressor map. The high flow rate requires a larger pipe diameter, which is more costly. For economic reasons, this is a rare case because the process pipe is designed to minimize the pipe diameter. The compressor choke is also not a destructive phenomenon. Therefore, surge receives more attention in compressor studies. Moreover, the high-efficiency compressor operating points are located close to the surge line.

Two methods have been developed to solve compressor surge. These methods are known as surge avoidance system (SAS) and active surge control system (ASCS) and explained as follows:

- Surge avoidance system (SAS)
  SAS works by defining a surge control line, which is located on the right side of the surge line, as a limit of the minimum compressor flow. It prevents the compressor operating point from reaching the surge line. The SAS method is implemented through a recycling flow mechanism or a blowing-off flow mechanism. The recycling flow mechanism uses a recycle line and a recycle valve. When the compressor operating point crosses the surge control line, the recycle valve will open to discharge fluid from the downstream line to the upstream line through the recycle line. This results in an increase in the compressor flow such that the compressor operating point will remain at the surge control line. The blow-

off flow mechanism uses a blow-off valve and the operation is similar to the recycling flow mechanism, but the downstream fluid is discharged to surrounding rather than recycled to the upstream line. The SAS works well for preventing a compressor from entering surge and has been applied in industrial compressors. However, applying SAS reduces the compressor operating envelope because the limit of minimum compressor flow is the surge control line rather than the surge line, and moreover, the recycling flow and blowing-off flow waste the energy.

- Active surge control system (ASCS)
  In contrast to SAS, which limits the compressor operating area by a surge control line, ASCS stabilizes surge by an active element such that the compressor operating point is allowed to cross the surge line into the stabilized surge area such that the operating envelope is enlarged. The active element, known as an actuator, is driven by a controller based on a state feedback control law. The ASCS method was introduced by Epstein et al. (1986).

ASCS provides an enlargement of the compressor operating envelope toward lower flows and an opportunity to reach higher compressor efficiencies. Several actuators have been applied in ASCS, and examples include moveable plenum wall (Williams and Huang, 1989), throttle (Pinsley et al., 1991), close coupled valve (Simon and Valavani, 1991), torque drive (Gravdahl et al., 2002), and active magnetic bearing (Yoon et al., 2012). Refer to Willems and de Jager (1999) for more actuators applied in ASCS. However, the implementation of ASCS in industrial compressors has not yet been reported. Safety could be a reason for this because a failure of ASCS may cause the compressor to enter a deep surge.

The compressor surge phenomenon is shown by the compressor pressure and the compressor mass flow oscillations. This motivates us to consider the surge phenomenon as a vibration problem. In most vibration problems, introducing or increasing damping is a solution to absorb the vibration. Vehicle suspension system is an example of a spring-mass-damper system, in which the damper is used to dampen the vehicle vibration excited by vertical velocity due to the road profile. The damper dissipates the vibration energy (kinetic energy) such that the oscillation will vanish. A vehicle suspension that uses a passive mechanical damper is called a passive suspension system. Studies have shown that the performance of vehicle suspension system can be considerably improved through the use of an active actuator rather than the passive mechanical damper (Uddin, 2009; Youn et al., 2014). A suspension system that uses an active actuator is called an active suspension system. The active actuator generates a force to counter the vibration such that the vibration vanishes. By using the same concept of vehicle suspensions, compressor surge should be stabilized by introducing a damping to the compression system.

Williams and Huang (1989) presented an active surge control that uses a movable plenum wall. The movable plenum wall is the active element for suppressing the compressor surge. They used a loud speaker as the movable plenum wall. The results of their experiments showed that the surge is stabilized and that the compressor operating area is enlarged to the left of the surge line. Gysling et al. (1991) developed a passive surge suppression system using a tailored structure. In the tailored structure, a movable wall supported by a spring and a damper was used to dissipate the vibration energy of the compressor surge. Arnulfi et al. (2001) extended this line of research and introduced a hydraulic oscillator as a passive mechanism for surge suppression. The system was analyzed using the nonlinear model, optimal parameters for the control structure were found, and the results were confirmed experimentally.

The three presented works on stabilizing compressor surge are essentially similar to the principle of vehicle suspension systems. The work of Williams and Huang (1989) is similar to an

active suspension system, and the works of Gysling et al. (1991) and Arnulfi et al. (2001) are similar to a passive suspension system. Motivated by the vehicle suspension system and the three aforementioned works, we are interested in developing an active damping by using a piston to suppress the compressor surge. The piston will be connected to the compressor plenum. We call this system a piston-actuated active surge control system (PAASCS). The principle of this system is similar to that of the movable plenum wall presented by Williams and Huang (1989), but the piston will provide more flexibility for practical implementations than the loud speaker. The PAASCS can be installed in current compression systems in a simple way such that the installation cost is minimized.

1.2 Scope of the Work

The scope of this work includes the following:

- System modeling
  This system modeling aims to develop a model of PAASCS. The model is a modification of the Greitzer compressor model (Greitzer, 1976) by including the effect of the piston dynamics to the compression system. The same assumptions as in the Greitzer model are applied.
- Control design and simulations
  The control law for PAASCS is developed based on the PAASCS model. The control law should be implementable in the experimental setup. The PAASCS is simulated to evaluate the system performance and improve the system if necessary.
- Piston design
  For research purposes, we require a piston that generates a high mass flow and is able to work at the maximum compressor pressure. Because such a piston is not available on the market, we design the piston and have it manufactured by our colleagues at the workshop at Department of Engineering Cybernetic, NTNU.
- Laboratory setup
  A compressor-pipeline setup is prepared and constructed at the Compressor Laboratory at Department of Engineering Cybernetic, NTNU, to test the PAASCS.
- Experimental test
  A hardware-in-loop test is performed to test the PAASCS and evaluate its performance.

1.3 List of Publications

The results of the work described in this thesis have been reported in the following publications:

1. Paper A: N. Uddin and J.T. Gravdahl, "Compressor Surge Control Using Piston Actuation", published in the *Proceedings of the ASME 2011 Dynamics System and Control Conference* (DSCC 2011) in Arlington, VA, USA, Oct 31 - Nov 2, 2011.
2. Paper B: N. Uddin and J.T. Gravdahl, "Piston-Actuated Active Surge Control of Centrifugal Compressor Including Integral Action", published in the *Proceedings of the 11th International Conference on Control, Automation and System* (ICCAS 2011) in KINTEX, Gyeonggi-do, South Korea, Oct 26-29, 2011.

3. Paper C: N. Uddin and J.T. Gravdahl, "Introducing Back-up to Active Compressor Surge Control System", published in the *Proceedings of the 2012 IFAC Workshop on Automatic Control in Offshore Oil and Gas Production* in Trondheim, Norway, May 31 - June 1, 2012.
4. Paper D: N. Uddin and J.T. Gravdahl, "Bond graph modeling of centrifugal compressor systems", published in the *Simulation: Transactions of the Society for Modeling and Simulation International 2015, Vol. 91(11) 998–1013*. The paper is an extension work of a published conference paper Uddin and Gravdahl (2012b).
5. Paper E: N. Uddin and J.T. Gravdahl, "A Compressor Surge Control System: Combination Active Surge Control and Surge Avoidance", published in the *Proceedings of the 13th International Symposium on Unsteady Aerodynamics, Aeroacoustics and Aeroelasticity of Turbomachines* (ISUAAAT13) in Tokyo, Japan, September 11-14, 2012.
6. Paper F: N. Uddin and J.T. Gravdahl, "Two General State Feedback Control Laws for Compressor Surge Stabilization", submitted to *The 24th Mediterranean Conference on Control and Automation in Athens, Greece, June 21-24, 2016.*
7. Paper G: N. Uddin and J.T. Gravdahl, "Active Compressor Surge Control System by Using Piston Actuation: Implementation and Experimental Results", accepted in *The 11th IFAC Symposium on Dynamics and Control of Process Systems, including Biosystems (DYCOPS-CAB 2016) in Trondheim, Norway, June 6-8, 2016.*

1.4 List of Contributions

The publications of this research have produced the following contributions:

1. Paper A: Introducing a new method for active surge control system (ASCS) by using piston actuation and including system modeling and control design.
2. Paper B: Improving the performance of PAASCS by using integral action to eliminate piston drift and minimize the required piston stroke.
3. Paper C and Paper E: Introducing a backup system for ASCS for fail-safe operation by using a blow-off mechanism and SAS, respectively.
4. Paper D: Modeling compression systems from an energy-flow perspective by using bond graph. Improving a model of a compressor equipped with a surge avoidance system by showing the effect of recycling flow to the inlet state. Analyzing the bond graph model of the compression system is able to describe energy flow during compressor surge and conclude two basic surge solutions: upstream energy injection and downstream energy dissipation.
5. Paper F: Presents two novel state feedback control laws for the basic surge solutions presented in D. Both state feedback control laws make the closed-loop systems globally asymptotic stable (GAS) and minimize the sensor requirements.
6. Paper G: Presents the implementation and experimental test results of the PAASCS.

1.5 Thesis Outline

- Chapter 1 Introduction
  This chapter describes the background and motivation of the work, scope of the work, and the list of publications and contributions.

- Chapter 2 Compressor Technology
  This chapter presents several types of compressors, their operating ranges, and a comparison of the compressors. The presentation is focused on dynamic compressors, compressor surge, and the surge solutions.
- Chapter 3 Piston-Actuated Active Surge Control System
  This chapter presents the highlights in developing PAASCS, piston design, laboratory setup and experimental test.
- Chapter 4 Conclusion and Remarks
  This chapter summarizes the work, defines future work, and concludes the thesis.
- Chapter 5 Publications
  This chapter presents the publications of the work results.

Chapter 2

Compressor Technology

This chapter provides general information about compressors, including compressor types, the operating ranges of the compressors, comparison of different compressor types, and selection of compressors. This chapter then focuses on dynamic compressors, which include centrifugal compressors and axial compressors. It describes the principle of the dynamics compressors operation, performance limitations, the compressor surge problem, and the compressor surge solutions.

A compressor is a device that compresses gas such that the pressure increases. Compression is required for a variety of purposes, such as providing air for combustion, transporting fluids through pipelines, providing compressed air for driving pneumatic tools, and circulating process fluids through certain processes (Boyce, 2003). Compressors are applied in many fields, such as natural gas pipeline systems, gas turbines, pneumatic systems, gas circulation in industrial processes, and refrigerators. Compressors are essential in many systems and equipment, including aircraft engines, automotive engines, chemical processes, air conditioning, and gas pipeline systems.

2.1 Compressor Types

There are several types of compressors. Based on the way to increase fluid pressure, the compressors can be classified into two types (Forsthoffer, 2005):

a. Positive displacement compressors
Positive displacement compressors work by trapping a volume of gas in a chamber and reducing the chamber volume such that the gas pressure increases. The pressure increase is calculated following Boyle's law (Nisenfeld, 1982):

$$p_2 = p_1 \frac{V_1}{V_2} \tag{2.1}$$

where p_2 is the discharge pressure, p_1 is the suction pressure, V_1 is the volume at suction, and V_2 is the volume at discharge. The positive displacement compressors are further classified into two types: reciprocating and rotary compressors. The rotary positive displacement compressors include rotary lobe, rotary vane, rotary screw and rotary liquid ring compressors.

b. Dynamic compressors
Dynamic compressors increase the gas pressure by accelerating the gas using a rotating

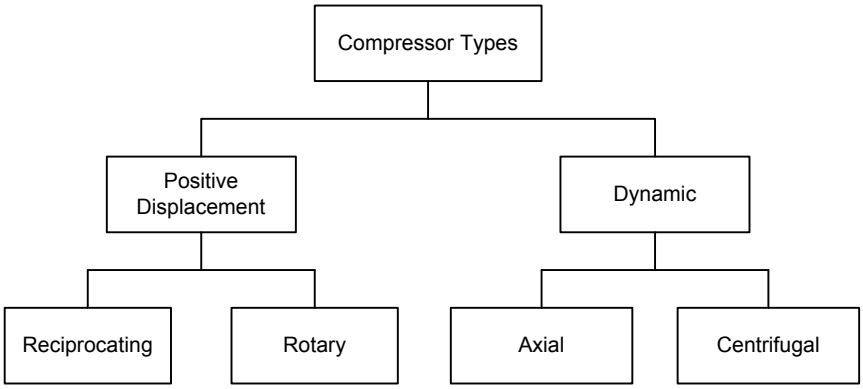

Figure 2.1: Compressor classification.

element, which increases to higher velocity and then decelerates. Following Bernoulli's equation:

$$p_1 + \frac{1}{2}\rho_1 v_1^2 + \rho_1 g h_1 = p_2 + \frac{1}{2}\rho_2 v_2^2 + \rho_2 g h_2, \tag{2.2}$$

where ρ is density, v is velocity, g is gravity, h is elevation, and the subscribes $_{1,2}$ denote the compressor inlet and the compressor discharge. Because the elevations of the compressor parts are not significantly different, the deceleration converts the kinetic energy into a pressure increases. There are two types of dynamic compressors: axial and centrifugal.

Figure 2.1 shows a diagram of the compressor classification.

2.2 Compressors Performance and Selection

Figure 2.2 shows the operating areas of different types of compressors. The positive displacement compressors dominate the low-flow-rate operating area (10^2 to 10^3 CFM[1]). The medium-flow-rate operating area (10^3 to 10^4 CFM) is dominated by centrifugal compressors. The multistage axial compressors operate in the high-flow-rate operating area (more than 10^4 CFM). Considering the compression results, positive displacement compressors provide a higher pressure ratio than dynamic compressors [2].

The application of the compressor type is dependent on the process requirements. The selection of compressors is influenced by several factors, such as compressor performance, investment costs, operating costs, maintenance costs, compressor cost, and environmental aspects. Dynamic compressors are commonly the first choice because they have the lowest maintenance costs, followed by rotary positive displacement compressors and reciprocating compressors Forsthoffer (2005).

[1] CFM: cubic feet per minute.
[2] Pressure ratio is the ratio of the compressor discharge pressure to the compressor inlet pressure.

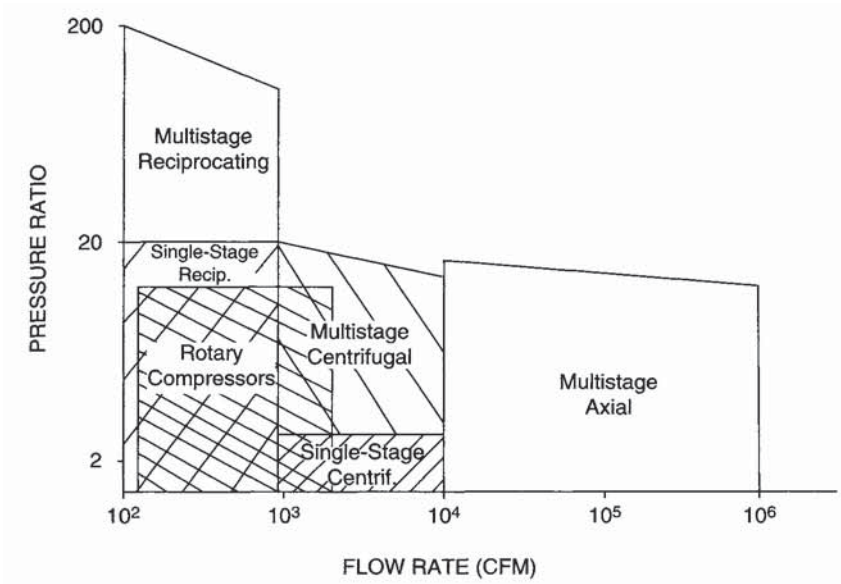

Figure 2.2: Application ranges of several compressor types (Brown, 2005).

Reciprocating compressors are generally the choice for processes with low flow rates and are preferred for high-pressure service. However, the advanced centrifugal compressor is able to produce higher pressure and operate at lower flow rates and may replace the reciprocating compressor. The disadvantages of reciprocating compressors are their higher maintenance requirements and the introduction of vibration to the system (Nisenfeld, 1982). According to Boyce (2003), reciprocating compressors were the most applied compressor in the process and pipeline industries up to and through the 1960s. In the 1960s, reciprocating compressors were replaced by centrifugal compressors. Centrifugal compressors have comparable efficiency to reciprocating compressors, but their maintenance costs are considerably lower. Today, centrifugal compressors are the main compressors used in the process and pipeline industries. A centrifugal compressor frequently operates for 2 to 3 years without shutting down.

Rotary compressors have applications over a broad range of flows and pressure. These compressors are generally more suitable for variable compression ratios and wide capacity ranges than the other types of compressors. Their most frequent application is the compression of "dirty" or corrosive gases, where special construction materials are needed. However, the application of rotary compressors is restricted by their higher capital cost (Nisenfeld, 1982).

Axial-flow compressors are primarily used in processes where efficiency is important, high flows, and low pressure ratios. Figure 2.3 shows a comparison of the typical efficiencies among rotary compressors, centrifugal compressors and axial compressors. The axial compressor has the highest efficiency, followed by the centrifugal compressor and the rotary compressor. However, an axial compressor is more expensive than a centrifugal compressor for the same performance class (Boyce, 2003). An example of an application for axial compressors is in aircraft engines.

The remainder of this chapter will only discuss dynamic compressors. Readers who are interested in positive displacement compressors are referred to (Brown, 2005; Forsthoffer, 2005; Bloch, 2006).

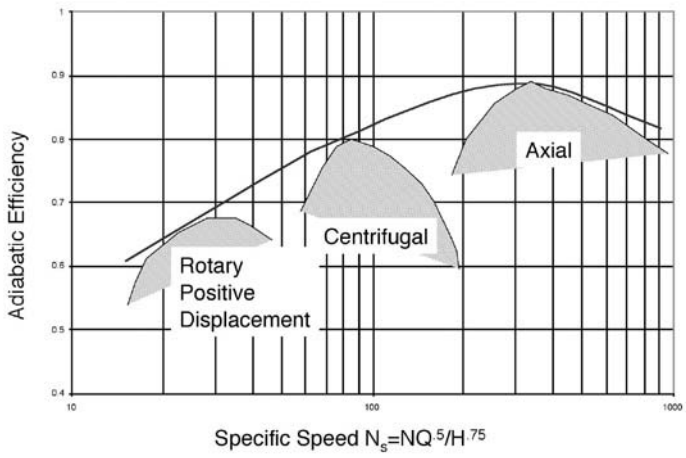

Figure 2.3: Adiabatic efficiency versus specific speed of different types of compressors (Boyce, 2003).

2.3 Dynamic Compressors

Dynamic compressors provide advantages of high reliability, high efficiency and low maintenance costs. Dynamic compressors work by accelerating and decelerating gas to obtain the pressure increase. The compressors can be divided into two types depending on the direction of the gas along the compressor process: centrifugal compressor and axial compressor. The principles of the both compressors operation are described in the following subsections.

2.3.1 Axial Compressors

The principles of axial compressor operation are explained in many compressor text books, for example, in Boyce (2003), and it is described as follows based on a diagram of a two-stage axial compressor shown in Figure 2.4. Gas enters the compressor through the inlet. The gas flow is directed by an inlet guide vane (IGV) such that the gas enters the first-stage rotor at the desired angle. The gas is accelerated by the rotor such that the gas velocity increases. The increase in gas velocity is converted to an increase in gas pressure by a diffusion process at the stator. The rotor and stator are a row of blades where the rotor is rotating and the stator is stationary. A pair of rotor and stator is called a compressor stage. An axial compressor commonly contains several stages. The pressure, temperature and velocity of the gas vary through the stages. The total pressure and temperature increase at the rotor, where energy is transferred to the gas. The rotor diameter, stator diameter, and the annulus area (the area between the shaft and shroud) decrease through the length of the compressor. The reduction in flow area is to compensate for the increasing gas density due to the compression process and to permit a constant axial velocity. A single-stage axial compressor produces a pressure ratio of approximately 1.1 to 1.4, and thus, a multi-stage configuration is commonly applied to obtain higher pressure ratios.

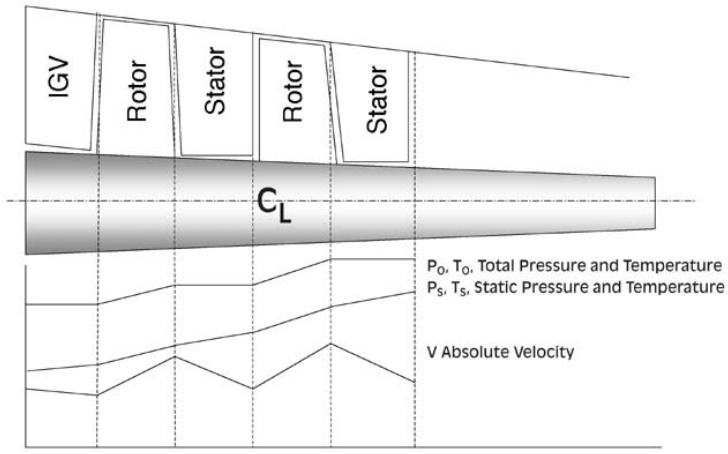

Figure 2.4: Axial compressor and the thermodynamic properties (Boyce, 2003).

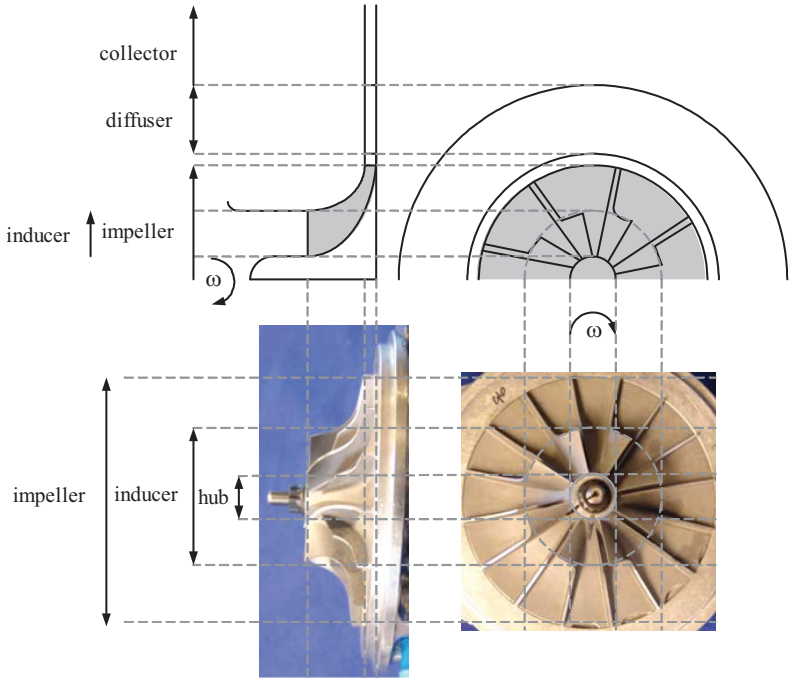

Figure 2.5: Centrifugal compressor parts (Bøhagen, 2007).

2.3.2 Centrifugal Compressor

The elements of a centrifugal compressor are shown in Figure 2.5. The principles of a centrifugal compressor operation are given in many compressor text books, for an example, in Boyce (2003),

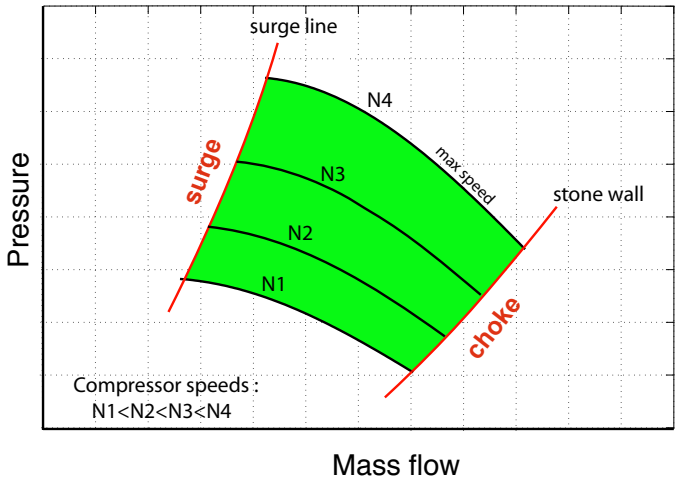

Figure 2.6: An illustration of a typical compressor map.

and is described as follows. Gas is drawn into the impeller eye and expelled outward by the high-speed rotating impeller. This process results in gas acceleration. The velocity of the fluid is converted to pressure, partially in the impeller and partially in the stationary diffusers. It is common in a compressor design that half of the pressure increase is obtained in the impeller and the other half in the diffuser. The diffuser consists of essentially of vanes, which are tangential to the impeller. These vane passage diverge to convert the velocity head into pressure energy. After exiting the diffuser, the air enters a scroll or collector and then to the compressor discharge. Centrifugal compressors range in size from pressure ratios of 1.3 per stage in the process industries, to 3 to 7 per stage in small gas turbines, and as high as 13 per stage on experimental models. The applied centrifugal compressors can be a single stage or multiple stages.

2.4 Performance Limitations of Dynamic Compressors

The operating area of a dynamic compressor is commonly shown by a chart of compressor discharge pressure versus compressor mass flow, and it is called a compressor map. A typical compressor map of dynamic compressors is shown in Figure 2.6. The operating area of the compressors is limited by the surge line at low mass flows and by stonewall at high mass flows. Operating a compressor across the surge line results in compressor surge, and operating it over the stonewall results in compressor choke.

A compressor surge is a system phenomenon that results from the inability of the compressor impeller (blades) to produce the amount of energy required by the process (Forsthoffer, 2005). The compressor surge is an aerodynamic instability in the compression system and results in an axisymmetric oscillation of the compressor flow and pressure (Gravdahl and Egeland, 1999). The oscillation results in pressure fluctuations, temperature fluctuations, and severe vibration in the compression system. It may lead to compressor damage, particularly to the rotating parts, such as blades and bearings.

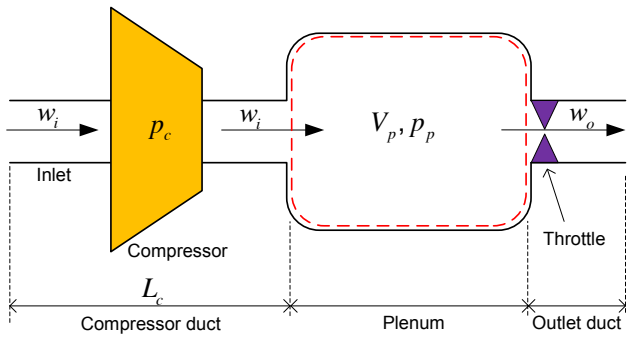

Figure 2.7: The Greitzer compression model.

Choke is a condition in which the compressor cannot pump any more gas. This condition occurs when the gas velocity relative to the blade is equal to the speed of sound (Nisenfeld, 1982). According to Forsthoffer (2005), the compressor can only operate in stonewall if the head (energy) required by the process system is low enough to allow the compressor to operate in this high-velocity region of the compressor map. For economic reasons, this is a rare case because the process pipe is designed to minimize the pipe diameter and therefore increase the head required at high flow rates. Stonewall is not a destructive phenomenon.

Surge gets a lot of attentions in compressor studies, design, and operation because this phenomenon may damage the compressor.

2.5 Compressor Surge

A model of compression system which is able to predict the transient response subsequent to perturbation from steady operating condition was introduced in (Greitzer, 1976). The model is known as the Greitzer compression model and shown in Figure 2.7. The Greitzer model was developed based on fluid dynamics laws (momentum equation and mass conservation) by the following assumptions: incompressible flow in the ducts with density equal to the ambient, fluid velocity in the plenum is negligible, uniform pressure throughout the plenum, process in the plenum is polytropic and adiabatic, and pressure drop along the ducts are negligible. Dynamics of the Greitzer compression model are given as follows:

$$\dot{w}_i = \frac{A_c}{L_c}(p_c - p_p) \tag{2.3}$$

$$\dot{p}_p = \frac{a_0^2}{V_p}(w_i - w_o), \tag{2.4}$$

where A_c is the compressor duct cross-sectional area, L_c is the effective length of the equivalent compressor duct, p_c is the compressor pressure rise, p_p is the plenum pressure, a_0 is the speed of sound, V_p is the plenum volume, w_i is the inlet mass flow, and w_o is the outlet mass flow. The plenum is representing a control volume of the downstream line in the compression system. The Greitzer compression model is mostly referred in compressor surge control studies.

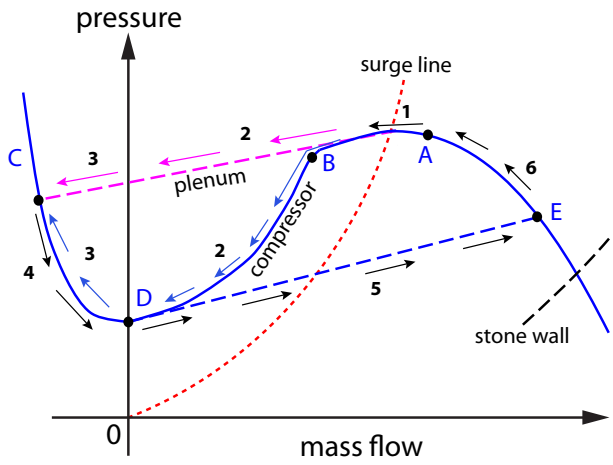

Figure 2.8: An illustration of compressor surge cycle.

A chronology of compresor surge is explained based on Figure 2.8 as follows (Gravdahl and Egeland, 1999; Uddin and Gravdahl, 2015):

1) A compressor is initially operating steadily at operating point A located in the stable area, but close to the surge line. This operation results in the plenum pressure being the same as the compressor discharge pressure. Due to a disturbance, for example, by closing the throttle, the compressor mass flow is reduced and the operating point should move to point B located on the left side of the surge line.
2) At the point B, the compressor discharge pressure is less than the plenum pressure. This condition causes the mass flow to decelerate, and the compressor produces less pressure discharge according to the compressor characteristic curve.
3) The mass flow continues to decelerate to zero and then to a negative value (reverse flow). The compressor acts like an orifice in reverse flow. The stored energy in the plenum accelerates the reverse flow until it reaches maximum reversal flow at point C.
4) After reaching the point C, the pressure is decreasing, and the reverse flow is decelerated and becomes zero mass flow at point D.
5) At the point D, the compressor begins a normal operation by accelerating the flow until point E.
6) The mass flow is reduced to build plenum pressure. However, the compressor operation from the point E is going to the point A and then to the point B such that the cycle repeats.

According to Forsthoffer (2005), a surge cycle produces large amounts of energy, which are absorbed by the mechanical components of the compressor and can result in a significant temperature increase inside the compressor. The gas flow will oscillate back and forth in the compressor with a frequency of up to 6 Hz. The flow oscillation is followed by a pressure oscillation and results in a rapid temperature increase, and thermal expansion can cause major damage during

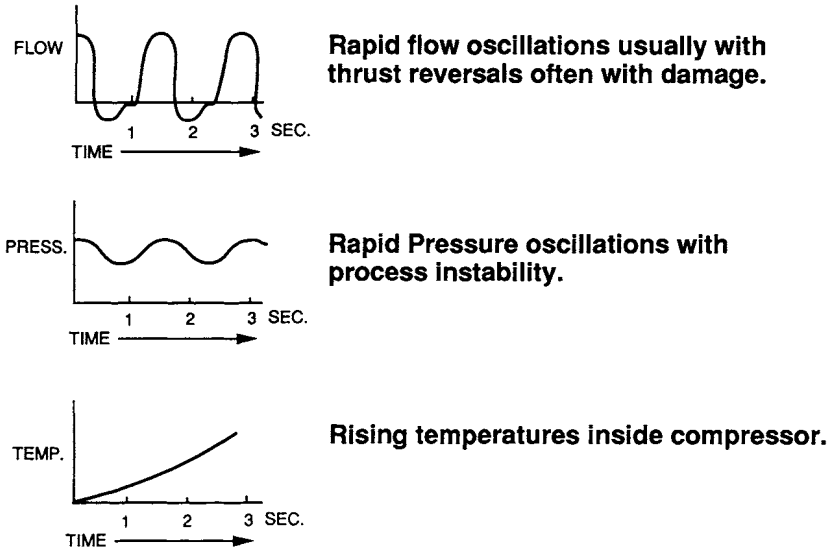

Figure 2.9: Flow, pressure and temperature during compressor surge (Forsthoffer, 2005).

surge. This phenomenon can occur most easily in axial compressors. Surge may heat up the system faster in axial compressors than in centrifugal compressors. Figure 2.9 shows the gas properties during compressor surge.

2.6 Compressor Surge Solutions

There are two kinds of surge solution: surge avoidance system and active surge control system. Both are described as follows including the industrial application.

2.6.1 Surge avoidance system

A surge avoidance system (SAS) is a common method for preventing surge in industrial compressors. This method works by recycling flow from downstream to upstream through a recycle line. Figure 2.10 shows the diagram of a compressor equipped with a SAS. Details of the diagram and notations are described in (Uddin and Gravdahl, 2015). A recycle valve is the actuator to control the recycling flow. The SAS works by comparing the compressor operating point to a line called the surge control line (SCL) as illustrated in the compressor map in Figure 2.11. The SCL is located to the right of the compressor surge line (SL) and becomes the minimum allowed mass flow in operating the compressor. The distance between the SCL and SL is called the surge margin. When the compressor operating point is crossing to the left side of the SCL, the recycle valve opens and flows the plenum fluid to the compressor inlet. The fluid flow causes the plenum pressure to decrease and the compressor mass flow to be accelerated such that the operating point moves to the SCL. This mechanism ensures that the operating point is not going to the surge condition. In some applications, for an example in aircraft engine, the SAS is implemented by blowing-off mechanism, where the downstream fluid is ejected to the atmosphere instead of

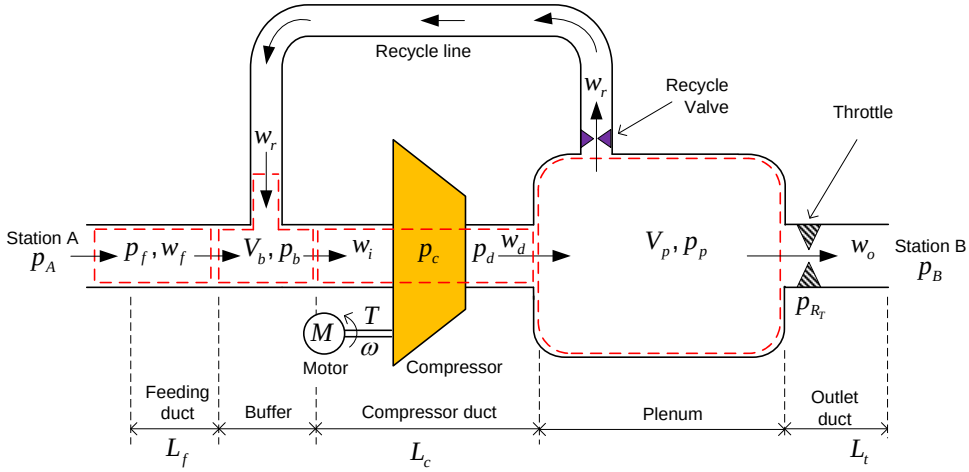

Figure 2.10: The model of a compressor equipped with a surge avoidance system (Uddin and Gravdahl, 2015).

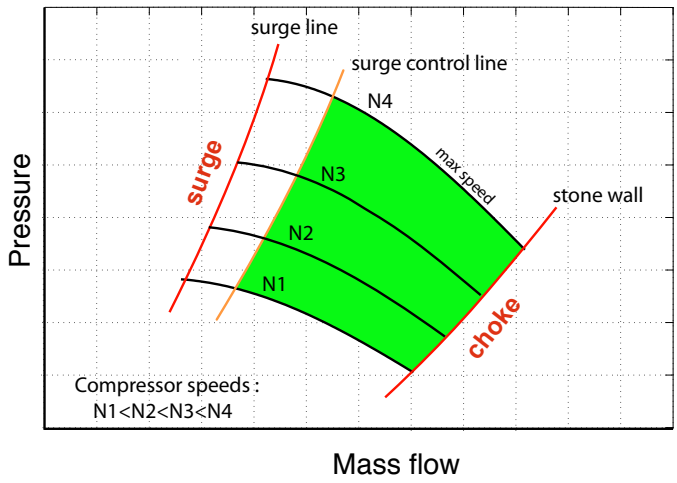

Figure 2.11: Operating area of a compressor equipped with a surge avoidance system.

recycled to the compressor upstream. The SAS works well for preventing a compressor from entering surge and has been applied in industrial compressors. However, applying SAS reduces the compressor operating envelope due to the defined surge control line. The recycling or blowing off of flow also wastes energy.

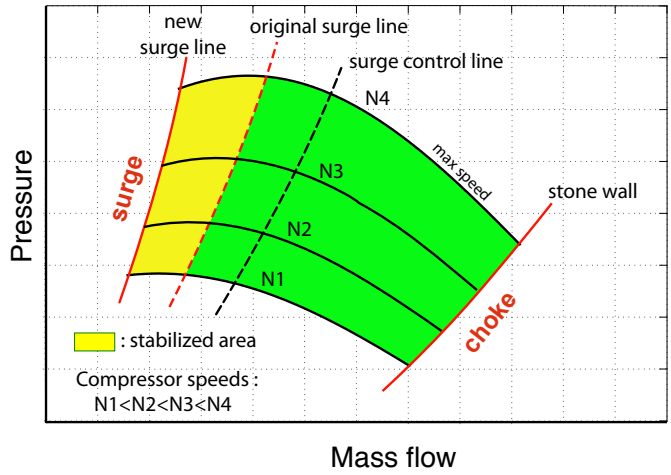

Figure 2.12: Operating area of a compressor equipped with an active surge control system.

2.6.2 Active Surge Control System

An active surge control system (ASCS) was first introduced by Epstein et al. (1986, 1989), and the main idea is to stabilize compressor surge by using an active element. The active element works based on a state feedback control. By using the ASCS, the compressor surge is stabilized and the compressor is safe to operate in the stabilized surge area. This makes the compressor operating envelope is enlarged toward the lower mass flow. Figure 2.12 illustrates the enlargement of the compressor operating area by applying the ASCS. The ASCS suppresses the surge line to the lower mass flow, as illustrated by a new surge line.

Several actuators have been applied in active surge control studies and examples includes moveable plenum wall (Williams and Huang, 1989), throttle (Pinsley et al., 1991), close coupled valve (Simon and Valavani, 1991), torque drive (Gravdahl et al., 2002), and active magnetic bearing (Yoon et al., 2012). Refer to (Willems and de Jager, 1999) for more actuators.

2.6.3 Industrial Compressor Surge Solution

SAS is commonly used in industrial compressors to prevent the compressor from entering surge. Although several studies on ASCS have proven the concept experimentally, to the best of our knowledge, the application of an active surge control system has not yet been reported. Developing an ASCS that is implementable in industrial compressors remains a research challenge. The implementation of such a system is determined by several factors, such as cost and safety. The cost is commonly influence by the ASCS cost, installation costs, and maintenance costs. The safety of implementing ASCS is very important because the ASCS allows the compressor to operate in a stabilized surge area. A failure of the ASCS will cause the compressor to surge and moreover to deep surge. An ASCS which is developed by considering the implementation factors will give more attraction to industries.

Chapter 3

Piston-Actuated Active Surge Control System (PAASCS)

This chapter describes the milestones in the development of PAASCS, the experimental test preparations, and the experimental test results. The preparations for the PAASCS experimental test include laboratory setup, piston design and manufacturing, and system implementation.

3.1 Milestones in PAASCS Development

The concept of PAASCS was presented in Gravdahl and Uddin (2012). The milestones in the design and development of PAASCS were presented in following papers:

1. Paper A
   This paper introduces the PAASCS, including modeling and control design. A model of PAASCS is shown in Figure 3.1 [1]. The PAASCS model is a modification of the Greitzer compressor model (Greitzer, 1976) by adding a piston. The assumptions in the Greitzer model mentioned in Section 2.5 are applied in the PAASCS model. The pressure at Station A (p_A) and pressure at Station B (p_B) are the ambient pressures and assumed to be equal. Fluid pressures in the system are measured relative to the ambient pressure. It is assumed that pressure drop along the ducts in the system are neglected. Therefore, the inlet pressure (p_i) is equal to p_A and the compressor discharge pressure (p_d) is equal to the compressor pressure rise (p_c). The dynamic equations of PAASCS are as follows:

$$\dot{w}_i = \frac{A_c}{L_c}(p_c - p_p) \tag{3.1}$$

$$\dot{p}_p = \frac{a_0^2}{V_p}(w_i - w_o - w_s), \tag{3.2}$$

   where w_i is the inlet mass flow, A_c is the compressor duct cross-sectional area, L_c is the effective length of the equivalent compressor duct, p_p is the plenum pressure, a_0 is the speed of sound, V_p is the plenum volume, w_o is the outlet mass flow, and w_s is the piston mass

[1] The notations of the model have been redefined to accommodate more complex compressor systems presented in other papers.

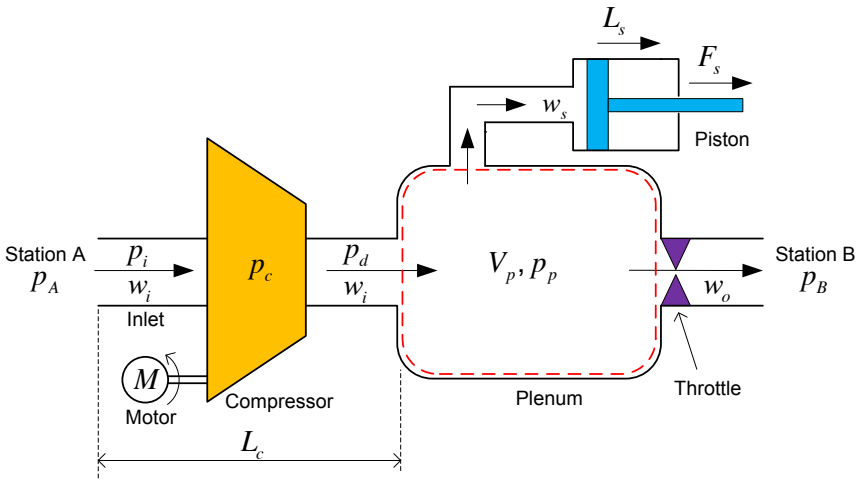

Figure 3.1: The model of a compression system equipped with a piston-actuated active surge control system.

flow. The plenum represents a control volume of the downstream line in a compression system. The piston mass flow is defined as:

$$w_s = \rho A_s \frac{dL_s}{dt} \tag{3.3}$$

where ρ is the fluid density, A_s is the piston cross-sectional area, and L_s is the piston position. The force to drive the piston is denoted by F_s in Figure 3.1.

Two control designs are presented. The first controller is designed using the backstepping method. This method proves the globally asymptotic stability (GAS) of the closed-loop system. However, the resulting state feedback control law is complicated and not practical for implementation. The second controller is a linear controller and is designed by linearizing the PAASCS dynamics. The state feedback control law is simpler because it is linear and requires state feedback from the plenum pressure and the piston velocity. However, the closed-loop system using the second controller is only guaranteed for locally asymptotic stability (LAS).

2. Paper B
The performance of PAASCS is evaluated. The linear quadratic method is applied to design the PAASCS controller. A simulation result shows that the piston is drifting during stabilizing surge such that the piston saturates at the end position. The piston saturation causes the PAASCS does not work properly and the compressor returns to surge. A solution for the piston drifting is presented by applying integral control action and the simulation results show that the drift is eliminated and moreover, applying a double-integral action results in eliminating the drift and minimizing the piston displacement. The minimizing piston displacement is a positive aspect for minimizing the piston size.
3. Paper C
Anticipating a failure in PAASCS that can cause the compressor to enter deep surge as

shown by the piston saturation case in Paper B, a backup system to the PAASCS is introduced. The backup system is used to recover the compressor from entering surge if the PAASCS should fail. This paper presents a study on applying an active surge control system by using a blow-off valve as the backup system for the PAASCS. Simulation results show that the backup system is able to recover the compressor from entering surge when the PAASCS fails. Two types of failures are presented: piston saturation and piston jamming.

4. Paper D
The work on backup systems for PAASCS is continued to apply SAS as the backup system. The SAS model described in (Egeland and Gravdahl, 2002) is applied. However, a numerical problem in the simulation appears when the operation is switched from PAASCS to SAS. The algorithm for switching the operating mode from PAASCS to SAS is the same as that for switching from PAASCS to ASCS using a blow-off valve in Paper C, where a numerical problem does not appear when the operation is switched from the PAASCS to the ASCS using a blow-off valve. Therefore, the SAS model needs to be evaluated.

   This paper presents compression systems modeling using bond graphs. Bond graph is a modeling method based on energy flow among the components in a system. Applying the bond graph in compression system modeling provides another modeling perspective, which is energy-based modeling rather than fluid dynamic laws. The bond graph applied to model a compression system equipped with a SAS. The modeling results in an improvement of the SAS model by taking into account the effect of recycling flow to the inlet state.

   Moreover, the bond graph is applied to model the Greitzer compression system. The energy flows among the components in the compression system system are described in the bond graph model. Two basis compressor surge solutions are identified through analysing the bond graph model. The two basic surge solutions are named upstream energy injection and downstream energy dissipation. Active surge control systems using several types of actuator are essentially implementing one of the two basic surge solutions. Therefore, we classify the active surge control systems into two types: upstream energy injection and downstream energy dissipation. All of the works on bond graph modeling for compressor systems are presented in (Uddin and Gravdahl, 2012b). Paper D is an extension of (Uddin and Gravdahl, 2012b) by providing more comprehensive explanations and extending to compressor network modeling.

5. Paper E
This paper presents a study of applying SAS as a backup system for the PAASCS, which applies the SAS model presented in Uddin and Gravdahl (2012b). Two failure scenarios are presented as in Paper C: piston saturation and piston jamming. The simulation results in this study show that the SAS is able to recover the compressor from entering surge when PAASCS fails.

6. Paper F
This paper presents two state feedback controls called ϕ-control and ψ-control for stabilizing compressor surge through upstream energy injection and downstream energy dissipation, respectively. Both state feedback controls are derived using the Lyapunov-based control method, and global asymptotic stability (GAS) of the closed-loop systems is proven. The ϕ-control only requires state feedback from the compressor mass flow sensor, and ψ-control only requires state feedback from the compressor discharge pressure and plenum pressure sensors.

7. Paper G
   This paper presents the implementation and experimental work on PAASCS in a laboratory-scale compressor test rig. The PAASCS controller uses the ψ-control introduced in Paper F. The experimental results show that PAASCS is able to stabilize surge and proof the concept of PAASCS.

3.2 Compressor Laboratory Facilities

An experimental test setup for PAASCS was prepared in parallel to the theoretical works for developing the PAASCS. A compressor test rig was constructed at the Compressor Laboratory at the Department of Engineering Cybernetics, NTNU. The major components applied in the compressor test rig are described as follows. Most of the components have been used in an experimental work on compressor surge control using torque drive (Bøhagen, 2007).

a. Compressor
   The setup uses a Vortech V-1 S-Trim Race M supercharger as the compressor. Unfortunately, the supercharger is obsolete and the technical information is not available in the Vortech's website any more. The following technical information of the supercharger and the drive refers to Bøhagen (2007). The supercharger has a maximum speed of 50000 rpm; maximum boosting pressure (pressure increase) of 20 PSI or 137.9 kPa, equivalent to a pressure ratio of 2.36; maximum flow of 1000 CFM; maximum power of 680 HP; and maximum efficiency of 72%. A compressor map of the Vortech V-1 S-trim supercharger[2] is shown in Figure 3.2. The compressor is driven by an 11 kW electric motor, ABB M3AA-160-MA2 with specific product code 3GAA-161-101-ASC. The motor is powered by 3-phase 240 VAC/40 A through an ABB frequency converter, ABB 11 kW ACS800 with specific product ACS800-01-0016-2+D150+L500+503. The motor has a nominal speed of 3000 rpm and can be operated up to 4500 rpm. The frequency converter is used to control the motor speed, and it also provides information about the motor speed based on the electric current supplied to the motor. The signal input to the frequency converter is 4-20 mA, and the signal output is 4-20 mA. The compressor shaft is connected to the motor shaft using a timing belt. The connection between the motor shaft and impeller shaft has a total gear ratio of 8.625. Therefore, the compressor can operate up to 38813 rpm.

b. Pressure sensors
   The pressure sensors used are Druck PTX610 sensors. These are high-performance pressure sensors, and the manufacturer claims that the output will not deviate from the straight line connecting zero full-scale output by more than 0.15%. The measurement range of the sensors is 0.9-1.6 bara with the sensor output of 4-20 mA.

c. Mass flow sensor
   The mass flow sensor used is an Endress+Hauser t-mass 65F80 sensor, specifically series 65F80-AE2AG1AAAAAA. It is a high-performance mass flow sensor for industrial gases and compressed air. The sensor is configured to measure flow at a range of 0-0.26 kg/s (Bøhagen, 2007). The sensor has high accuracy, with a measurement error of 2% of the measured value. The signal output of the sensor is 4-20 mA.

[2]The figure's title is Vortech V S-trim Compressor Map, but it has been confirmed by Vortech through an email correspondence that the figure is showing the Vortech V-1 S-trim compressor map.

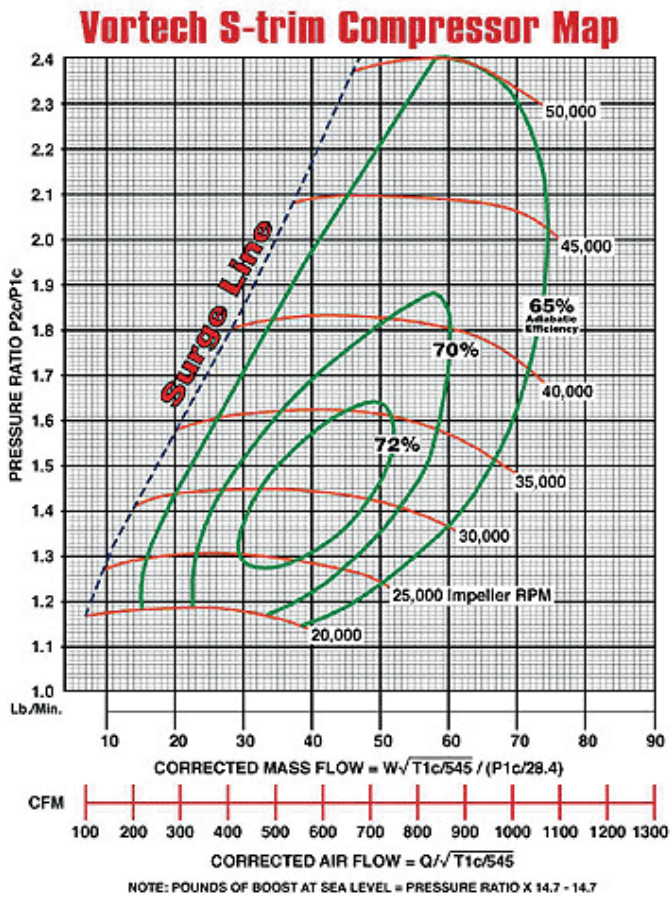

Figure 3.2: Compressor map of Vortech V-1 S-trim supercharger (Vortech, 2015)

d. Pipeline and Plenum
The employed pipeline is polypropylene pipe because it is inexpensive and easy to use for constructing a pipeline setup. The dimensions of the pipe are 75 mm and 70 mm for the outer and inner diameters, respectively. A cylindrical vessel with a volume of $0.1m^3$ is installed at the downstream line and used as a replacement for a long pipe, which is not possible to construct in the laboratory due to space limitations. A plenum is a control volume of the downstream line. The plenum volume is an accumulation of the cylindrical vessel volume and the downstream-pipe volume.

e. Throttle
A throttle is installed at the outlet duct to adjust the outlet flow. The throttle used is a Siemens 2-port seat valve PN10 with a flanged connection, with serial number VVF31.80, and driven by an electro-hydraulic actuator, SKD60. The actuator receives a 0-10 VDC input signal for controlling the valve position and provides feedback as a 0-10 VDC signal representing the valve position. The valve response is not quite fast, where the valve is typically applied in building systems. The throttle is used to adjust the outlet flow and not

for surge control purposes such that a fast response valve is not necessary.

f. Control Unit
A dSPACE board DS1103 PPC is used to construct a hardware-in-loop (HIL) simulation. The Matlab and Simulink algorithm codes are embedded in the dSPACE board. The dSPACE board is used to execute the algorithm in real time, send command signals to actuators through a DAC (digital-to-analog converter), and receive measurement signals from the sensors through an ADC (analog-to-digital converter). The dSPACE board has a 20-channel ADC with signal input in the range of 0-10 VDC and an 8-channel DAC with signal output in the range of 0-10 VDC. Because some of the sensors and actuators use signals of 4-20 mA, signal converters are required. The dSPACE board provides a dSPACE Control Desk software for designing a human machine interface (HMI). The HMI is used for allowing the operator to control and monitor the HIL simulation.

g. Signal Converters
Signal converters are used to convert 0-10 VDC signals to 4-20 mA signals and vice versa. The used signal converters are Siemens 3RS1705-1FD00 and Nokeval 641.

3.3 Compressor Test Rig

3.3.1 Initial Compressor Test Rig Setup

An initial compressor test rig setup is constructed as shown in Figure 3.3. Eight pressure sensors are installed at three locations in the setup described as follows, where the fluid pressure is measured relative to the ambient pressure.

- Pressure measurement at the inlet
Two pressure sensors, PT_1 and PT_2, are installed at the compressor inlet using a pitot tube. The PT_1 is used to measure the total pressure while the PT_2 to measure the static pressure.
- Pressure measurement at the compressor discharge
Four pressure sensors are installed at the compressor discharge, two of which (PT_3 and PT_4) are installed using a pitot tube and the other two (PT_5 and PT_6) are installed at the pipe wall. The PT_3 is used to measure the total pressure while the PT_4, PT_5, and PT_6 to measure the static pressure.
- Pressure measurement at the plenum
Two pressure sensors, PT_7 and PT_8, are installed at the cylindrical vessel wall. Both sensors measure the static pressure in the vessel.

The compressor discharge pressure (p_d), which is equal to compressor pressure rise (p_c), is measured using pressure sensor PT_3. The plenum pressure is approximated by the average of pressure measurement outputs of PT_7 and PT_8. The pitot tubes used in the setup are Endress+Hauser deltaset DPP50-A1F2A11Y tubes. A mass flow sensor is installed in the downstream line between the compressor discharge and the cylindrical vessel. A throttle is installed at the outlet line to adjust the mass flow.

A personal computer (PC) in the setup is connected to a dSpace system, in which Matlab and Simulink codes are embedded to construct a real-time system. The dSpace system is connected to actuators and sensors through DAC and ADC, respectively. The DAC converts digital signals from the dSpace processor into analog signals and sends the analog signals to the actuators. The

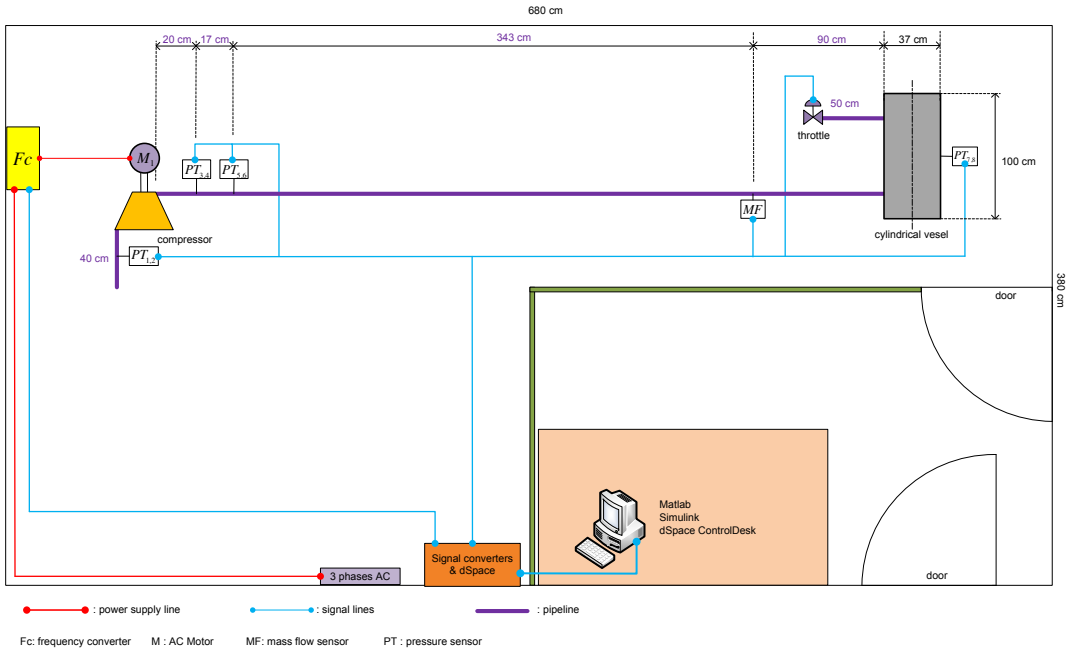

Figure 3.3: The diagram of initial compressor test rig setup in Compressor Laboratory, Dept. of Engineering Cybenetics, NTNU.

DAC provides analog signals in the range of 0 to 10 volts. The ADC receives the analog signals from the sensors, converts the analog signals into digital signal, and sends the digital signal to the dSpace processor. The ADC receives analog signals in the range of 0 to 10 volts.

The operation of the compressor test rig is controlled and monitored through a human machine interface (HMI) as shown in Figure 3.4. The HMI was created using Control Desk software which is included in the dSpace system package.

A performance test on the initial compressor test rig setup is required to evaluate the performance of all components in the setup, to generate a compressor map, and to identify compressor surge. A performance test was performed on the setup by running the compressor at a constant speed and reducing the throttle opening gradually until the compressor to enter surge. The compressor mass flow and compressor discharge pressure at a steady operating point for each throttle setting are recorded. The performance test is repeated for different compressor speeds. The recorded data of the compressor mass flow and compressor discharge pressure are plotted to generate a compressor map, and the result is shown in Figure 3.5.

Figure 3.6 shows the measurement outputs of the mass flow sensor and pressure sensors when the throttle opening is reduced. The figure shows that mass flow sensor response is very slow and has a time delay. The mass flow sensor requires more than 10 seconds to obtain a steady

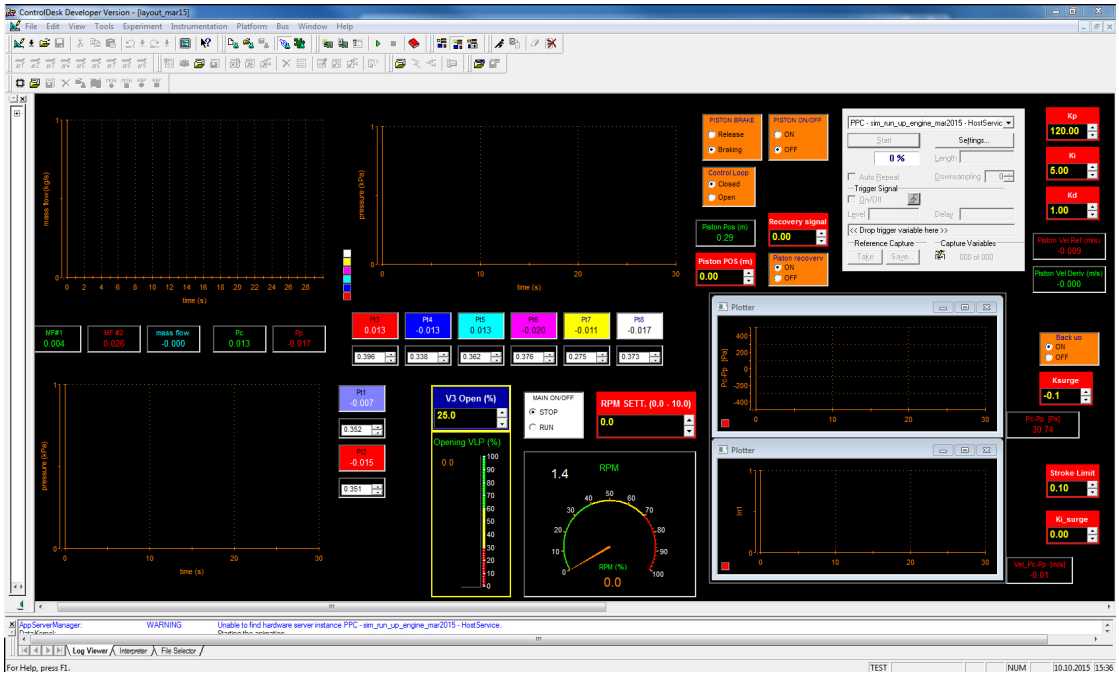

Figure 3.4: The human machine interface (HMI) for the compressor test rig operations.

measurement, whereas the pressure sensors are considerably faster. Pressure sensor PT_1 measures the total pressure at the inlet. The output of pressure sensor PT_1 is approximately zero, which is the ambient pressure because all pressure measurements are measured relative to the ambient pressure. Pressure sensor PT_2 measures the static pressure at the inlet. The output of pressure sensor PT_2 is negative because the inlet fluid is sucked by the compressor. Pressure sensor PT_3 measures the total pressure at the compressor discharge, and pressure sensor PT_4 measures the static pressure at the compressor discharge.

Because a compressor surge can occur at frequencies up to 6 Hz (Forsthoffer, 2005), the mass flow sensor will not be able to capture the mass flow oscillation during compressor surge. As a solution, the mass flow will be measured using a pitot tube and will be described in the next subsection.

3.3.2 Mass Flow Measurement Using a Pitot Tube

Flow measurement using a pitot tube is commonly applied in aircraft and wind tunnel. A pitot tube is equipped with two pressure sensors to measure the total pressure (p_t) and static pressure (p_s). Figure 3.7 shows a pitot tube installed in a pipe. The mass flow in a pipe is calculated using the following equation:

$$\bar{w} = A_c\sqrt{2\rho(p_t - p_s)}, \tag{3.4}$$

where $\bar{w}$ is the calculated mass flow and A_c is the pipe cross-sectional area. The pitot tube installed at the inlet duct of the initial compressor test rig setup is applied in measuring the inlet

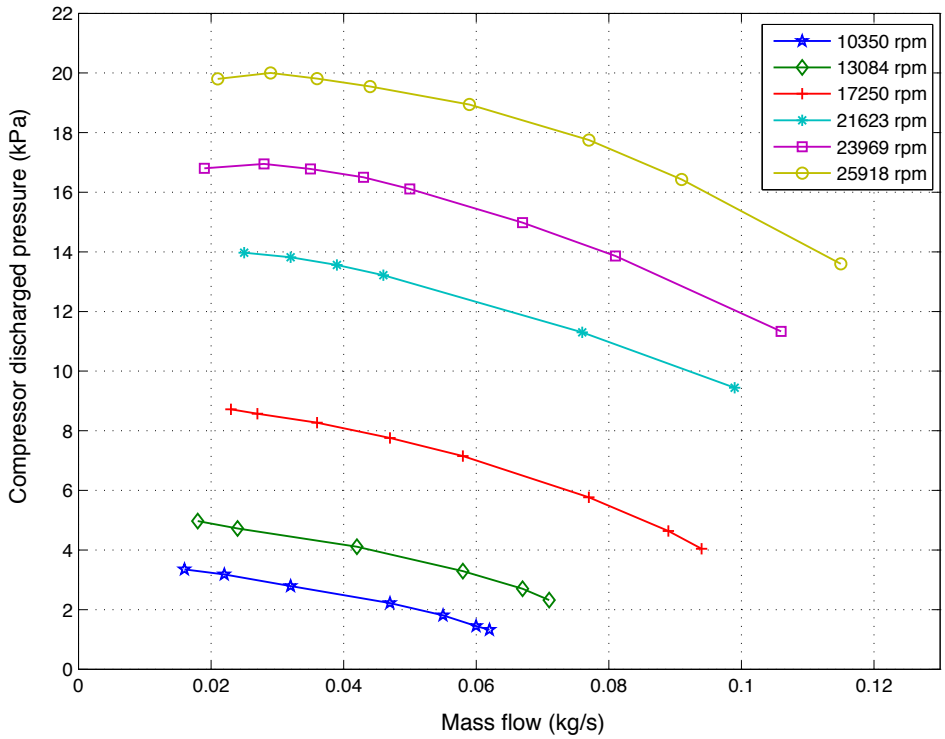

Figure 3.5: The resulting compressor map from a performance test on the initial compressor test rig setup.

mass flow. It is assumed that the fluid density is constant and equal to the ambient fluid density, which is 1.2041 kg/m^3.

The calculated mass flow is validated by the measurement data of the mass flow sensor. Figure 3.8 shows the relationship of the calculated mass flow based on the pitot tube measurement and the measured mass flow using mass flow sensor of several steady compressor operating points for different rotational speeds. The relationships of both data are approximated by a linear function. The linear function is then used to correct the calculated mass flow such that the corrected mass flow of the pitot tube mass flow measurement is as follows:

$$w = 0.45\bar{w} - 0.0035, \tag{3.5}$$

where w is the corrected mass flow. The main reasons for this correction are a misalignment of the pitot tube installation and incorrect air density.

3.3.3 Compressor surge test on the initial compressor test rig setup

A compressor surge test was performed on the initial compressor rig setup by running the compressor at 23960 rpm and reducing the throttle opening such that the compressor enters surge.

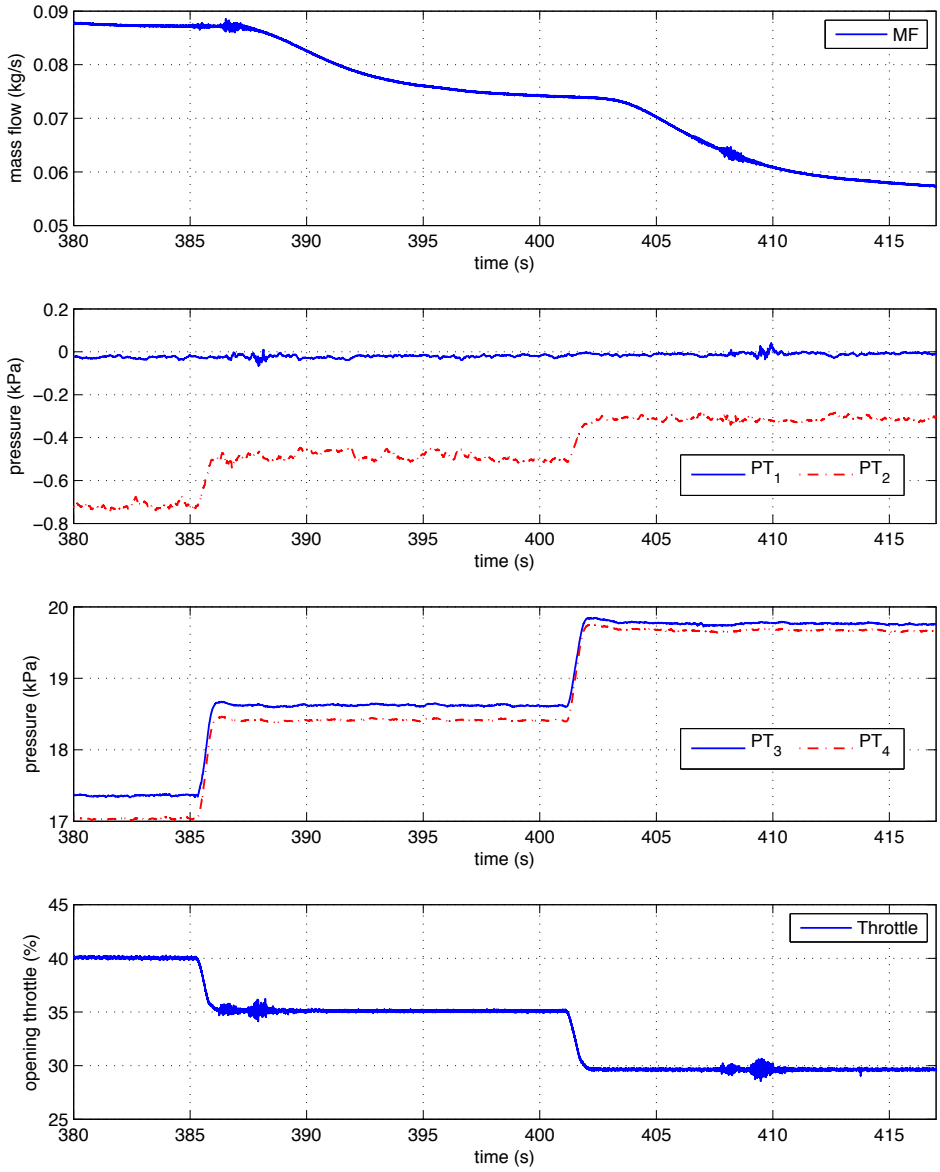

Figure 3.6: The measurement outputs of the mass flow sensor and pressure sensors in the compressor test rig when the throttle opening is reduced.

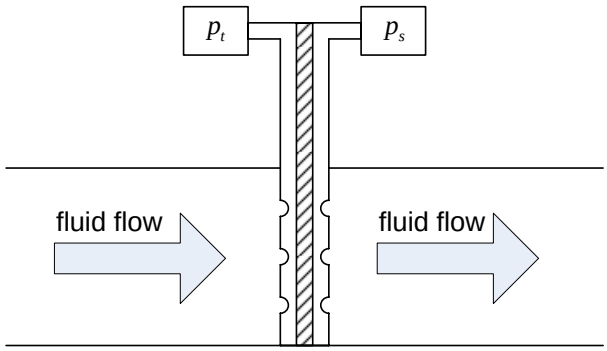

Figure 3.7: Diagram of a pitot tube installed in a pipe.

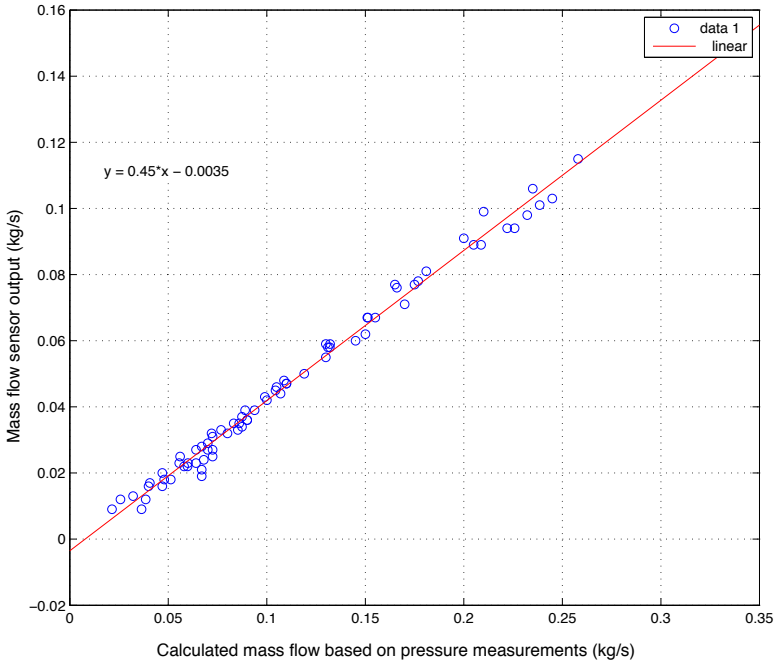

Figure 3.8: The relationship of the calculated mass flow based on pressure measurements (mass flow measurement using a pitot tube) and the measured mass flow using a mass flow sensor of several steady compressor operating points for different rotational speeds.

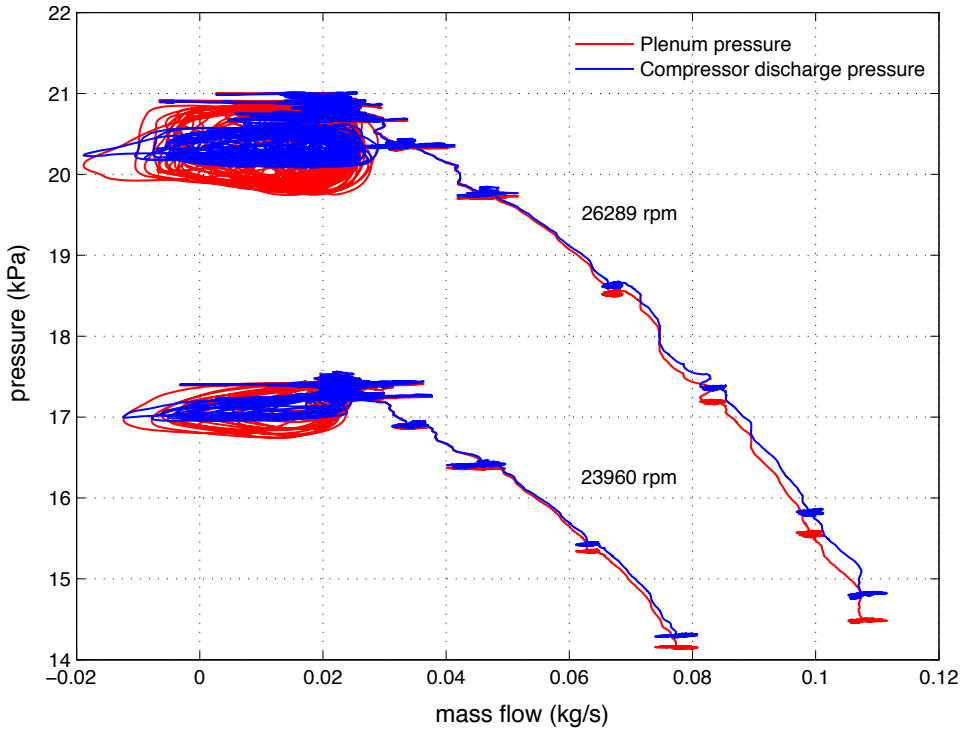

Figure 3.9: The compressor surge test results using the initial compressor rig setup.

The test was repeated for the 26289 rpm compressor speed to gain a stronger flow oscillation during compressor surge.

Figure 3.9 shows the plot of the compressor discharge pressure and the plenum pressure against the compressor mass flow obtained from both compressor surge tests on the initial compressor test rig setup. The mass flow in the figure was obtained through a mass flow measurement using pitot tube. The compressor was experiencing deep surge in the test for both compressor speeds, where the reverse flows were observed physically in the inlet.

Figure 3.10 shows the measurement of compressor states during the compressor surge at compressor speeds 26289 rpm. It is shown that the pressures are oscillating with frequency of 3 Hz. The pressure oscillation frequency is the compressor surge frequency. The mass flow measurement using the mass flow sensor were not able to capture the flow oscillation during compressor surge, while the mass flow measurement using pitot tube was able to capture the mass flow oscillation during surge. This indicates that the mass flow measurement using pitot tube has a fast response which is sufficient for capturing surge. However, the mass flow measurement using pitot tube during surge was not accurate as the mass flow should be negative for the reverse flow and remains a further study. Because a reliable mass flow sensor for measuring compressor surge is not available in the setup, the surge phenomenon will be presented in terms of pressure oscillation in this study.

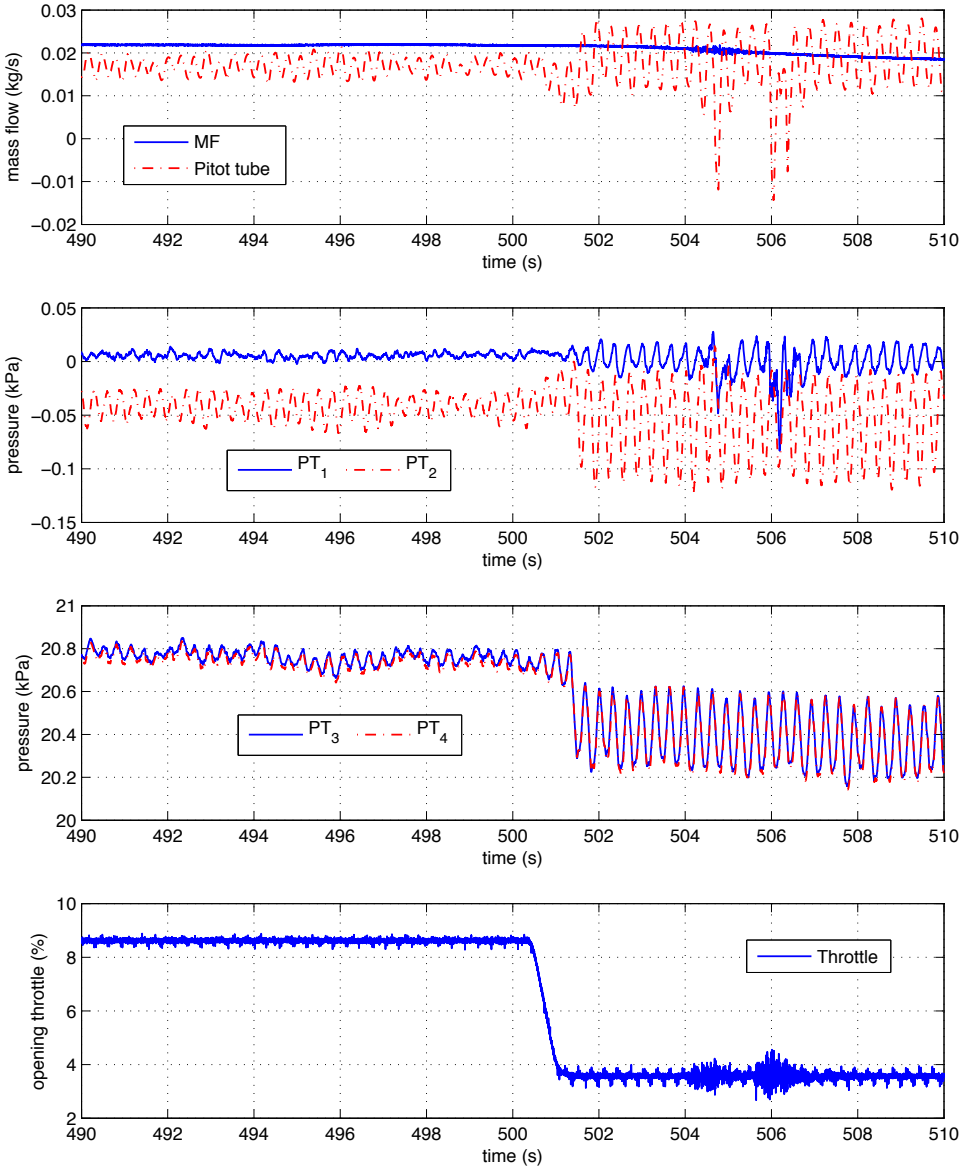

Figure 3.10: The compressor states during compressor surge at a compressor speed of 26289 rpm.

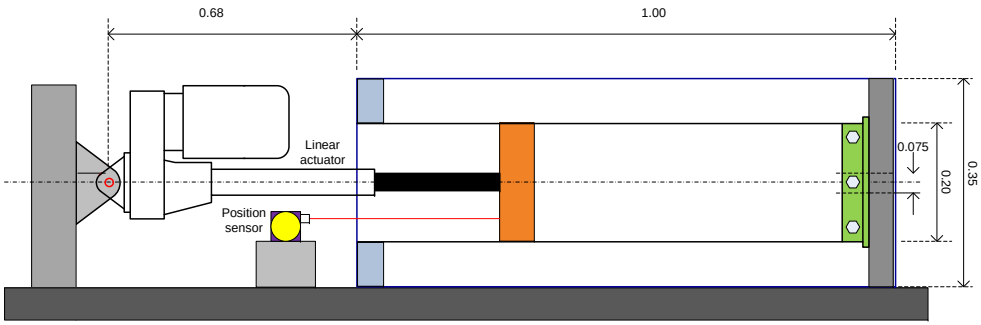

Figure 3.11: Piston design.

3.3.4 Piston for PAASCS

The remaining component in the compressor test setup was a piston, which is the actuator of the PAASCS. The specifications of the piston should be determined by simulating the PAASCS closed-loop system. However, a proper control law for PAASCS was not yet established at that time. The control law should be practically implementable and make the closed-loop system GAS. The exact specifications of the piston could not yet be determined. The result of compressor surge test on the initial setup shows that the maximum compressor pressure rise of the compressor at 26289 rpm is 21 kPa. We defined 26289 rpm as the maximum compressor speed for operating the compressor test rig setup, and thus, the piston should be able to work up to pressures of 21 kPa. Because the exact specifications of the piston were not available, we decided to have a piston that is able to generate the highest possible mass flow and work at pressures up to 21 KPa. A piston of this type was not available on the market, and thus, we had to construct it.

A piston was designed and shown in Figure 3.11. The piston is driven by an electric linear actuator. The piston was initially designed to have a diameter of 35 cm, and thus, it requires a linear actuator to generate a force of 2020 N. Considering speed, maximum displacement and force, we decided to use a Servomech UAL4RV2C500 (3x230volt, 1.1 kW) with a Toshiba VF-S11 frequency converter as the linear actuator to drive the piston. The linear actuator has a maximum speed of 44 cm/s, maximum displacement of 50 cm and maximum force of 1700 N. It was the fastest linear motor available on the market that can generate a high force and long displacement. Because the linear motor produces less force, the piston diameter has to be reduced. Considering friction and avoiding high load to the linear actuator, the piston diameter is reduced to 20 cm such that it only requires a force of 660 N to move the piston. It is expected that the piston will move at maximum speed with the lower load. The piston displacement is sensed by a SP1-50 spring-loaded potentiometer. The piston was constructed by our colleagues, Per Inge Snildal and Terje Haugen, at the workshop of Department of Engineering Cybernetics, NTNU. The constructed piston is shown in Figure 3.12, and the piston specifications are presented in Table 3.1.

A system identification of the piston was performed in Uddin and Gravdahl (2016b) and resulted in a transfer function

$$G(s) = \frac{L_s(s)}{u_s(s)} = \frac{0.251}{s(s + 5.405)} \tag{3.6}$$

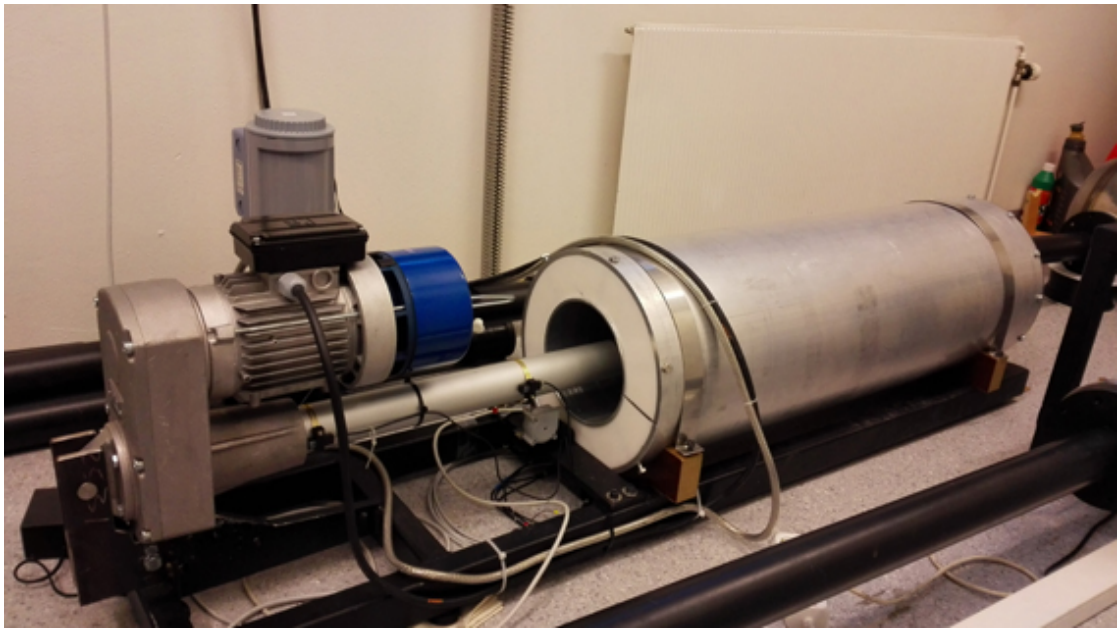

Figure 3.12: The constructed piston.

Table 3.1: Piston Specifications

Nomenclature	Detail
Piston diameter	20 cm
Displacement	± 25 cm
Max speed	44 cm/s
Max flow (ρ=1.2 kg/s)	0.0166 kg/s
Max pressure	54 kPa

where L_s is the piston displacement in meters and u_s is the piston input in volts. The idle piston position is in the middle such that the piston displacement is in the range of ±25 cm. The mass flow generated by the piston is given by:

$$w_s = \rho A_s \frac{dL_s}{dt} = \rho A_s \left(\frac{0.251}{s + 5.405} \right) u_s \tag{3.7}$$

where ρ is the air density and A_s is the piston cross-sectional area.

3.3.5 Final Compressor Test Rig Setup

A diagram and photograph of the final compressor test rig setup are shown in Figure 3.13 and Figure 3.14, respectively. The piston is installed between the plenum and throttle. The final compressor test rig setup has a longer pipe on the line between the plenum and throttle than

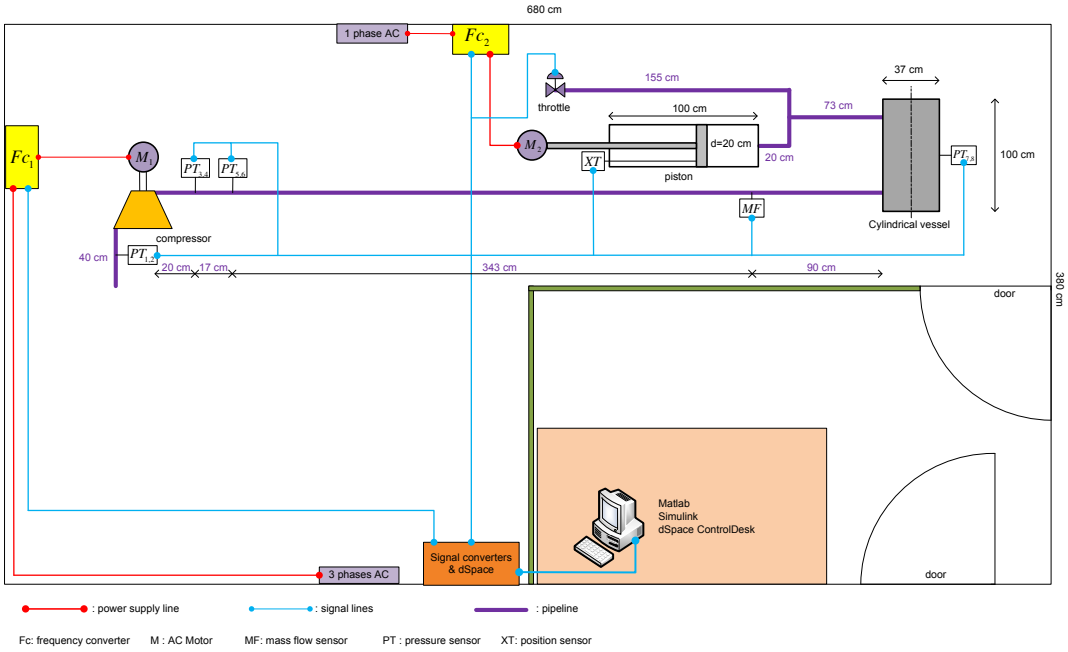

Figure 3.13: The diagram of final compressor test rig setup in Compressor Laboratory, Dept. of Engineering Cybenetics, NTNU.

Table 3.2: PAASCS Test Setup Parameters

Parameter	Value	Unit	Parameter	Value	Unit
a_0	340	m/s	V_p	0.12	m^3
L_c	0.8	m	A_c	0.0038	m^2
ρ	1.2041	kg/m^3	A_s	0.0314	m^2

the initial compressor test rig setup. Parameters of the final compressor rig setup are presented in Table 3.2. It is assumed that the L_c is twice the compressor inlet duct length and that the plenum volume is the accumulation of the cylindrical vessel volume, the downstream pipe volume, and the half piston volume. The pressures and mass flow measurements strategy in the final compressor test rig setup is the same as in the initial compressor test rig setup, where the mass flow is calculated based on the pressure measurements using pitot tube installed at the inlet, the compressor discharge pressure (p_d) is obtained using the pressure sensor PT_3, and the plenum pressure (p_p) is the average of the measured pressures using pressure sensors PT_7 and PT_8.

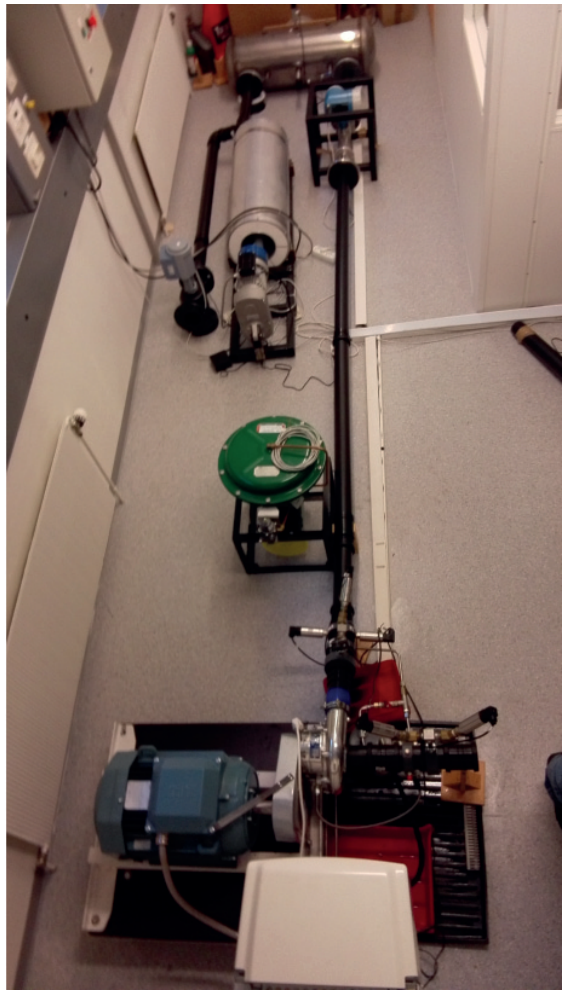

Figure 3.14: A photograph of the final compressor test rig setup.

The pipe extension and piston installation in the final setup cause the system characteristics to change such that a compressor performance test was required. A performance test was performed on the final setup by running the compressor at 23978 rpm and 26287 rpm for eight operating points. The initial operating point is with a throttle opening of 40% and reduced gradually at 5% up to the final operating point where the throttle opening was 5%. The eight operating points are labelled by alphabet A to H, where operating point A is with throttle opening 40% and H is with throttle opening 5%.

Figure 3.15 shows the results of the compressor performance test at 23978 rpm, where the compressor surge is shown particularly in Figure 3.16. The compressor discharged pressure was oscillating with peak to peak amplitude of around 250 Pa and the oscillation frequency of around 3 Hz. Figure 3.17 shows the results of the compressor performance test at 26287 rpm and the compressor surge is shown particularly in Figure 3.18. The compressor discharged pressure was

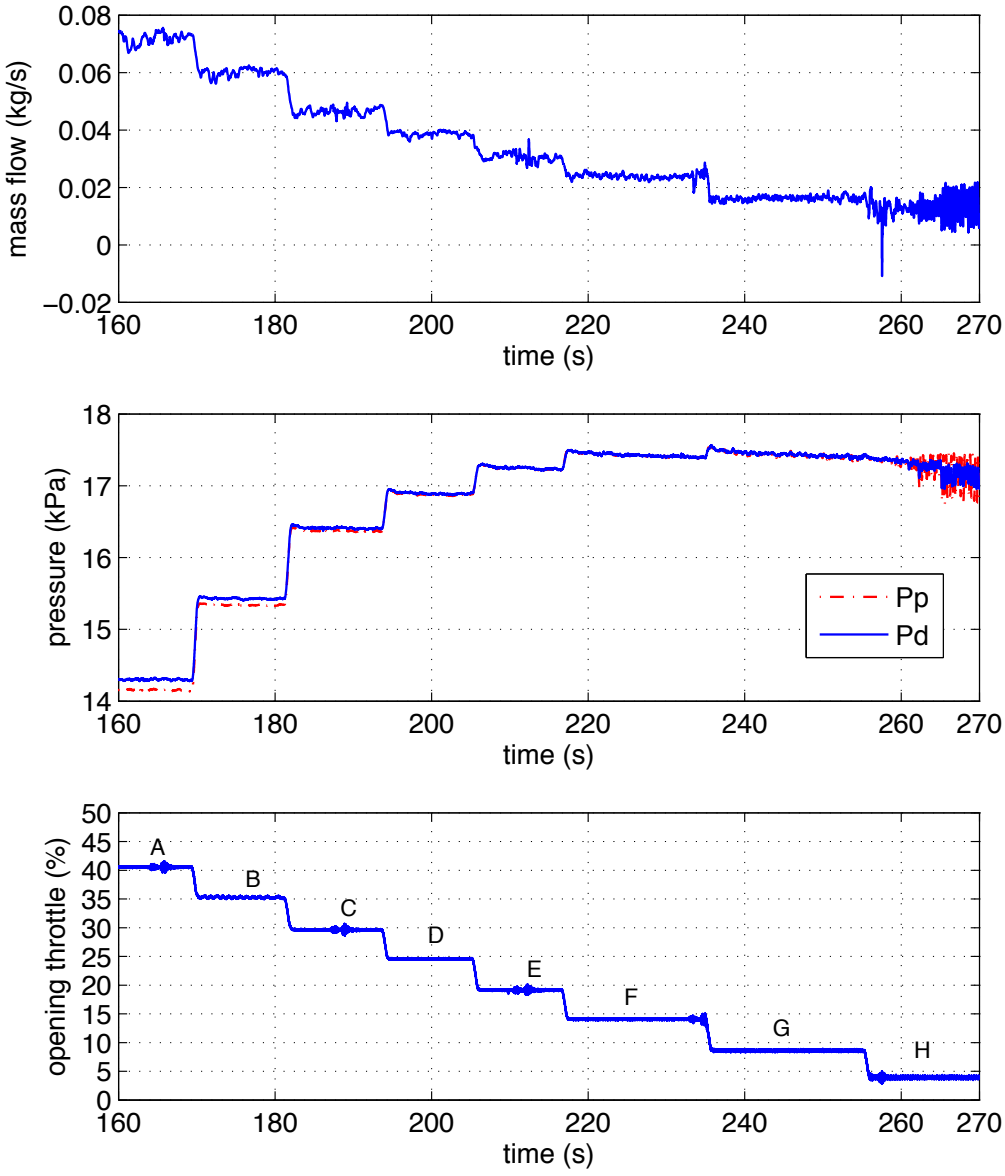

Figure 3.15: The compressor time response of several throttle settings at a compressor speed of 23978 rpm.

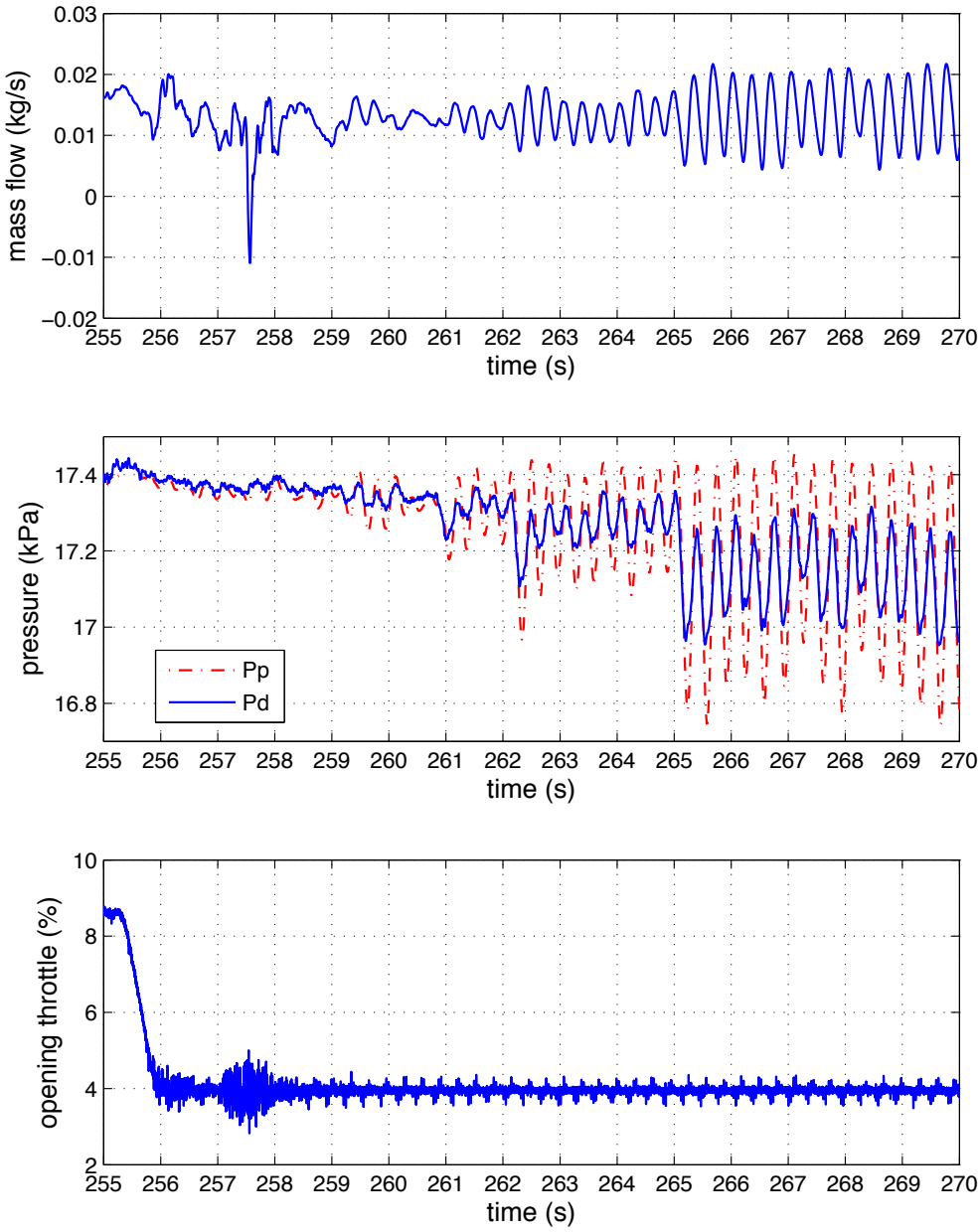

Figure 3.16: The compressor time response during surge at a compressor speed of 23978 rpm.

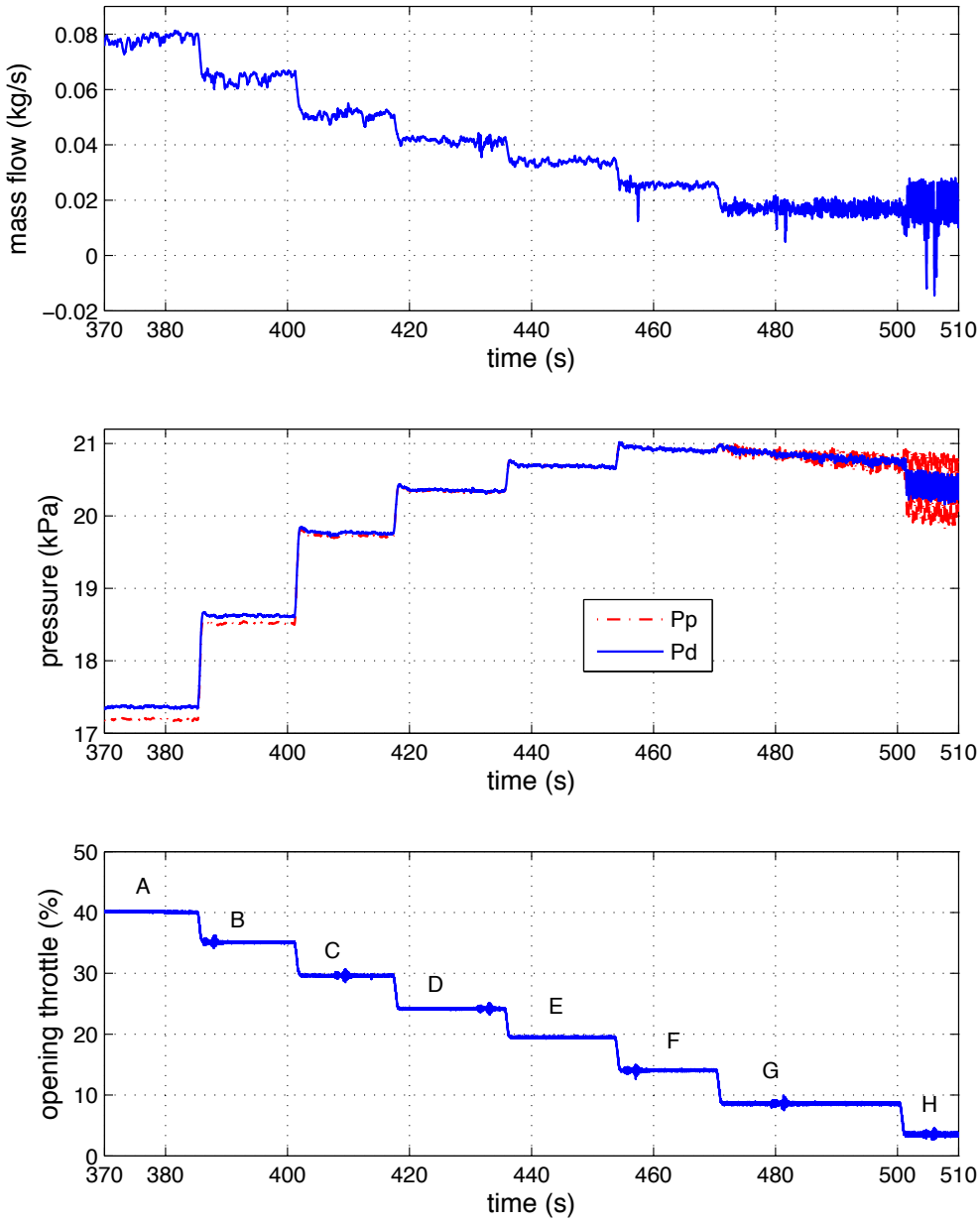

Figure 3.17: The compressor time response of several throttle settings at a compressor speed of 26287 rpm.

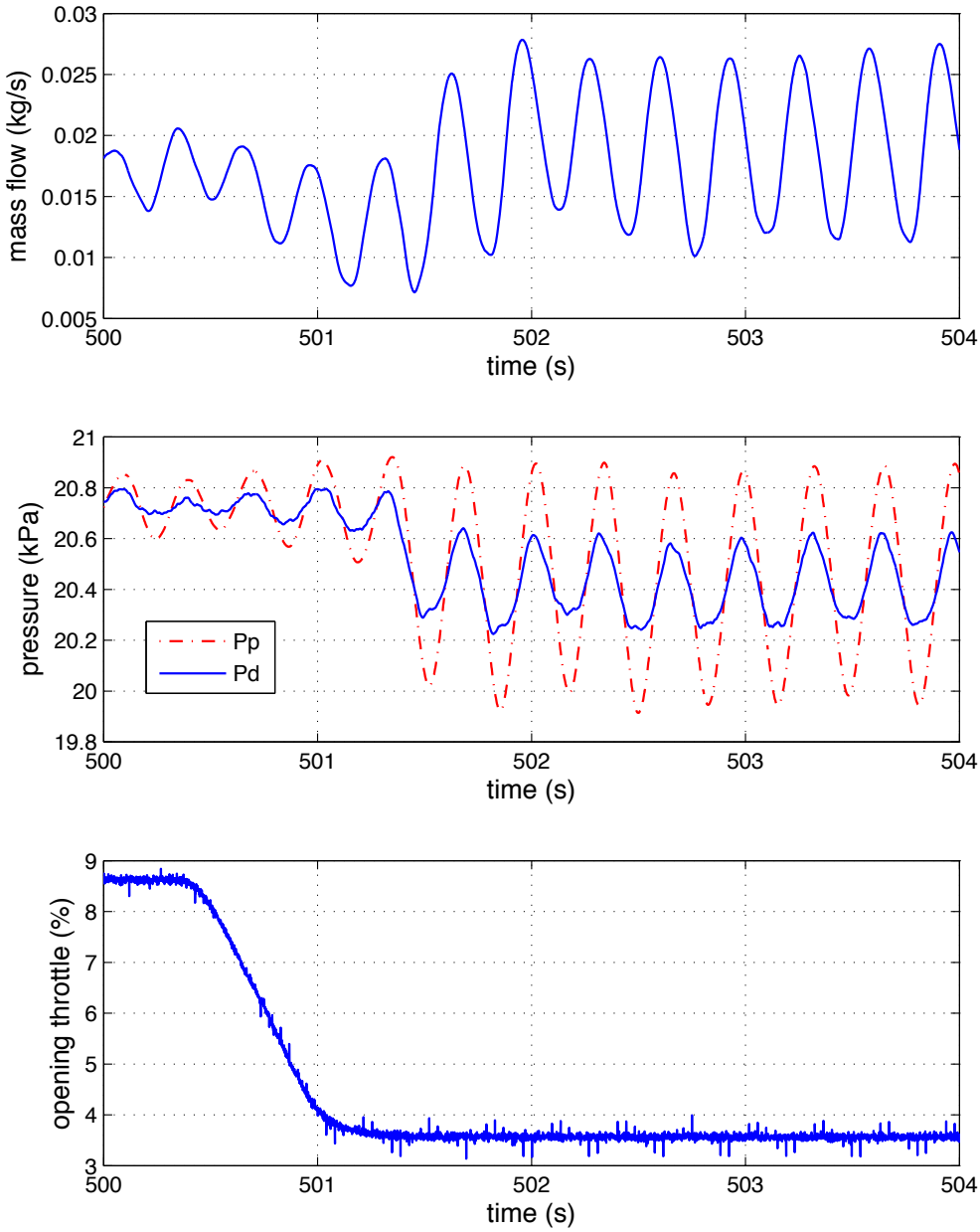

Figure 3.18: The compressor time response during surge at a compressor speed of 26287 rpm.

oscillating with frequency of around 3 Hz and peak to peak amplitude of around 380 Pa. The figures also show that the throttle is not very accurate, and thus, the measured throttle opening is not exactly the same as the set point, specially for the smaller throttle openings.

The measured data of the compressor mass flow and compressor pressure are applied in generating a compressor performance curve of the final compressor test rig setup. The curve describes the compressor operating points, including stable and unstable operation region. The stable compressor operating curve is generated by a cubic approximation of the measured data up to right before compressor surge. Those are shown by "*Approximation 1*" for each compressor speed in Figure 3.19, and the peaks of the curves are the surge points. The unstable compressor operating curve is estimated using a cubic function introduced in (Moore and Greitzer, 1986) and given as follows:

$$p_c\left(w_i\right) = p_{c_0} + H\left[1 + \frac{3}{2}\left(\frac{w_i}{W} - 1\right) - \frac{1}{2}\left(\frac{w_i}{W} - 1\right)^3\right] \tag{3.8}$$

where p_{c_0} is the shut-off value of the axisymmetric characteristic, W is the semi-width of the cubic axisymmetric compressor characteristic, and H is the semi-height of the cubic axisymmetric compressor characteristic; refer to (Moore and Greitzer, 1986) for more detailed definitions.

The value of H is approximated by the amplitude of the compressor discharged pressure (p_d) oscillation of compressor surge as shown in Figure 3.16 and Figure 3.18 for compressor speeds 23978 rpm and 26287 rpm, respectively. The value of W is determined by using the peak point of curve "Approximation 1" where the mass flow of the peak point is equal to $2W$. The value of p_{c_0} is approximated by subtracting the pressure of the peak point of curve "Approximation 1" with $2H$. The estimated compressor performance curves in unstable operating area for the both compressor speeds are shown by "Approximation 2" in Figure 3.19.

3.4 PAASCS Implementation

The PAASCS is an active surge control system in the type of downstream energy dissipation (Uddin and Gravdahl, 2015). A ψ-control was introduced in (Uddin and Gravdahl, 2016a) to establish a globally asymptotic stability (GAS) for the closed-loop of this type of active surge control system and given in the following theorem.

Theorem 3.1. *A ψ-control to generate flow out from the plenum $w_u = -k_u(p_c - p_p)$ with the control gain $\frac{2B_1}{B_2}k_m < k_u < \frac{2B_1}{B_2}k_n$, where $B_1 = \frac{A_c}{L_c}$, $B_2 = \frac{a_0^2}{V_p}$, $k_m = \frac{\partial p_c}{\partial w_i}\Big|_{\max}$ and $k_n = \frac{\partial p_p}{\partial w_o}\Big|_{\min}$, makes the operating point of the closed-loop compression system equipped with PAASCS globally asymptotically stable (GAS).*

By using the cubical function in (3.8), the compressor map for 26287 rpm in Figure 3.19, and the compressor test rig setup parameter in Table 3.2, it is obtained $k_m = \frac{3H}{2W} = 2.5909 \times 10^4$ Pa.s/kg and $k_n = \frac{2p_p}{w_o}\Big|_{\min} = 3.3684 \times 10^5$ Pa.s/kg, $B_1 = 0.0047$, and $B_2 = 963330$. The calculation of the ψ-control gain results in $2.555 \times 10^{-4} < k_u < 3.3 \times 10^{-3}$. We choose the surge control gain $k_u = 4 \times 10^{-4}$ for the experimental test.

A block diagram of the PAASCS closed-loop system is presented in Figure 3.20. The surge controller is the ψ-control which provides a command signal to the piston to generate mass flow w_u based on a feedback of pressure different between the compressor discharge pressure

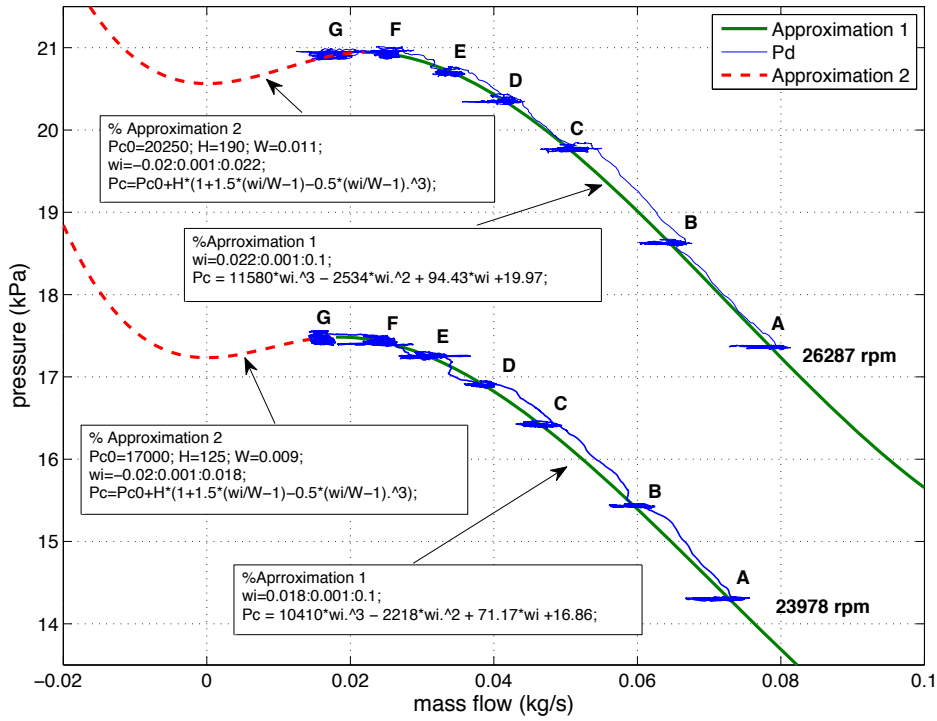

Figure 3.19: The resulting compressor performance curves of operating the compressor at 23978 rpm and 26287 rpm using the final compressor rig setup.

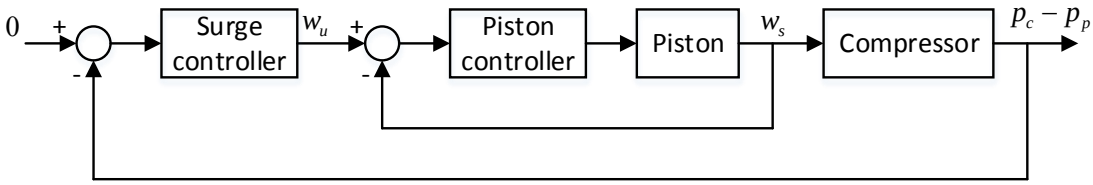

Figure 3.20: Block diagram of PAASCS.

and plenum pressure. Because the piston generates mass flow w_s, an inner loop with a piston controller is introduced to make w_s close to w_u.

The PAASCS block diagram is implemented according to the test setup facility, as shown in Figure 3.21. The piston controller is a PID control with $k_p = 120$, $k_i = 5$, and $k_d = 1$. The piston

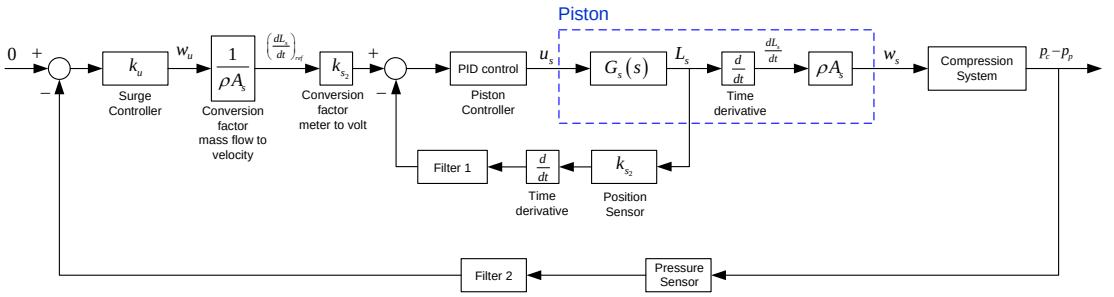

Figure 3.21: Block diagram of PAASCS implementation.

mass flow is calculated by:

$$w_s = \rho A_s \frac{dL_s}{dt} \tag{3.9}$$

where ρ is the fluid density, A_s is the piston area, and $\frac{dL_s}{dt}$ is the piston velocity. The fluid density is assumed to be constant and equal to the ambient air density in this case. The assumed fluid density is of course not correct as the fluid density of compressed fluid should be greater than the ambient fluid density. The assumption is taken to simplify the system implementation. Considering the block diagram of PAASCS implementation Figure 3.19, it is shown that the fluid density is used as a conversion factor in converting mass flow to velocity. Applying fluid density less than the actual makes the conversion factor greater than the correct conversion factor, and it is similar to increasing the surge control gain. In fact, the correct air density is unknown as not air density sensor is available in the setup, but the range of surge control gain is known. Based on the range of surge control gain, which is $2.555 \times 10^{-4} < k_u < 3.3 \times 10^{-3}$, the defined surge controller with $k_u = 4 \times 10^{-4}$ should tolerate the incorrect fluid density up to eight times of the ambient air density.

Because the piston is not equipped with a velocity sensor but rather with a position sensor, the piston velocity is obtained by taking a time derivative of the position sensor output. The position sensor output is voltage, which is proportional to the position with a conversion factor of k_{s_2}. The value of k_{s_2} is obtained through calibrating the position sensor. The used filter for piston-position measurement (Filter 1) is the first-order low-pass Butterworth filter with pass band frequency 20π rad/s, while the used filter for pressure measurement (Filter 2) is the first-order low-pass Butterworth filter with pass band frequency 60π rad/s. The block diagram is implemented in a Simulink model and embedded into a dSpace board to construct a hardware-in-loop (HIL) simulation.

3.5 Experimental Test Results

Experimental tests were performed by operating the final compressor test rig setup at a constant compressor speed and then reducing the throttle opening gradually up to a 5% opening such that the compressor enters surge. The PAASCS was activated when the compressor was in surge to stabilize the compressor surge. The results of two experimental tests of the PAASCS at compressor speeds 24335 rpm and 23550 rpm are presented.

Figure 3.22 shows the experimental result at compressor speed 24335 rpm. The compressor test rig was operating at a constant compressor speed 24335 rpm and throttle opening of 5%, and the compressor was entering surge as shown by the pressure oscillations since $t = 475$ seconds. The PAASCS controller was then turned on at $t = 482$ seconds as shown by Control ON in the figure and suppressed the pressure oscillation such that the compressor surge was stabilized. The PAASCS controller was then turned off at $t = 513$ seconds, and as shown, the compressor was driven back to surge.

Another test result is presented in Figure 3.23, where the compressor run at 23550 rpm. The compressor speed is lower than that in the previous test. This test result shows that the compressor surge was stabilized when the controller was activated. The compressor returned to surge again when the controller was turned off.

Both test results show that the actual piston velocity was not exactly following the reference signal given by the surge controller. An investigation in Uddin and Gravdahl (2016b) showed that the piston bandwidth is 1.2 Hz , which is quite low compared to the surge frequency of 3 Hz. The piston response is very slow such that not able to follow the reference signal.

The piston was also experiencing some drift as shown in Figure 3.22. Integral control recommended in (Uddin and Gravdahl, 2011b) to eliminate piston drift was applied, but it did not show any improvement in this experimental test. The slow response of the piston could be the main reason of it.

Nevertheless, surge was stabilized with the current piston and proves the concept of PAASCS experimentally.

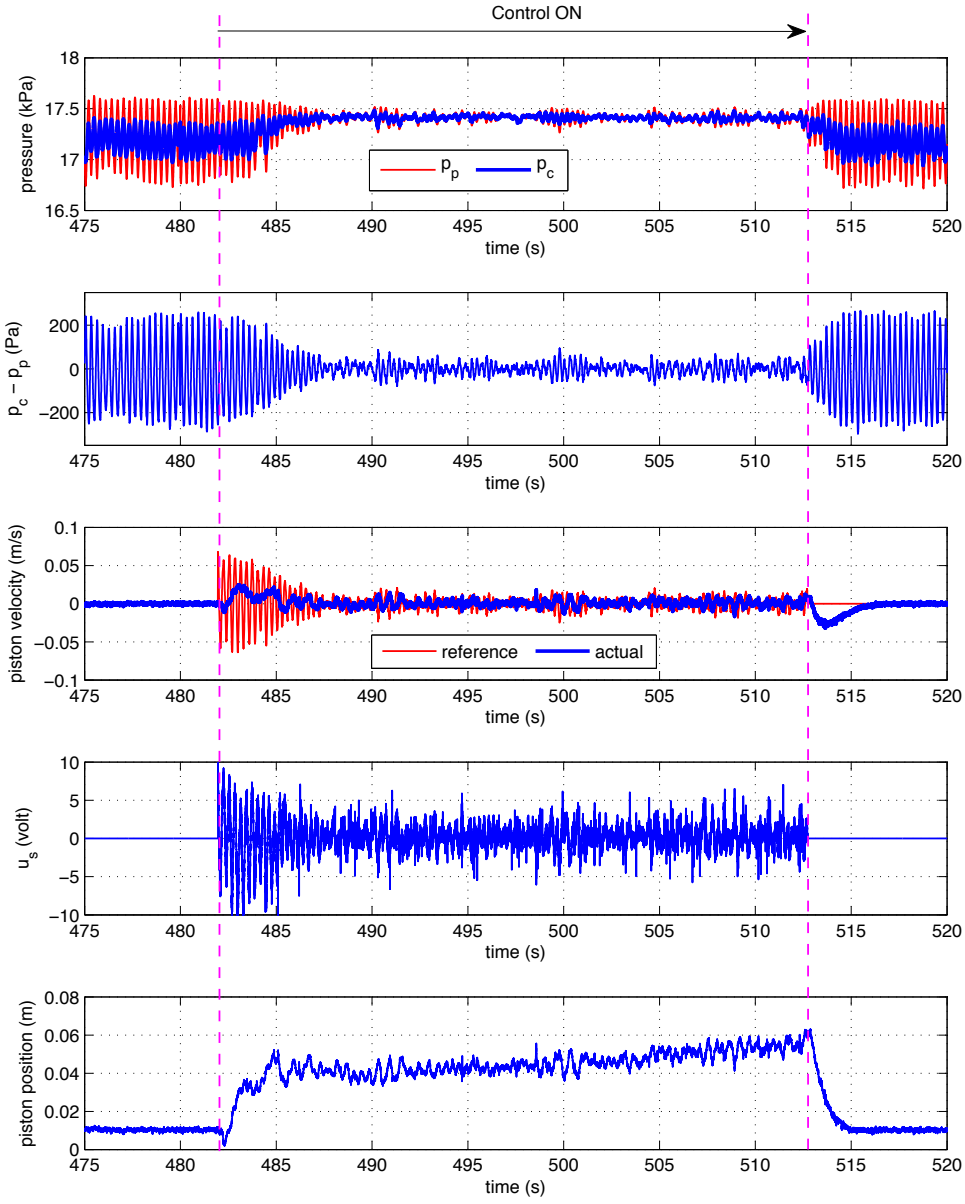

Figure 3.22: Experimental test result of PAASCS at 24335 rpm.

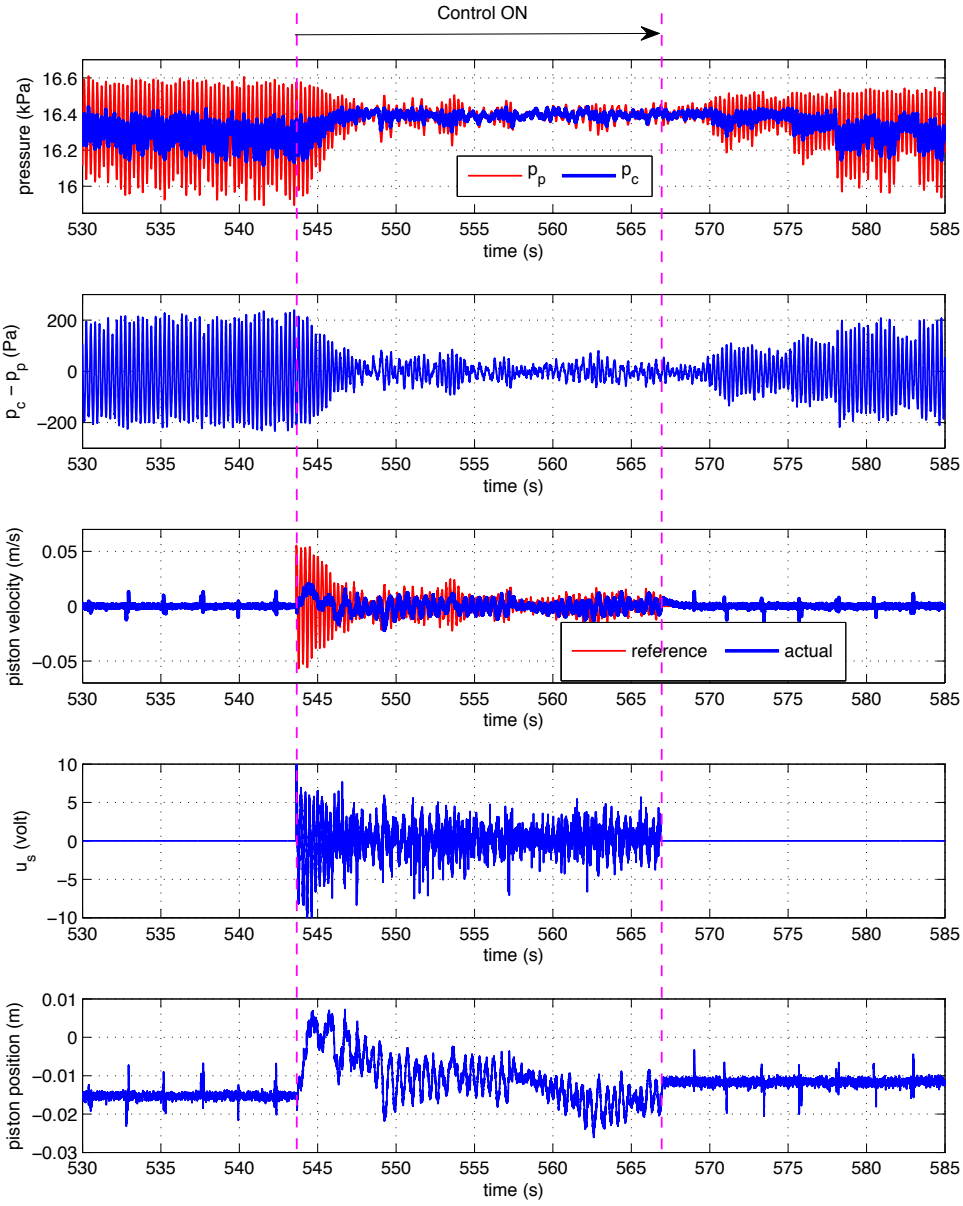

Figure 3.23: Experimental test result of PAASCS at 23550 rpm.

Chapter 4

Conclusions and Future Works

4.1 Conclusions

A study on the development of a new method for an active compressor surge control system using piston actuation has been presented. The method is called piston-actuated active surge control system (PAASCS). The study included system modeling, control design, piston design, system implementation, and experimental tests. The conclusions of this study are as follows:

a. The theoretical works including simulation results showed that the PAASCS is able to stabilize compressor surge, and global asymptotic stability (GAS) of the closed-loop system is proven.

b. Two methods for improving the PAASCS were presented. 1) Applying integral control action to eliminate piston drift under steady state operation and to minimize the piston displacement. 2) Introducing a backup system by using another surge control method for fail-safe operation.

c. Modeling a compression system based on energy flow using bond graphs was able to identify two basic solutions for compressor surge: upstream energy injection and downstream energy dissipation. The PAASCS is classified into the downstream energy dissipation. The simple and systematic modeling of compression systems for control design purposes using bond graphs was demonstrated.

d. Two general state feedback control laws were formulated using Lyapunov base control methof for both basic surge solutions in Paper F. These are called ϕ-control for upstream energy injection and ψ-control for downstream energy dissipation. The ϕ-control only requires feedback from the compressor mass flow, whereas the ψ-control requires feedback from pressure measurements at the compressor discharge and in the plenum. Both state feedback control laws make the closed-loop systems GAS.

e. The ψ-control was applied in the PAASCS. It was implemented in Matlab/Simulink and embedded in the dSpace system to construct a hardware-in-loop (HIL) simulation for the experimental test. The experimental test results show that the PAASCS is able to stabilize a compressor surge and proves the concept of PAASCS. These results also confirm the ψ-control experimentally.

f. The experimental test results showed that the piston response is very slow to follow the reference signal. The investigation showed that the piston bandwidth is 1.2 Hz which is

too low compare to the compressor surge frequency of 3 Hz. The slow piston limits the PAASCS performance in stabilizing the compressor surge.

4.2 Future Works

Recommendations for further works to improve the PAASSC are as follows:

a. The performance of PAASCS can be improved by using a better linear actuator with a higher bandwidth. It is expected that the linear actuator will be able to follow the reference command signal as close as possible. Considering the experimental results, the piston diameter can be reduced such that a linear actuator with a lower force can be applied.

b. It was shown that the piston mass flow is proportional to the piston velocity by assuming a constant fluid density. The piston velocity was obtained by taking the time derivative of the piston position measurement. It can be improved by using a velocity sensor rather than using a position sensor and taking the time derivative.

c. The mass flow in the test setup was measured using a pitot tube due to the slow response of the available mass flow sensor. The pitot tube mass flow measurement has a faster response, but it was not able to provide a correct measurement during compressor surge. The assumption of constant fluid density and equal to ambient air density could be a potential reason for the incorrect measurement because the reverse flow from the compressor downstream has a higher density than the ambient fluid. It is recommended to consider the varying fluid density in the system, which can be approximated as a function of temperature. Another solution for the mass flow measurement is to use an observer as introduced in Bøhagen and Gravdahl (2002) and Backi et al. (2013). A part of the mass flow measurement problem was resolved thanks to ψ-control, which does not require feedback from the mass flow measurement. However, having a sufficient mass flow measurement will provide a better representation of the trajectories of the compressor states during surge and the stabilization.

d. Studies on introducing a backup system to the PAASCS were presented theoretically. The experimental work has not yet been accomplished and is recommended for a future work.

Chapter 5

Original Publications

This chapter contains six conference papers and a journal paper.

Paper A Active Compressor Surge Control Using Piston Actuation

Published in the *Proceedings of the ASME 2011 Dynamics System and Control Conference* (DSCC 2011) in Arlington, VA, USA, Oct 31 - Nov 2, 2011.

Is not included due to copyright

Paper B Piston-Actuated Active Surge Control of Centrifugal Compressor Including Integral Action

Published in the *Proceedings of the 11th International Conference on Control, Automation and System* (ICCAS 2011) in KINTEX, Gyeonggi-do, South Korea, Oct 26-29, 2011.

Is not included due to copyright

Paper C Introducing Back-up to Active Compressor Surge Control System.

Published in the *Proceedings of the 2012 IFAC Workshop on Automatic Control in Offshore Oil and Gas Production* in Trondheim, Norway, May 31 - June 1, 2012.

Proceedings of the 2012 IFAC Workshop on Automatic Control in Offshore Oil and Gas Production, Norwegian University of Science and Technology, Trondheim, Norway, May 31 - June 1, 2012

FrAT2.4

Introducing Back-up to Active Compressor Surge Control System ⋆

Nur Uddin * **Jan Tommy Gravdahl** *

* *Engineering Cybernetics, Norwegian University for Science and Technology, O.S. Bragstads plass 2D, Trondheim, Norway N-7491*
nur.uddin@itk.ntnu.no, Jan.Tommy.Gravdahl@itk.ntnu.no

Abstract: A novel method for introducing a back-up system to an active compressor surge control system is presented in this paper. Active surge control is a promising method for extending the compressor map towards and into the unstable area at low mass flow by stabilizing the surge phenomenon. The method also has potential for allowing operation at higher efficiencies. However, a failure in the active surge control system may endanger the compressor by entering deep surge as the compressor is allowed to operate in the stabilized surge area. We propose the use of a back-up system applied to the active system to keep the compressor safe should the active system fail. This paper present an active compressor surge control system with piston actuation combined with a blow off system as the back-up. Performance of the combined system is evaluated by simulating the system in situations where the piston is saturated or jammed. The combination results in a system with increased performance by taking advantage of both systems.

Keywords: centrifugal compressor, compressor surge, piston-actuated active surge control system, blow off surge control system, combined surge control system.

1. INTRODUCTION

The operating area of compressors can be described by plotting compressor pressure rise against flow for varying compressor speed. This is called the compressor map. The stable operating area is limited for low mass flows by the so-called surge line and for high mass flows by the stone wall or choke line. Operation of a compressor at flows below the surge line would drive the compression system into an instability known as surge. This is an axisymmetric oscillation of mass flow and pressure rise and is followed by severe vibrations in the compression system. The vibrations may reduce the reliability of the system and large amplitude vibrations may lead to compressor damage, especially to compressor blades and bearings.

Most industrial compressors are equipped with a surge avoidance system ensuring that the compressor does not enter the surge area. These surge avoidance systems usually work by recycling flow from downstream to upstream when the operating point reach a surge control line that is located to the right of the surge line. Such surge avoidance schemes successfully ensure safe operation, but the introduction of the surge control line reduces the usable size of compressor map, thereby restricting the compressor operational envelope.

Surge stabilization by using active control system was proposed by Epstein et al. (1989) and since then a number of theoretical and experimental results have been published. A number of different actuators and control methods have been applied, as summarized by Willems and de Jager (1999). Recent developments in this field include the work by Arnulfi et al. (2001) on hydraulic actuators as well as Bøhagen and Gravdahl (2008) on drive torque actuation. Williams and Huang (1989) proposed to employ a movable plenum wall as an actuator for the surge control problem. Their experimental results showed that the developed system, using a loudspeaker as the movable wall, was able to stabilize surge and enlarge the operating area in the low mass flow region of the compressor map. This inspires the piston-actuation surge control in the current work.

Active surge control systems have mainly been implemented in university laboratories and have not yet found wide spread use in industrial compression systems. One reason for this is safety. Although active surge control is a promising method for compressor map enlargement, the enlarged area is open loop unstable, and failure in the active system will cause the compressor to go unstable and enter surge. The introduction of a back-up system is therefore necessary.

Active surge control using a blow off valve was presented by Willems and de Jager (1998). In principle, this is quite similar to a surge avoidance system using recycle, but the blow off valve is controlled by a control law that actively stabilizes the equilibrium or operating point instead of using a control line. This approach stabilized surge and the compressor map was enlarged to the left side of the surge line. The control system was so-called one-sided as it was only able to discharge flow from plenum and not inject flow into plenum. An active surge control system with piston actuation was introduced by Uddin and Gravdahl (2011a) where the surge stabilization relies on a piston which can both draw flow from the plenum or inject flow into the

⋆ This work was supported Siemens Oil and Gas Solutions Offshore through the Siemens-NTNU collaboration project.

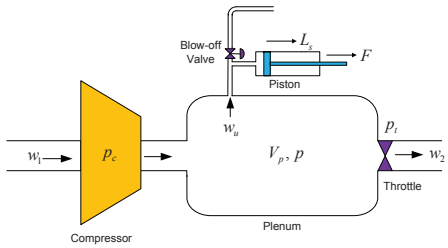

Fig. 1. Compression system equipped with a piston.

plenum. However, there are two situations that could cause this active system to fail: 1) actuator saturation caused by limited the maximum piston stroke, and 2) actuator fault such as jamming of the piston.

This paper presents an active compressor surge control system with piston actuation combined with a blow off system as back-up. Blow off system is a common method of controlling surge and piston-actuation was introduced, but the two methods are combined for the first time in this paper. Performance of the combined system is evaluated by simulating the saturation and jamming of the piston. The combination is expected to give a better system performance by taking the advantage of each method. A study case is presenting an application of the combined surge control method in a centrifugal compression system. Instability at low mass flow in a centrifugal compressor is dominated more by occurring surge than stall. Fontaine et al. (1999) presented a comparison of linear and non-linear control for axial compressor and concluded that linear control works well for compressor surge problem but not for both surge and stall. Based on their result, we are applying linear control design for the both surge control methods.

The paper consists of five sections including introduction in Section I. Section II describes compressor dynamics and compressor characteristic. Section III describes control design for piston-actuated active surge control law, blow off surge control law and active surge control including back-up. Simulation results are presented in Section IV. Finally, conclusions and future works are presented in Section V.

2. COMPRESSOR DYNAMICS

A model of a compression system equipped with a piston actuator combined with a blow off valve for surge control is shown in Fig. 1. The compression system dynamics was introduced by Greitzer (1976) and given as follows:

$$\dot{w_1} = \frac{A_c}{L_c}\left[p_c\left(w_1\right) - p\right] \tag{1}$$

$$\dot{p} = \frac{a_0^2}{V_p}\left[w_1 - w_2\left(p\right) - w_u\right] \tag{2}$$

where w_1 is the compressor mass flow, w_2 is the throttle mass flow, w_u is the control mass flow, p_c is the compressor pressure rise, p is the plenum pressure, a_0 is the speed of sound, V_p is the plenum volume, A_c is the inlet duct cross section area, L_c is the length of the inlet duct. The control mass flow w_u is applied for surge control and will be controlled by the piston or the blow off valve.

Non-dimensionalization of the equations were done by using factors: $\frac{1}{2}\rho U^2$ for pressure, $\rho U A_c$ for mass flow, $\frac{1}{\omega_H}$ for time and L_c for length and resulting in:

$$\dot{\phi}_1 = B\left[\psi_c\left(\phi_1\right) - \psi\right] \tag{3}$$

$$\dot{\psi} = \frac{1}{B}\left[\phi_1 - \phi_2(\psi) - \phi_u\right] \tag{4}$$

where $B = \frac{U}{2\omega_H L_c}$ and $\omega_H = a_0\sqrt{\frac{A_c}{V_p L_c}}$. The notation ϕ_1 is the non-dimensional compressor mass flow, ϕ_2 is the non-dimensional throttle mass flow, ϕ_u is the non-dimensional control mass flow, ψ_c is the non-dimensional compressor pressure rise, ψ is the non-dimensional plenum pressure, B is the Greitzer's constant, U is the mean rotor velocity, ω_H is the Helmholtz resonator frequency, ρ is the fluid density and τ is the non-dimensional time. The non-dimensional throttle mass flow was defined by Gravdahl and Egeland (1997):

$$\phi_2 = \gamma_T\sqrt{\psi}. \tag{5}$$

A compressor pressure rise characteristic is modeled by a qubic function as introduced by Moore and Greitzer (1986):

$$\psi_c\left(\phi_1\right) = \psi_0 + H\left[1 + \frac{3}{2}\left(\frac{\phi_1}{W} - 1\right) - \frac{1}{2}\left(\frac{\phi_1}{W} - 1\right)^3\right] \tag{6}$$

where ψ_o is the shut-off value of the axisymmetric characteristic, W is the semi-width of the cubic axisymetric compressor characteristic, and H is the semi-height of the cubic axisymetric compressor characteristic, consult Moore and Greitzer (1986) for more detailed definition.

A compressor operating point is an intersection point between compressor pressure rise ψ_c and throttle pressure drop ψ_T. The throttle pressure drop is given by:

$$\psi_T\left(\phi_2\right) = \frac{1}{\gamma_T^2}\phi_2^2, \tag{7}$$

where γ_T is the throttle setting. Four different compressor operating points based on the compressor data given in Table 1 are shown in Fig. 2. Point A is a stable operating point with the throttle setting $\gamma_T = 0.7$. The compressor is operating at surge point when the throttle setting is $\gamma_T = 0.6$ as shown by point B. A throttle setting less than 0.6 brings the compressor into surge, for example: point C with $\gamma_T = 0.5$ and D with $\gamma_T = 0.3$. It can be shown that operating points located at positive compressor characteristic slope are unstable and thereby leading to surge, see Gravdahl and Egeland (1999).

3. SURGE CONTROL DESIGN

3.1 System State Equation

For notational convenience, define the system states as follows:

$$x_1 = \phi_1,\ x_2 = \psi, \tag{8}$$

Table 1. SIMULATION PARAMETERS

Parameter	Value	Unit	Parameter	Value	Unit
U	68	m/s	a_0	340	m/s
V_p	0.1	m^3	A_c	0.0038	m^2
L_c	0.41	m	ρ	1.2041	kg/m^3
m_s	1	kg	A_s	0.0038	m^2
ψ_o	0.352	-	W	0.25	-
H	0.18	-			

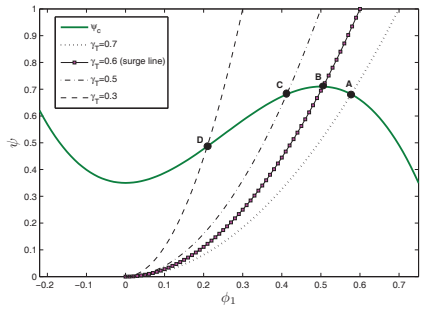

Fig. 2. Compressor and throttle characteristics.

and constants as follows:

$$b_1 = B,\ b_2 = \frac{1}{B} \tag{9}$$

such that the dynamics (3) and (4) can be written as:

$$\dot{x}_1 = b_1 \left[\psi_c\left(x_1\right) - x_2\right] \tag{10}$$

$$\dot{x}_2 = b_2 \left[x_1 - \phi_2\left(x_2\right) - \phi_u\right]. \tag{11}$$

Define deviation from an operating point as follows:

$$\tilde{x}_1 = x_1 - x_{10},\ \tilde{x}_2 = x_2 - x_{20},\ \tilde{\phi}_u = \phi_u - \phi_{u_0} \tag{12}$$

where (x_{10}, x_{20}) is the compressor operating point. The ϕ_{u_0} is assummed to be zero as the piston is idle during steady operation. The blow off valve is working only if the piston should fail. Transforming the system dynamics (10) and (11) into new state coordinates (12) results in:

$$\dot{\tilde{x}}_1 = b_1 \left[\tilde{\psi}_c\left(\tilde{x}_1\right) - \tilde{x}_2\right] \tag{13}$$

$$\dot{\tilde{x}}_2 = b_2 \left[\tilde{x}_1 - \tilde{\phi}_2\left(\tilde{x}_2\right) - \tilde{\phi}_u\right] \tag{14}$$

where the compressor pressure rise, throttle pressure drop and control mass flow in the new coordinates are defined by:

$$\tilde{\psi}_c\left(\tilde{x}_1\right) = -k_3\tilde{x}_1^3 - k_2\tilde{x}_1^2 - k_1\tilde{x}_1 \tag{15}$$

$$\tilde{\phi}_2\left(\tilde{x}_2\right) = \gamma_T\sqrt{\left(x_{20} + \tilde{x}_2\right)} - \gamma_T\sqrt{x_{20}} \tag{16}$$

with $k_1 = \frac{3Hx_{10}}{2W^3}\left(x_{10} - 2W\right)$, $k_2 = \frac{3H}{2W^3}\left(x_{10} - W\right)$ and $k_3 = \frac{H}{2W^3}$.

The compression system described in (13) and (14) is stabilized by control mass flow $\tilde{\phi}_u$ which can be generated by the piston or blow off valve depending on the chosen surge control method shown in Fig. 3. The details of the control laws are explained in the next parts.

3.2 Piston-actuated active surge control

Active surge control system using a piston was improved by using integral control in Uddin and Gravdahl (2011b). Piston-actuated active surge control is stabilizing surge by injecting flow into the plenum or drawing flow from the plenum by moving the piston. Define control mass flow generated by the piston as:

$$\tilde{\phi}_u = \tilde{\phi}_p, \tag{17}$$

which is a function of the piston velocity as

$$\tilde{\phi}_p = b_3\tilde{x}_3, \tag{18}$$

where b_3 is a constant given by

$$b_3 = \frac{1}{2B}\left(\frac{A_s}{A_c}\right) \tag{19}$$

and $\tilde{x}_3$ is nondimensional piston velocity defined by

$$\tilde{x}_3 = \frac{d}{d\tau}\left(\frac{L_s}{L_c}\right). \tag{20}$$

The notation A_s is for the piston cross section area, A_c is the inlet duct cross section area, L_s is the piston stroke and L_c is the length of the inlet duct. The closed loop piston dynamics including integral action is given as follows:

$$\dot{\tilde{x}}_3 = b_4\left[b_5\tilde{x}_2 + \tilde{u}_p\right] \tag{21}$$

$$\dot{\tilde{x}}_4 = \tilde{x}_3 \tag{22}$$

$$\dot{\tilde{x}}_5 = \tilde{x}_4. \tag{23}$$

The notation b_4 is a constant defined by $b_4 = \frac{2B^2}{M_s}$ with M_s is the non-dimensional piston mass given by $M_s = \frac{m_s}{\rho A_c L_c}$ where m_s is the piston mass. The notations $\tilde{u}_p$ is piston control force and b_5 is a constant defined by $b_5 = \frac{A_s}{A_c}$. The states $\tilde{x}_3$ is the piston velocity, $\tilde{x}_4$ is the piston stroke, and $\tilde{x}_5$ is time integral of the piston stroke. A state feedback control law for the piston control force is defined by:

$$\tilde{u}_p = -K_p\tilde{x}_p \tag{24}$$

where K_p is the control gain and $\tilde{x}_p = [\tilde{x}_1, \tilde{x}_2, \tilde{x}_3, \tilde{x}_4, \tilde{x}_5]^T$. Uddin and Gravdahl (2011b) applied linear quadratic regulator for the linearized the system around operating point A. The computational resulted in a control gain

$$K_p = [\,4303.2\ \ -2157.2\ \ 1707.9\ \ 1719.9\ \ 316.2\,] \tag{25}$$

and closed loop eigenvalues at $s_{1,2} = -1.2400 \pm 2.1987i$, $s_3 = -2.3043$ and $s_{4,5} = -0.1838 \pm 0.1824i$. All eigenvalues are located in the left half plane (LHP) such that the system locally asymptotically stable. An alternative control law using feedback from plenum pressure and piston displacement only can be found in Uddin and Gravdahl (2011a).

3.3 Blow off surge control

Blow off surge control is stabilizing surge by discharging the plenum fluid out of the compression system. The control mass flow is defined by:

$$\tilde{\phi}_u = \tilde{\phi}_b. \tag{26}$$

The blow off flow is adjusted by a blow off valve and the function is defined by:

$$\tilde{\phi}_b = \gamma_b(\tilde{u}_b')\sqrt{x_{20} + \tilde{x}_2} \tag{27}$$

where $\gamma_b(\tilde{u}_b')$ is the opening valve as a function of control signal u_b' with nominal value in the range of $0 \leq \gamma_b(\tilde{u}_b') \leq 1$. For simplicity, define $\gamma_b(\tilde{u}_b') := \tilde{u}_b$ such that

$$\tilde{\phi}_b = \tilde{u}_b\sqrt{x_{20} + \tilde{x}_2}. \tag{28}$$

Notice that this actuator model does not include actuator dynamics as in (21)-(23). The compressor dynamics with a blow off line are then defined by:

$$\dot{\tilde{x}}_1 = b_1\left[\tilde{\psi}_c(\tilde{x}_1) - \tilde{x}_2\right] \tag{29}$$

$$\dot{\tilde{x}}_2 = b_2\left[\tilde{x}_1 - \tilde{\phi}_2(\tilde{x}_2) - \tilde{\phi}_b\right]. \tag{30}$$

Linearization around an operating point results in

$$\dot{\tilde{x}}_b = A_b\tilde{x}_b + B_b\tilde{u}_b \tag{31}$$

where

$$\tilde{x}_b = [\,\tilde{x}_1\ \tilde{x}_2\,]^T, \tag{32}$$

$$A_b = \begin{bmatrix} -b_1k_1 & -b_1 \\ b_2 & \dfrac{-b_2\gamma_T}{2\sqrt{x_{20}}} \end{bmatrix}, B_b = \begin{bmatrix} 0 \\ -b_2\sqrt{x_{20}} \end{bmatrix}. \tag{33}$$

A state feedback control for the blow off valve is given by:

$$\tilde{u}_b = -K_b\tilde{x}_b. \tag{34}$$

Linearizing the system (29)-(30) around operating point A and applying pole placement method by selecting closed loop poles at -1.09 ± 1.32 results in

$$K_b = [1.1666 - 0.9978]. \tag{35}$$

The poles was selected such that the blow off valve will not be saturated. Another possibility would be to use saturated control like in Willems et al. (2002). The pole selection was also intended to makes the closed loop system using blow off valve has greater damping and shorter natural frequency than the one using piston. It was due to the control mass flow in closed loop system with blow off valve has one direction and not bidirection as in the closed loop system with piston. It was demonstrated in Willems et al. (2002) that a compression system described by (29)-(30) is stabilizable with positive feedback blow off. The lower constraint on $\tilde{u}_b$ does not affect the stability of the linearized system but reduces the range of stabilizing control gains.

3.4 Active surge control with back-up

This active surge control system with back-up is combining the piston actuation and blow off valve to generate a control mass flow $\tilde{\phi}_u$ for surge control purpose. The piston surge control is the main system and operates by default. The blow off surge control is the back-up system and works if the main system should fail. The main system is said to have failed if the piston is saturated or the piston is jammed. The failure in the system is detected by observing the piston velocity $\tilde{x}_3$ and the piston control law output

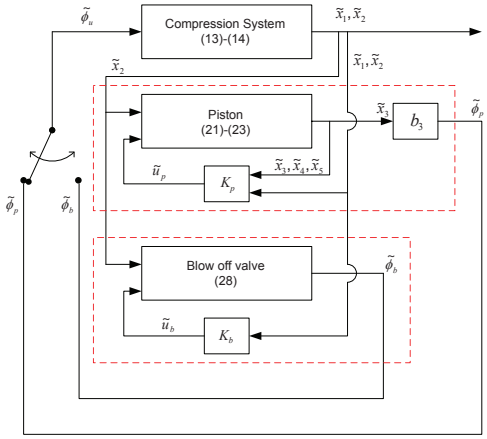

Fig. 3. Control diagram with switching operation of active surge control with piston actuation and blow off valve.

$\tilde{u}_p$. The control law for this combined system is defined as follows:

$$\tilde{\phi}_u = \begin{cases} \tilde{\phi}_p \\ \tilde{\phi}_b \quad \text{for } \tilde{u}_p \neq 0 \wedge \tilde{x}_3 = 0 \end{cases} \tag{36}$$

where $\wedge$ is AND logic operator. The back-up system is only applied to save the compressor from entering surge when the main active surge control system should fail. Block diagram of the active surge control system including back-up is shown in Fig. 3.

4. SIMULATION

The performance of the active compressor surge control with back-up is evaluated by simulating piston saturation and piston jammed conditions. Four active surge control systems are simulated in both conditions for comparison. The first active surge control system called "Active I " is a piston-actuated active surge control system with piston stroke up to ± 0.35. The second active surge control system called "Active II" is a piston-actuated active surge control system with maximum stroke ± 0.15. The third active surge control system called "Active III" is a blow off active surge control system. The fourth active surge control system called "Active IV" is a piston-actuated active surge control system with maximum stroke ± 0.15 combined with blow off active surge control system as the back-up. The simulation scenario is initialized by operating the compressor at point A with throttle setting $\gamma_T = 0.7$ then at $\tau = 20$ the throttle is reduced to $\gamma_T = 0.5$ and then to $\gamma_T = 0.3$ at $\tau = 100$. The valve closing rate is 0.04 per non-dimensional time unit.

First simulation was done by simulating the system in normal condition and the result is shown in Fig. 4. The Active I controller performed well in stabilizing surge. The Active II controller was not able to stabilize surge as the control law required a piston stroke beyond the saturation limit. Moreover, closing throttle to $\gamma_T = 0.3$ causes the

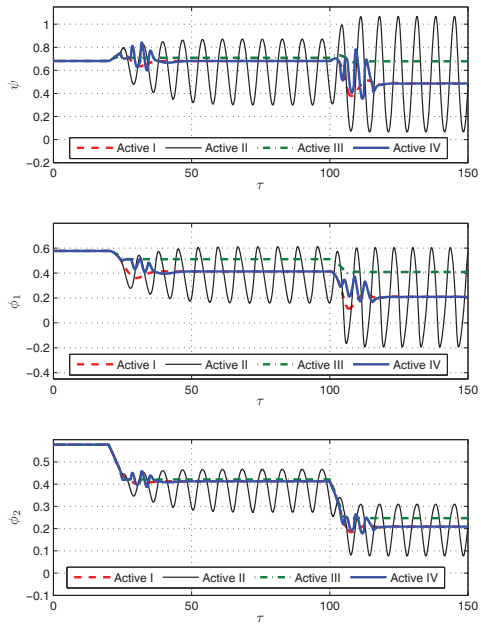

Fig. 4. Compressor states in a condition where the pistons of Active II and Active IV should be saturated.

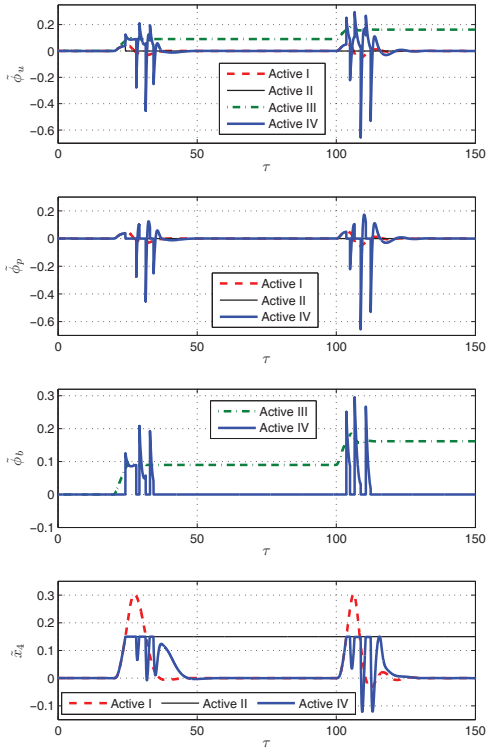

Fig. 5. Control mass flow and piston stroke in a condition where the pistons of Active II and Active IV should be saturated.

"un-actuated" compressor to enter deep surge. The Active III controller stabilized surge, but the steady state is higher than the desired due to the blow off moved the system to a new equilibrium. The Active IV controller was able to stabilize surge and blew off some flow to compensate the piston saturation. Only using Active I and Active IV, the compressor operates stable at the desired operating point in the left side of the original surge line. Fig. 5 shows the control mass flow and piston stroke of the four systems. The Active IV control mass flow is a result of switching operation between the piston and the blow off valve according to control law (36). Fig. 6 shows the piston velocity, piston position, and piston control force of Active IV.

The second simulation is done by assuming that the piston is jammed at $\tau = 112$. At that time γ_T will be 0.3. The simulation is only performed for Active I, Active III and Active IV, as Active II has been failed to stabilize surge under saturation. Fig. 7 is showing the results. The Active I was entering deep surge when the piston was jammed. The jammed piston did not affect to the Active III as piston was not used in the system. Active IV was able to keep the compressor in stable operation by blowing off flow when the piston is jammed and the compressor operating point moved to the stabilized operating point by the back-up system which is exactly the same as the operating point of Active III.

5. CONCLUSIONS AND FUTURE WORKS

5.1 Conclusions

Piston-actuated active surge control combined with blow off surge control as back-up was presented. Active surge control system with piston actuation which is able to discharge flow from plenum and inject flow into plenum showed better performance than the blow off surge control system which is only able to discharge flow from plenum. The simulation result showed that the combined system can both enlarged the compressor map and still keep safe operation even though the piston should fail. Providing longer piston stroke or applying some control method may avoid piston saturation, however a back-up system is still needed to assure safe compressor operation, for instance if the piston should jam.

5.2 Future works

This work is continued by: 1) analyzing the region of attraction of each surge control system and the combined system, 2) applying non-linear control in each surge con-

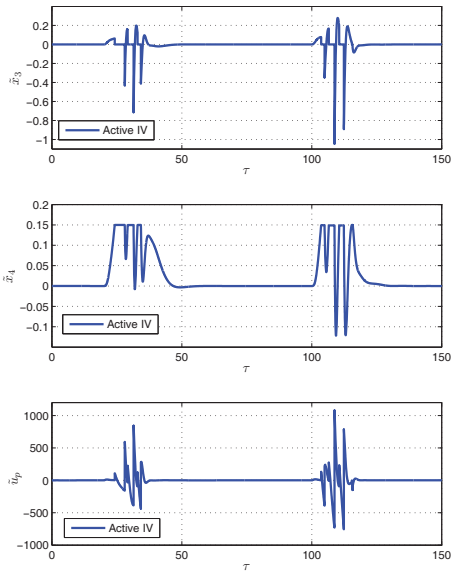

Fig. 6. The piston states and control force of Active IV in a condition where the piston should be saturated.

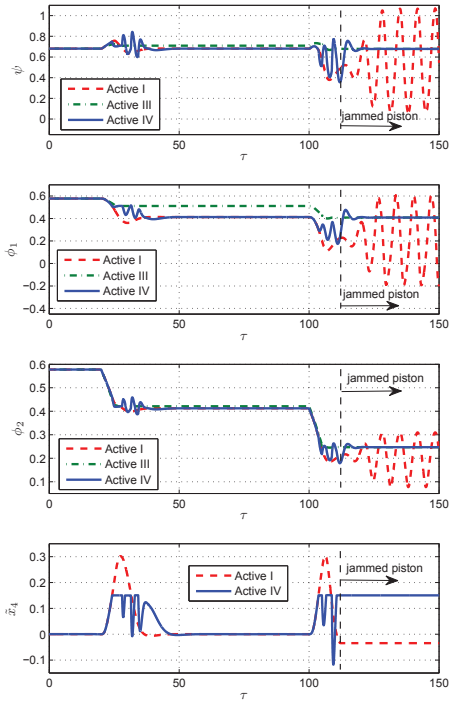

Fig. 7. Compressor states and piston stroke in a condition where the pistons of Active I and Active IV are jammed at $\tau = 112$.

trol, 3) stability analysis of the switching between the two mode, and 4) experimental test in a laboratory scale.

REFERENCES

Arnulfi, G.L., Giannattasio, P., Micheli, D., and Pinamonti, P. (2001). An innovative device for passive control of surge in industrial compression system. *J. Turbomachinery*, 123, 473–782.

Bøhagen, B. and Gravdahl, J.T. (2008). Active surge control of compression system using drive torque. *Automatica*, 44, 1135–1140.

Epstein, A.H., Williams, J.E.F., and Greitzer, E.M. (1989). Active suppression of aerodynamics instability in turbo machines. *J. Propulsion and Power*, 5, 204–211.

Fontaine, D., Liao, S., Panduano, J., and Kokotovic, P. (1999). Linear vs. nonlinear control of an axial flow compressor. In *Proc. of Conf. on Control and Application*, 921–926.

Gravdahl, J.T. and Egeland, O. (1997). Compressor surge control using a close-coupled valve and backsteeping. In *Proc. of the American Control Conference*.

Gravdahl, J.T. and Egeland, O. (1999). *Compressor surge and rotating stall: Model and control*. Springer Verlag, London.

Greitzer, E.M. (1976). Surge and rotating stall in axial flow compressor, part I: Theoritical compression system model. *J. Engineering for Power*, 98.

Moore, F.K. and Greitzer, E.M. (1986). A theory of post stall transients in an axial compressors system: Part I-Development of equation. *J. Engineering for Gas Turbine and Power*, 108, 68–76.

Uddin, N. and Gravdahl, J.T. (2011a). Active compressor surge control using piston actuation. In *Proc. of the ASME Dynamics System and Control Conference*.

Uddin, N. and Gravdahl, J.T. (2011b). Piston-actuated active surge control of centrifugal compressor including integral action. In *Proc. of the 11th Int. Conference on Control Automation and System*, 991–996.

Willems, F. and de Jager, B. (1998). Active compressor surge control using a one-side controlled bleed/recycle valve. In *Proc. of the 37th IEEE Conf. on Decission and Control*, 2546–2551.

Willems, F. and de Jager, B. (1999). Modeling and control of compressor flow instabilities. *Control System Magazine*, 19, 8–18.

Willems, F., Heemels, W.P.M.H., de Jager, B., and Stoorvogel, A.A. (2002). Positive feedback stabilization of centrifugal compressor surge. *Automatica*, 38, 311–318.

Williams, J.E.F. and Huang, X.Y. (1989). Active stabilization for compressor surge. *J. Fluid Mech.*, 204, 245–262.

Paper D Bond Graph Modeling of Centrifugal Compression Systems.

Published in the *Simulation: Transactions of the Society for Modeling and Simulation International 2015, Vol. 91(11) 998–1013*
The paper is an extension work of Uddin and Gravdahl (2012b), which was presented in International Conference on Bond Graph Modeling (ICBGM), Genoa, Italy, 2012.

Simulation

Applications

Simulation: Transactions of the Society for Modeling and Simulation International
2015, Vol. 91(11) 998–1013

DOI: 10.1177/0037549715612124
sim.sagepub.com
SAGE SCS

Bond graph modeling of centrifugal compression systems

Nur Uddin and Jan Tommy Gravdahl

Abstract

A novel approach to model unsteady fluid dynamics in a compressor network by using a bond graph is presented. The model is intended in particular for compressor control system development. First, we develop a bond graph model of a single compression system. Bond graph modeling offers a different perspective to previous work by modeling the compression system based on energy flow instead of fluid dynamics. Analyzing the bond graph model explains the energy flow during compressor surge. Two principal solutions for compressor surge problem are identified: upstream energy injection and downstream energy dissipation. Both principal solutions are verified in bond graph modelings of single compression system equipped with a surge avoidance system (SAS) and single compression system equipped with an active control system. Moreover, the bond graph model of single compressor equipped with SAS is able to show the effect of recycling flow to the compressor upstream states which improves the current available model. The bond graph model of a single compression system is then used as the base model and combined to build compressor network models. Two compressor networks are modeled: serial compressors and parallel compressors. Simulation results show the surge conditions in both compressor networks.

Keywords

bond graph, compressor modeling, compressor surge, surge avoidance system, active surge control system, serial compressors, parallel compressors

1. Introduction

A centrifugal compressor is basically used to increase gas pressures. The compressor operating area is described by a plot of the compressor pressure against the flow for different compressor speeds known as a compressor map. Figure 1 shows an example of a compressor map. The stable compressor operating area is limited by a surge line (SL) for lower flow. Operating the compressor at a flow lower than the SL would cause the compressor to go into an unstable condition known as surge. It is an axisymmetric oscillation of the compressor flow and the compressor-produced pressure followed by severe vibrations. The vibrations may reduce the reliability of the compression system and large-amplitude vibrations may lead to compressor damage in particular to the compressor blades and bearings, and also damage to pipe connections.

Surge phenomena are of interest as higher compressor efficiency operating points are located near the SL and some processes require low mass flow at high pressure. However, operating in such points may endanger the compressor because a disturbance could bring the compressor into the surge area. There is a trade-off between operating the compressor at a higher efficiency and the stability. Two methods have been developed to overcome the surge problem, as follows:

(a) *Surge avoidance system* (SAS). SAS works by introducing a surge control line (SCL) located at a certain margin to the right of the SL as illustrated in Figure 1. The margin is known as the surge margin (SM). The SAS has a recycle line and a recycle valve. The recycle valve is controlled by a controller which compares the compressor inlet mass flow to a reference mass flow. The reference mass flow is the mass flow at the SCL for a related compressor speed. The recycle valve will open

Department of Engineering Cybernetics, Norwegian University of Science and Technology, Norway

Corresponding author:
Nur Uddin, Department of Engineering Cybernetics, Norwegian University of Science and Technology, O.S. Bragstads plass 2D, Trondheim N-7491, Norway.
Email: nur.uddin@itk.ntnu.no

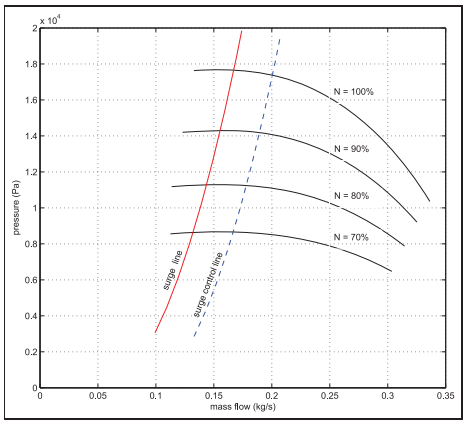

Figure 1. A typical compressor map for different rotational speeds, *N*.

when the inlet flow is less than the reference mass flow. It results in recycling flow from the downstream line to the upstream line and increasing the compressor inlet flow to be the same as the reference mass flow. This mechanism makes the SCL be the lower limit for the compressor flow and the compressor operation will not reach the SL. Such surge avoidance schemes successfully ensure the safe operation and are widely used for industrial compressors. However, introducing the SCL reduces the usable size of the compressor map and thereby restricting the compressor operational envelope.

(b) *Active surge control system* (ASCS). ASCS works by stabilizing surge. It was initialized by Epstein et al.[1] who introduced surge stabilization by using an active element. This method could enlarge the operating envelope towards the lower mass flow in the stabilized area. Since then a number of theoretical and experimental results on active surge control systems have been published and several different actuators have been introduced as summarized by Willems and de Jager,[2] examples include: closed couple valve, bleed valve, throttle valve, gas injection, variable plenum, and variable guide vanes. Active surge control by using variable speed drives,[3] piston actuation,[4] and active magnetic bearing[5] have also been reported. Although ASCS enlarges the operating envelope which can improve the compressor performance, it has not yet been applied in an industrial system. The safety of implementing ASCS is a serious issue, since a failure in ASCS may bring the compressor into the surge.[6]

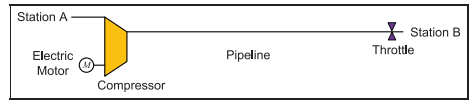

Figure 2. A pipeline system with a single compressor.

A natural gas pipeline system is an example of an industrial compressor application. Several compressors are commonly operated simultaneously in such a system. The compressors can be arranged in serial, parallel, or serial–parallel. Serial compressors are used to gain higher pressure and parallel compressors to gain higher flow. It has been reported that the compressors operation consumes a significant portion of the transmitted gas in the pipeline system. Optimizing the compressors operation is a solution that minimizes the operating cost. Mathematical models of compressors in pipeline networks are required for the design and optimization of the network. Several works on compressors network modeling have been presented.[7,8,9,10,11,12,13,14] The modelings were focused on stable operating area and assumed the compressors would not enter surge as the compressors are equipped with SAS. However, it is still possible that the compressors in the network could enter surge, for an example due to the SAS failure. It is of interest to further investigate surge in such a compressor network. A model of compressors in a network which can simulate surge is required for this purpose, and to the best of our knowledge such a model cannot be found in the existing literature.

A model of a single compression system which is able to predict the transient response of a compression system subsequent to a perturbation from steady operating conditions has been introduced by Greitzer.[15] The model is then known as the Greitzer compression model. The Greitzer model was developed based on fluid dynamics laws. Another modeling of the compression system by using a bond graph has also been presented by Uddin and Gravdahl.[16] Both modelings resulted in the same system dynamics which can be used to predict the transient response including a surge condition. A bond graph is a modeling method based on energy flow which is universal and systematic.[17,18] The universality provides the same description in modeling a system with various energy domains. A bond graph is systematic such that several simple models can be combined to build a complex model and the dynamic equations of the system is obtained in a straightforward manner by investigating energy flow in the storage elements. Therefore, the bond graph model of a single compression system can be extended to model more compression systems, for example, compressor networks as presented in this paper. The modeling of compressor networks will be done by combining the bond

graph models of single compressor systems. The discussion is limited to incompressible flow and constant compressor speed. This paper is an extension of the work of Uddin and Gravdahl[16] by presenting a more detailed description of bond graph modelings of the compression system and compressor networks.

2. Single compression system

A simple diagram of a gas pipeline with a single compressor is shown in Figure 2. The electric motor rotates the compressor blades such that the gas at station A is pulled into the compressor through an inlet. The gas is then accelerated towards the compressor impeller, de-accelerated at the compressor diffuser, and collected in the compressor volute before being discharged. Such processes result in a gas pressure rise. The gas is then discharged and directed to the station B through the pipeline. A throttle is installed before the pipeline outlet to adjust the flow arriving at station B. A model of such a compressor system which is able to predict the transient response subsequent to a perturbation from steady operating condition was introduced by Greitzer in 1976.[15] The model is known as the Greitzer compressor model. The Greitzer model was developed based on fluid dynamics laws (momentum equation and mass conservation) and used the following assumptions: quasi-steady compressor behavior, uniform pressure throughout the plenum, isentropic fluid behavior in the plenum, incompressible flow in the duct, negligible throttle inertance, quasi-steady flow through the throttle, and constant ambient conditions.

Following the Greitzer model, the pipeline compression system in Figure 2 is modeled as in Figure 3. The model is identical to the Greitzer model except the addition of a motor drive which generates torque τ to rotate the compressor with rotational speed ω, which is also covered by Fink et al.[19] and Gravdahl and Egeland.[20] Furthermore, by neglecting friction flow along the pipeline, the inlet pressure (p_i) is equivalent to the pressure at station A (p_A), the inlet mass flow (w_i) is equivalent to the discharged mass flow (w_d), and the outlet pressure (p_o) is equivalent to the pressure at station B (p_B). The space inside downstream pipeline is modeled as a plenum with volume V_p and pressure p_p. It is assumed that the mass flow through the plenum is steady and the pressure is uniform, that there is no pressure drop. A throttle is applied to adjust the outlet flow (w_o) and thereby generating throttle pressure drop (p_{R_T}) between the plenum and the outlet. The dynamic equations of the Greitzer compression system is given as follows:[15]

$$\dot{w}_i = \frac{A_c}{L_c}(p_c - p_p) \tag{1}$$

$$\dot{p}_p = \frac{a_0^2}{V_p}(w_i - w_o) \tag{2}$$

where A_c is the compressor duct cross-sectional area, L_c is the effective length of the equivalent compressor duct, p_c is the compressor pressure rise, and a_0 is the speed of sound. The compressor pressure rise is typically presented in a compressor map as a function of mass flow and compressor speed which is commonly provided by the compressor manufacturer. A compressor map can also be generated by performing a compressor test to collect several compressor operating data (e.g. pressure, mass flow and speed) and approximated by one of two following mathematical functions:

(a) Compressor pressure rise approximation for a constant compressor speed:[21]

$$p_c(w_i) = p_{c_0} + H\left[1 + \frac{3}{2}\left(\frac{w_i}{W} - 1\right) - \frac{1}{2}\left(\frac{w_i}{W} - 1\right)^3\right] \tag{3}$$

where p_{c_0} is the shut-off value of the axisymmetric characteristic, W is the semi-width of the cubic axisymmetric compressor characteristic, and H is the semi-height of the cubic axisymmetric compressor characteristic; consult Moore and Greitzer[21] for more detailed definitions.

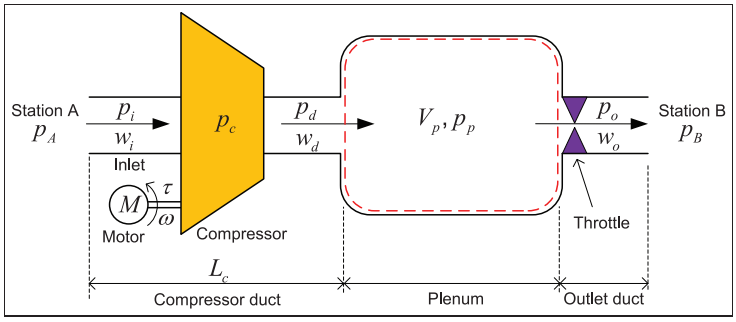

Figure 3. Model of a single compression system.

Table 1. Effort and flow of various system domains.

Energy domain	Effort (e)	Flow (f)
Translational mechanics	Force F [N]	Velocity v [m/s]
Rotational mechanics	Torque τ [Nm]	Angular velocity ω [rad/s]
Electrical	Voltage E [V]	Current i [A]
Hydraulics	Total pressure p [N/m^2]	Volume flow q [m^3/s]
Pneumatics	Total pressure p [N/m^2]	Volume flow q [m^3/s]
Thermodynamics	Temperature T [K]	Entropy flow S [J/(Ks)]

(b) Compressor pressure rise approximation for varying compressor speed:[3]

$$p_c(\omega, w_i) = \left(1 + \frac{\mu d_2^2\omega^2 - 0.5d_1^2(\omega - \alpha w_i)^2 - 4k_f w_i^2}{4c_p T_{01}}\right)^{\frac{\kappa}{\kappa-1}} \quad (4)$$

where ω is the compressor speed, d_1 is the mean inducer diameter, d_2 is the impeller diameter, k_f is the fluid friction constant, T_{01} is the inlet stagnation temperature, c_p is the specific heat at constant pressure, c_v is the specific heat at constant volume, and $\kappa = \frac{c_p}{c_v}$ is the ratio of specific heat. Consult Gravdahl et al.[3] for more detailed definitions of μ and α.

The outlet mass flow is given by

$$w_o = u_T k_T \sqrt{p_p - p_o} \quad (5)$$

where u_T is the throttle opening with the range value from 0 to 100% and k_T is the throttle constant.

3. Bond graph modeling

Bond graph is a modeling method based on energy transfer among the components in a system. The energy is transferred through the components port. The energy transfer is shown as a line with a half arrow which is called a bond. The half arrow is showing the energy transfer direction. A bond has two variables: effort (e) and flow (f) to describe energy. Table 1 shows the definitions of effort and flow of various energy domains. Multiplication of effort and flow results in power P,

$$P = ef \quad (6)$$

It is common to place an effort variable above or on the left of a bond and a flow variable below or on the right of a bond. The direction of effort is shown by a perpendicular bar at the tip of a bond which known as the causality. The flow direction is always opposite to the effort direction.

Bond graph modeling defines components in a system as: effort source (S_e), flow source (S_f), resistance (R), inertia (I), capacitor (C), transformer (TF), and gyrator (GY). Source effort is a component which supplies effort. Source flow is a component which supplies flow. Resistance is a component which dissipates energy. Inertia is a storage element which integrates the effort. Capacitor is a storage element which integrates the flow. A transformer is a component which converts effort at one port into effort at another port with the transformer ratio n and separately converts the flow in the opposite direction with the same transformer ratio. A gyrator is a component which relates the effort of one port to the flow of another port with the gyrator ratio r, and vice versa. If the conversion ratio depends on another variable, the transformer is called a modulated transformer (MTF) and the gyrator is called a modulated gyrator (MGY).

A bond graph component is connected by a bond to another component or junction. A junction is a connecting point and the energy is neither stored nor dissipated. There are two types of junctions:

(a) 0-junction, which connects bonds with equal effort and the total flow is zero

$$f_1 + f_2 + \cdots + f_n = 0 \quad (7)$$

$$e_1 = e_2 = \cdots = e_n \quad (8)$$

(b) 1-junction, which connects bonds with equal flow, and the total effort is zero

$$f_1 = f_2 = \cdots = f_n \quad (9)$$

$$e_1 + e_2 + \cdots + e_n = 0 \quad (10)$$

Dynamic equations of a bond graph model are obtained by an effort–flow relation of the storage energy elements (C and I). A more detailed description of bond graphs can be found in the bond graph literature.[22,17,18]

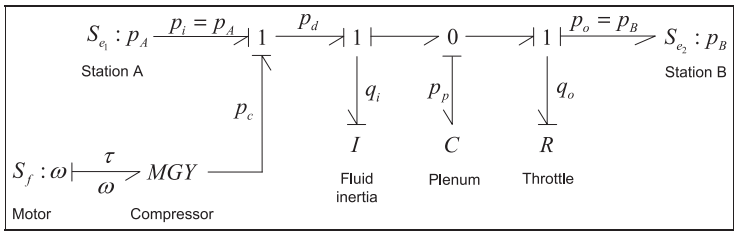

Figure 4. Bond graph model of the single compression system.

4. Bond graph model of a single compression system

The single compression system shown in Figure 2 includes several physical domains. The transmitted gas is in the pneumatic domain, the electric motor transfers energy from the electrical domain into the mechanical domain, the compressor transfers energy from the mechanical domain into the pneumatic domain, and the valve dissipates the pneumatics energy into heat. There are energy transfer from the pneumatic energy into heat due to friction flow along the pipeline and the mechanical energy into heat due to friction in the rotating parts of the compressor. Taking all of the domains into account in the system makes the system modeling extremely complicated. Limiting the modeling scope of the compression system by using several assumptions is necessary as in the Greitzer model. By considering only the pneumatics domain and the mechanical domain of the motor drive, using the same assumptions as in the Greitzer model, and assuming that friction on the piping is insignificant, the components in the single compression system shown in Figure 3 are modeled as follows.

(i) Stations A and B are modeled as effort source elements S_{e_1} and S_{e_2} as both are providing pressure p_A and p_B, respectively.

(ii) The electric motor provides angular velocity to the compressor and is modeled by a flow source element S_f.

(iii) The compressor converts the angular velocity into fluid pressure is a kind of gyrator. Since the produced pressure is also dependent on the mass flow, the compressor is defined as a modulated gyrator MGY. The gyrator ratio is given the compressor pressure rise which can be approximated by (3) for a constant compressor speed and (4) for varying compressor speed. This study is only considering compressors at a constant compressor speed.

(iv) The fluid inertia along the compressor duct is modeled by an inertia element (I).

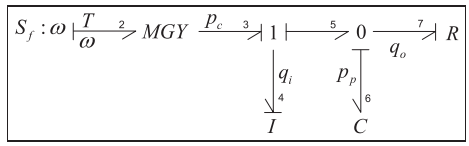

Figure 5. Simplified bond graph model of the single compression system.

(v) The pipeline volume or plenum provides a capacitance effect and is modeled by a capacitor element (C).

(vi) The throttle produces flow resistance and is modeled by a resistor element (R). Flow resistance due to friction in the pipeline is assumed to be extremely small compared with the throttle resistance and is neglected. Then the effort and flow relation in the throttle is given in (5).

Following the bond graph procedures,[18,17] the bond graph model of a single compression system is given in Figure 4.

By assuming that pressures at station A and B are equivalent to the ambient pressure and the pressures in the system are measured relative to the ambient pressure, the compressor pressure discharge is equal to the compressor pressure rise ($p_d = p_c$). Therefore, the bond graph model can be simplified as shown in Figure 5. The bonds in the model are identified by index numbers started by number two. Table 2 shows the effort and flow of each bond in the model.

The compressor dynamics are obtained by the effort–flow relation at storage energy elements (C and I) connected by bonds number 4 and 6, respectively, and given as follows:

$$I\frac{df_4}{dt} = e_3 - e_5 \tag{11}$$

$$\dot{q}_i = \frac{1}{I}(p_c - p_p) \tag{12}$$

Table 2. Effort and flow of the compressor model.

Bond	Effort	Flow	Note
2	$e_2 = \tau$	$f_2 = \omega$	—
3	$e_3 = p_c$	$f_3 = q_i$	—
4	$e_4 = e_3 - e_5$	$f_4 = q_i$	Inertia: $e_4 = I\frac{df_4}{dt}$
5	$e_5 = p_p$	$f_5 = q_i$	-
6	$e_6 = p_p$	$f_6 = f_5 - f_7$	Capacitor: $f_6 = C\frac{de_6}{dt}$
7	$e_7 = p_p$	$f_7 = q_o$	Resistor: $f_7 = \frac{1}{R}e_7$

$$C\frac{de_6}{dt} = f_5 - f_7 \tag{13}$$

$$\dot{p}_p = \frac{1}{C}(q_i - q_o) \tag{14}$$

The relation of mass flow and volume flow is given by

$$w = \rho q \tag{15}$$

where ρ is the fluid density. Since the flow is assumed as incompressible flow, the fluid density is constant and Equations (12) and (14) can be expressed in mass flow as

$$\dot{w}_i = \frac{\rho}{I}(p_c - p_p) \tag{16}$$

$$\dot{p}_p = \frac{1}{\rho C}(w_i - w_o) \tag{17}$$

By defining $I = \frac{\rho L_c}{A_c}$ and $C = \frac{V_p}{\rho a_0^2}$, Equations (16) and (17) are equivalent to (1) and (2), respectively.

5. Energy analysis of compressor surge

Compressor surge is defined as a condition at which the pressure developed by the compressor is less than the pressure in the system (downstream).[23] It occurs due to inability of the impeller to produce the amount of required energy for the process system.[24] It results in an axisymmetric oscillation of mass flow and pressure as shown by a limit cycle. The chronology of surge is explained as follows (refer to Figure 6).[25]

(1) A compressor initially operates at steady state at operating point A located in the stable area, though near the surge line (SL). This operation results in the plenum pressure being the same as the discharge pressure. Due to a disturbance, for example, by reducing the throttle opening for a certain value such that the compressor mass flow is reduced, the operating point is moving to B located to the left of the SL.

(2) At point B, the compressor discharge pressure is a bit lower than the plenum pressure, which makes the mass flow decelerate as formulated in (16), and the compressor produces less pressure discharge according to the compressor characteristic curve. The mass flow continues to decelerate to zero.

(3) The mass flow deceleration continues to negative flow (reverse flow). The compressor acts like an orifice in the reverse flow. The stored energy in the plenum accelerates the reverse flow until it reaches the maximum reversal flow which is at point C.

(4) After reaching point C, the plenum pressure is rapidly decreasing and the reverse flow is decelerated to zero at point D.

(5) At point D, the compressor begins to the normal operation by accelerating the flow until point E.

(6) The mass flow is then reduced to build plenum pressure. However, the compressor operation from point E is going to point A and then to point B such that the cycle repeats.

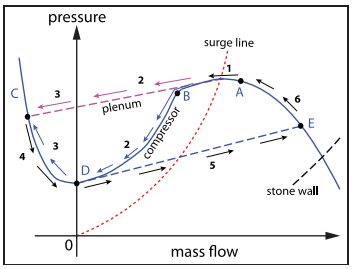

Figure 6. Compressor surge cycle.

Surge occurs due to the compressor pressure discharge (p_c) being less than the plenum pressure (p_p) which results in decelerating the inlet mass flow such that the operating point crosses the SL. The bond graph model shown in Figure 5 expresses p_c as e_3 at bond 3 and p_p as e_5 at bond 5, respectively. Both the bonds are connected together with bond 4 by a 1-junction and the equations are given as follows:

$$e_4 = I\dot{f}_4 = e_3 - e_5 \tag{18}$$

$$f_3 = f_4 = f_5 \tag{19}$$

where f_4 is the inlet volume flow. Surge occurs when $e_3 < e_5$ or e_4 is negative. It can be eliminated by maintaining e_4 non-negative through the following methods.

(a) *Increasing* e_3. Effort e_3 is the effort output of the gyrator (compressor) where the input–output relation is given by

$$e_3 = rf_2 \tag{20}$$

where r is the gyrator ratio. Effort e_3 (compressor pressure rise) can be increased by increasing f_2

(motor speed). It is illustrated in Figure 1 and shown by Gravdahl et al.[3] that the compressor produces a higher pressure at higher motor speeds for the same mass flow.

(b) *Decreasing* e_5. Effort e_5 comes from the 0-junction. Based on the junction properties, the connected bonds have the same effort ($e_5 = e_6 = e_7$) and only one bond has an effort inward to the junction, i.e. the bond of the C element (e_6). The relation between effort and flow in the C element is given by

$$e_6 = \frac{1}{C}\int f_6 dt + e_6(0) \tag{21}$$

where the flows equation in the 0-junction is given by

$$f_6 = f_5 - f_7 \tag{22}$$

The effort e_6 can be reduced by making f_6 negative, which can be done by increasing f_7. Reducing f_5 may also result in f_6 becoming negative. However, this is not physically possible because f_5 is the compressor mass flow (w_1) and reducing the mass flow will bring the compressor into surge. Flow f_7 is the flow of the R element (throttle), where the relation between flow and effort is given by

$$f_7 = \frac{1}{R}e_7 \tag{23}$$

Flow f_7 can be increased by reducing the R value which means increasing the throttle opening.

The direct methods to eliminate surge are by increasing the compressor speed and/or the throttle opening. However, those options are not always applicable, for example if surge occurs when shutting down the compressor, where the motor speed and the mass flow should decrease. We introduce terms of upstream energy injection for increasing e_3 and downstream energy dissipation for reducing e_5 as the two principals for solving the compressor surge. Both principal solutions will be evaluated through a discussion about compressor surge control in the next section.

6. Surge control solutions

Two methods to overcome compressor surge have been presented, i.e. the surge avoidance system (SAS) and the active surge control system (ASCS). We are going to use a bond graph to model the systems implementing both methods. The models will show explicitly how to maintain $e_4 > 0$ in a practical system or in an experimental setup.

6.1. Surge avoidance system

A SAS is commonly used as surge solution in industrial compressors. SAS introduces a surge control line (SCL) located at a certain margin to the right of the surge line (SL). The distance between SCL and SL is called the surge margin (SM) and is defined as[26]

$$SM = \frac{w_{SCL} - w_{SL}}{w_{SCL}} \tag{24}$$

where w_{SL} is mass flow at the SL and w_{SCL} is mass flow at the SCL for corresponding compressor speed. SAS has a recycle line and a recycle valve. The recycle valve is controlled by a controller which compares the compressor mass flow to a reference mass flow (w_{SCL}). When the compressor operating point is crossing the SCL ($w_i < w_{SCL}$), the SAS controller gives a command to the recycle valve to open such that the plenum fluid is flowing back to the compressor inlet through the recycle line. The recycling flow reduces the plenum pressure and the compressor mass flow is accelerated such that the operating point goes to the SCL ($w_i = w_{SCL}$).

The recycling flow (w_r) is giving an additional fluid flow to the upstream such that the inlet states will be affected. The effect is investigated by considering a capacitance effect in the space around the connection of the feeding line, the recycle line, and the inlet line. The space is then called a buffer, as shown in Figure 7.

A bond graph is applied to model the compression system equipped with a SAS as shown in Figure 7. The same assumptions as in modeling the single compression system are applied. By following the bond graph procedures, in particular on causality, we have to take into account the inertia effect in the feeding line (I_f) due to the recycling flow; otherwise, we cannot get a proper causality at the 0-junction connecting the buffer (C_b). The fluid inertia along the compressor duct is modeled by I_c, the capacitance effect in the plenum is modeled by C_p, the throttle is modeled by R_T and the recycle valve is modeled by R_r.

The resulting bond graph model is shown in Figure 8. The model shows that the recycle line is decreasing the downstream (plenum) energy and increasing the upstream (inlet) energy. The dynamic equations of the model are obtained by evaluating the effort–flow relation at the storage elements (I_f, C_b, I_c, and C_p) and given as follows:

$$\dot{w}_f = -\frac{1}{I_f}p_b \tag{25}$$

$$\dot{p}_b = \frac{1}{C_b}\left[w_f + w_r - w_i\right] \tag{26}$$

$$\dot{w}_i = \frac{1}{I_c}\left[p_b + p_c - p_p\right] \tag{27}$$

$$\dot{p}_p = \frac{1}{C_p}\left[w_i - w_o - w_r\right] \tag{28}$$

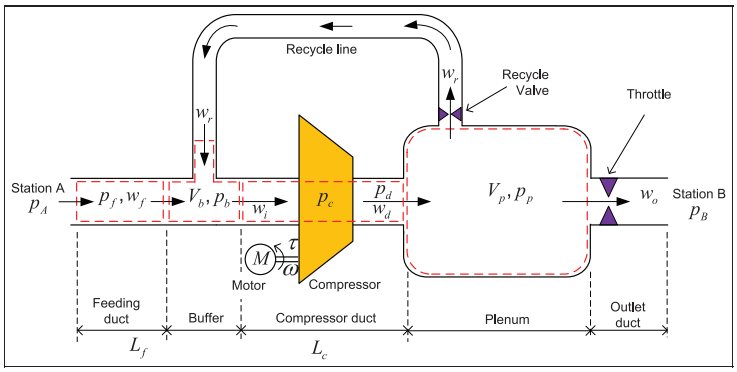

Figure 7. A compression system equipped with a surge avoidance system (SAS).

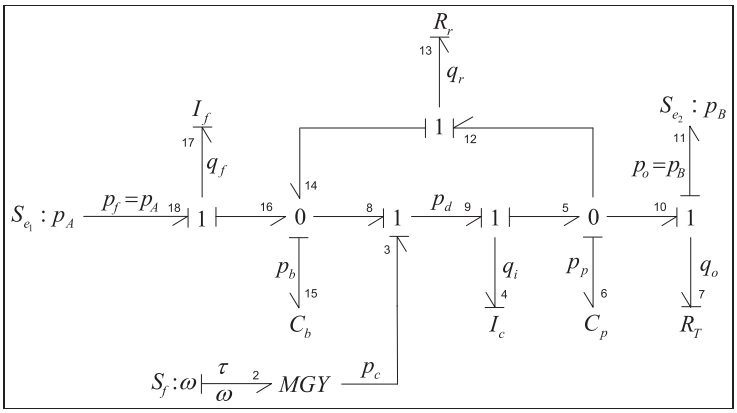

Figure 8. Bond graph model of the compression system equipped with a SAS.

where $I_f = \frac{\rho L_f}{A_f}$, $C_b = \frac{V_b}{\rho a_0^2}$, $I_c = \frac{\rho L_c}{A_c}$, and $C_p = \frac{V_p}{\rho a_0^2}$. Here V_b denotes the volume of the buffer, L_f denotes the length of the feeding duct, and A_f denotes the cross-sectional area of the feeding duct. Equations (25) and (26) show the effects of recycling flow to the compressor inlet states which improves the model presented by Gravdahl and Egeland[25] by showing the effect of the recycling flow to the feeding flow.

A recycle valve is similar to a throttle; however, it usually has a faster actuation than the throttle. The recycled mass flow is defined by

$$w_r = k_r u_r \sqrt{(p_p - p_b)} \tag{29}$$

where k_r is the recycle-valve constant and u_r is the valve opening control signal with the range value of 0 to 100%. The recycle valve is controlled by a controller which compares the inlet mass flow to the reference mass flow (w_{SCL}) to compute u_r. We demonstrate a PI (proportional and integral) controller for the SAS as follows:

$$u_r = K_p w_e + K_i \int w_e \, dt \tag{30}$$

where K_p is the proportional gain, K_i is the integrator gain, and w_e is the error mass flow. The error mass flow is defined by

$$w_e = w_{SCL} - w_i \tag{31}$$

Table 3. Simulation parameters.

Parameter	Value	Unit	Parameter	Value	Unit
U	68	m/s	a_0	340	m/s
V_b	0.009	m^3	V_p	0.9	m^3
L_f	0.41	m	L_c	0.41	m
$A_c = A_f$	0.0038	m^2	ρ	1.2041	kg/m^3
p_{c_0}	16646	Pa	W	0.0775	kg/s
H	500	Pa	$k_T = k_r$	0.75	$Pa^{-0.5}kg/s$
k_{T_S}	0.6	$Pa^{-0.5}kg/s$	k_{T_p}	1.5	$Pa^{-0.5}kg/s$
w_{SL}	0.155	kg/s	w_{SCL}	0.2	kg/s

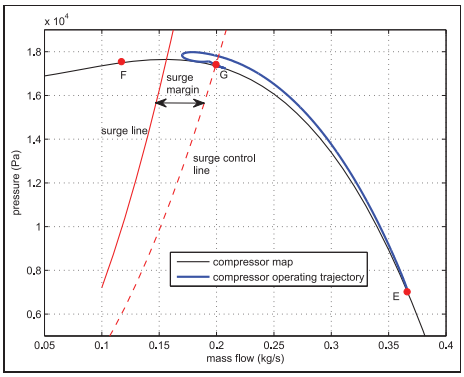

Figure 9. Trajectory of the compression system equipped with a SAS when the compressor should be entering surge.

An example simulation of a compression system equipped with a SAS using the parameters in Table 3 and the control gain $K_p = 5$ and $K_i = 10$ is given as follows.

A compressor is initially operating at steady state at point E where the throttle is fully open ($u_T = 100\%$) as shown in Figure 9. The throttle opening is then reduced to $u_T = 20\%$ at $t = 40$ s such that the compressor should operate at point F located to the left of the SCL, which is in the surge area. The operating point is moving from E to the left and crossing the SCL such that the SAS controller detects $w_i < w_{SCL}$ and gives a command to the recycle valve to open. Figure 9 shows the mass flow and pressure trajectories of the simulation and Figure 10 shows the system time responses. The plenum fluid is recycled to the inlet ($w_r > 0$) such that compressor mass flow stays at the SCL ($w_{SCL} = 0.2$ kg/s). The pressure fluctuation in the buffer (p_b) shows the effect of the recycling flow to the inlet states. The magnitude of the buffer pressure fluctuation is dependent on the pipe size and the recycled mass flow. The steady-state value of the feeding flow (w_f) is the mass flow at point F.

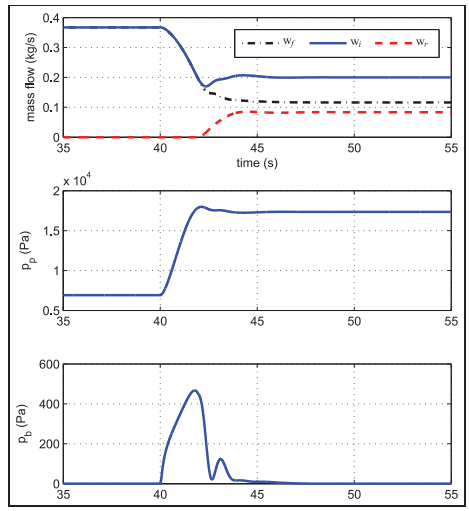

Figure 10. The time responses of a compression system when the SAS is preventing the compressor from entering surge.

6.2. Active surge control system

An ASCS works to stabilize compressor surge such that the compressor can operate in the stabilized surge area. This enlarges the compressor operating envelope to the lower mass flow. The ASCS method has been implemented experimentally by several different actuators and some of them are illustrated together in Figure 11.

As described in Section 5 for two basic solutions for compressor surge, the different actuators for ASCS can be classified as follows.

(i) *Upstream energy injection*. The examples of upstream energy injection are fluid injection,[27] close-coupled valve,[28] drive torque control,[29] and active magnetic bearing.[5] Defining a new bond

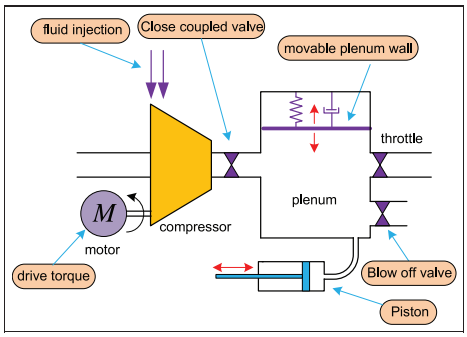

Figure 11. Several types of active elements applied in an active surge control system (ASCS).

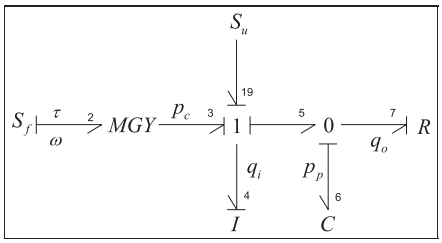

Figure 12. Bond graph model of active surge control in a class of upstream energy injection.

graph component S_u as an active component for injecting energy, the bond graph model of a compressor equipped with upstream energy injection ASCS is shown in Figure 12. The model shows that S_u gives additional effort to the 1-junction and the effort equation the junction is given by

$$e_4 = e_3 + e_{19} - e_5 \tag{32}$$

where e_{19} is an additional effort from the active element to maintain e_4 being non-negative. The examples of implementing e_{19} can be found in additional upstream pressure by fluid injection,[27] additional compressor-produced pressure by controlling the compressor speed through the drive torque control,[29] and additional compressor-produced pressure by controlling the axial clearance between the impeller and the static shroud using an active magnetic bearing.[5]

(ii) *Downstream energy dissipation*. The example of downstream energy dissipation are movable plenum wall,[30,31] piston actuation,[4] and blow-off valve.[32] A bond graph model of a compressor

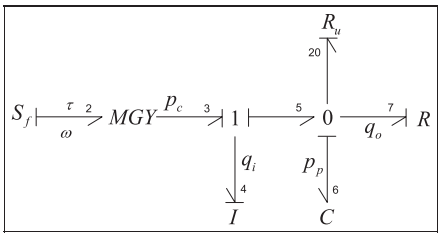

Figure 13. Bond graph model of active surge control in a class of downstream energy dissipation.

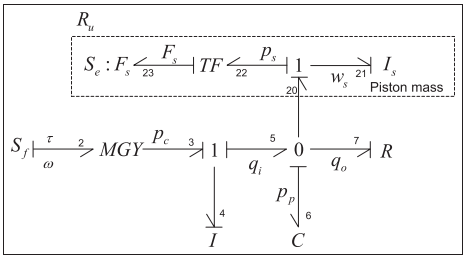

Figure 14. Bond graph model of active surge control using piston actuation.

equipped with a downstream energy dissipation ASCS is shown Figure 13, where R_u is an active component for dissipating energy. The flow equation at the 0-junction is given by

$$f_5 = f_6 + f_7 + f_{20} \tag{33}$$

$$f_6 = f_5 - f_7 - f_{20} \tag{34}$$

The active element R_u is mainly dissipating the downstream energy by creating additional flow out of the system (plenum control volume). The implementations of R_u can be found in a movable plenum wall,[30,31] piston actuation,[4] and a blow-off valve.[32]

The active elements S_u and R_u are not always single components, but they can be a subsystem consisting of several components as given by the following example of ASCS using a piston actuation. Details of the system are described by Uddin and Gravdahl.[4] The bond graph model of a compressor equipped with ASCS using piston actuation and the detailed model inside the R_u is shown in Figure 14. The active element R_u consists of a source effort S_e to generate force F_s, a transformer TF which transforms the force F_s into pressure p_s, and an inertia I_s which is the piston mass.

The ASCS using a close-coupled valve is of the type of upstream energy injection. The valve is placed between the compressor discharge and the plenum. Closing the valve

will reduce flow from the compressor discharge to the plenum and increase the upstream pressure. The bond graph model is shown in Figure 15.

7. Modeling of compressor networks

A compressor network is commonly applied in industry to satisfy a process requirement, e.g. flow and pressure. The compressor network can be serial, parallel, or serial–parallel configurations. The serial configuration is used to attain a higher pressure rise, while the parallel configuration is to gain higher mass flow, and the serial–parallel configuration is to attain both higher mass flow and higher pressure rise. This section presents bond graph modeling of the compressor networks in serial and parallel configurations. The modeling uses the same assumptions as in modeling the single compression system in the previous section.

7.1. Bond graph modeling of serial compressors

Figure 16 shows two compressors in a serial configuration. The first compressor outlet is connected to the second compressor inlet such that the fluid properties are the same. A throttle is installed at the outlet of the second compressor to adjust the flow in both compressors. Pressure drop along the pipeline is denoted as p_{R_L} and assumed to be accumulated at the outlet. Therefore, total pressure drop at the outlet denoted by p_R is an accumulation of pressure drop along the pipeline p_{R_L} and pressure drop due to a throttle p_{R_T} if available. Total pressure drop at the first outlet is solely due to the pipeline pressure drop ($p_{R_1} = p_{R_{L_1}}$) and the total pressure drop at the second outlet is due to the pipeline pressure drop and the throttle pressure drop ($p_{R_2} = p_{R_{L_2}} + p_{R_T}$). Several approximations to calculate pressure drop due to fluid friction along the pipeline can be found in Menon.[33]

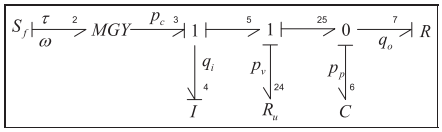

Figure 15. Bond graph model of active surge control using close-coupled valve.

In this serial connection, we assume that the first outlet states are equal to the second inlet states such that $p_{o_1} = p_{i_2}$ and $w_{o_1} = w_{i_2}$. Bond graph model of the serial compressors is shown in Figure 17.

Dynamics equations of the serial compressor networks are obtained by the effort–flow relation of the storage elements (I_1, C_1, I_2 and C_2) and given as follows:

$$\dot{w}_{i_1} = \frac{A_{c_1}}{L_{c_1}}\left(p_{i_1} + p_{c_1} - p_{p_1}\right) \tag{35}$$

$$\dot{p}_{p_1} = \frac{a_0^2}{V_{p_1}}\left(w_{i_1} - w_{i_2}\right) \tag{36}$$

$$\dot{w}_{i_2} = \frac{A_{c_2}}{L_{c_2}}\left(p_{p_1} - p_{R_1} + p_{c_2} - p_{p_2}\right) \tag{37}$$

$$\dot{p}_{p_2} = \frac{a_0^2}{V_{p_2}}\left(w_{i_2} - w_{o_2}\right) \tag{38}$$

The outlet mass flow of the second compression is defined as

$$w_{o_2} = k_{T_s} u_T \sqrt{p_{p_2} - p_{R_2} - p_{o_2}} \tag{39}$$

where k_{T_s} is the throttle constant for the serial compressors configuration. Figure 18 shows the compressor maps of a single compressor and a serial interconnection of two such identical single compressors where the pipeline pressure drop is neglected.

Serial compressors are characterized by the same mass flow through each compressor unit and the overall pressure rise is an accumulation of the pressure rise at each unit, which is twice in this case. Therefore, serial compressors are applied to produce a higher pressure rise. Serial compressors might be found in a process with a higher pressure requirement or in a long pipeline gas transportation system to compensate for the pressure drop. The surge point (the peak of compressor map) of the serial

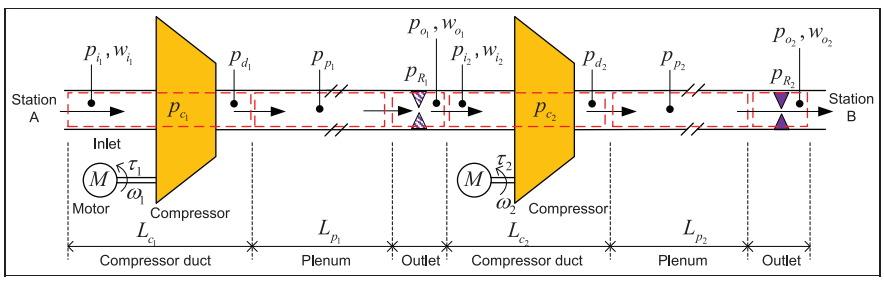

Figure 16. Two serial compressors.

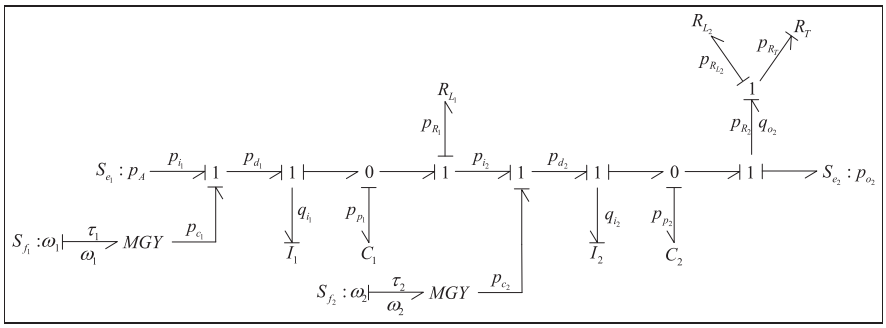

Figure 17. Bond graph model of two serial compressors.

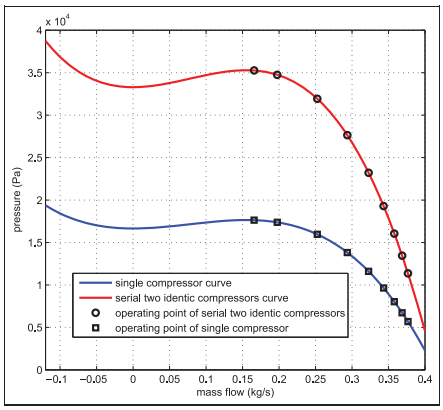

Figure 18. Compressor map of a single compressor and two identical compressors in serial configuration.

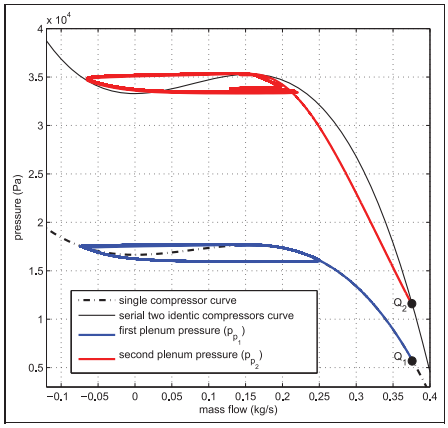

Figure 19. Serial compressor operating trajectory.

compressors is located at the same mass flow as the single compressor surge point.

The surge simulation of two identical compressors in serial configuration is now presented. The pipeline pressure drop is neglected. The first and second compressors are initially operating steadily at throttle opening $u_T = 100\%$ as the operating points are shown by Q_1 and Q_2 in Figure 19, respectively. The operation points are then changed by reducing the throttle opening to $u_T = 20\%$ at $t = 40$ s. The result is that both compressors are entering surge. Figure 19 shows the system trajectories and Figure 20 shows the time responses.

7.2. Bond graph modeling of parallel compressors

Parallel compressors are used to attain a higher total mass flow by connecting several compressor discharge lines into one line. The discharged lines should have the same pressure to avoid back flow. A model of a pipeline system with two compressors in parallel is shown in Figure 21 and the bond graph model is shown in Figure 22.

The dynamic equations of the parallel compressors are derived by evaluating the effort–flow relation of the storage elements (I_1, I_2, and C) in the bond graph model and given as follows:

$$\dot{w}_{i_1} = \frac{A_{c_1}}{L_{c_1}}\left(p_{i_1} + p_{c_1} - p_p\right) \tag{40}$$

$$\dot{w}_{i_2} = \frac{A_{c_2}}{L_{c_2}}\left(p_{i_2} + p_{c_2} - p_p\right) \tag{41}$$

$$\dot{p}_p = \frac{a_0^2}{V_p}\left(w_{i_1} + w_{i_2} - w_o\right) \tag{42}$$

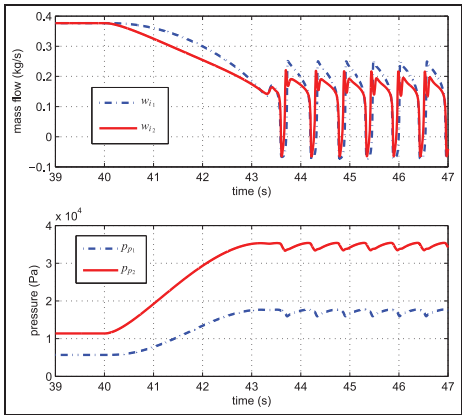

Figure 20. Mass flow and pressure of two serial compressors in surge condition.

The outlet flow is defined as

$$w_o = k_{T_p} u_T \sqrt{p_p - p_R - p_o} \tag{43}$$

where k_{T_p} is the throttle constant for the parallel compressors configuration. Figure 23 shows the compressor maps of a single compressor and the parallel configuration of the two identical single compressors where the pipeline pressure drop is neglected.

Surge simulation of two parallel identical compressors by ignoring the pipeline pressure drop is now presented. Both compressors are initially operating steadily at throttle opening $u_T = 100\%$ as the operating points are shown by P_2 for the two compressors in parallel and P_1 for each single compressor. The operation point is then changed at $t = 40$ s by reducing the throttle opening to $u_T = 20\%$. The result is that compressors are entering surge as shown by Figure 24 for the system trajectories and Figure 25 for the time responses.

8. Conclusions

Bond graph modeling of compressor networks has been presented. The Greitzer model was used as the reference such that the developed model can represent the transient response of the fluid dynamics. The modeling was started by developing a bond graph model of a single compression system. The resulted bond graph model was used as the basic model to build more complex compression system models. The bond graph model of the single compression system was analyzed to explain compressor surge. Solutions to compressor surge control were presented as upstream energy injection and downstream energy dissipation. The bond graph model of the compression system with SAS improves the current model by showing the effect of recycling flow to the feeding flow. Several actuators applied in the ASCS were classified into the upstream energy injection and the downstream energy dissipation, and modeled by using bond graph. The modelings of

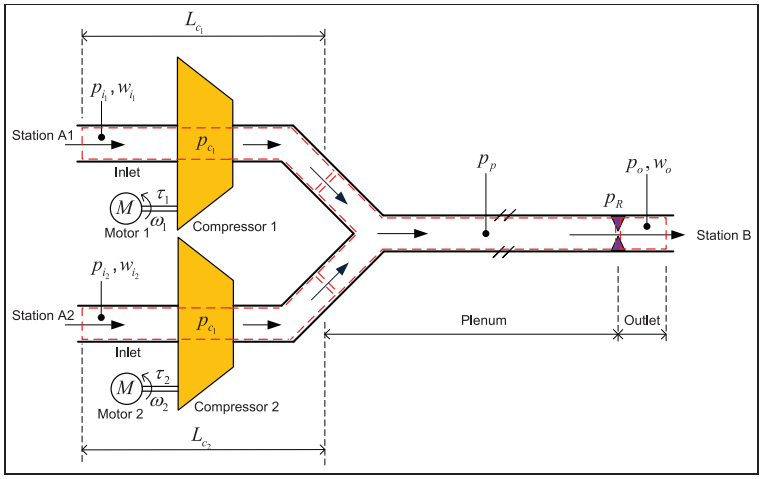

Figure 21. Two parallel compressors.

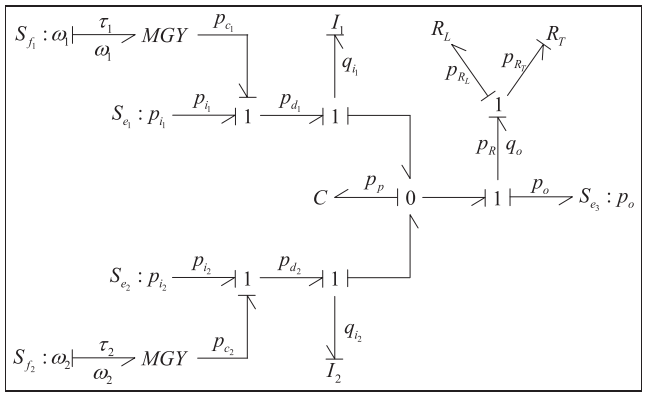

Figure 22. Bond graph model of two parallel compressors.

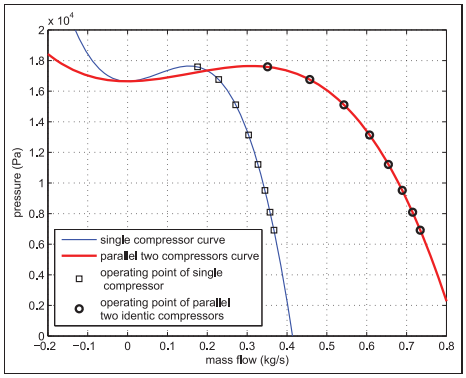

Figure 23. Compressor map parallel.

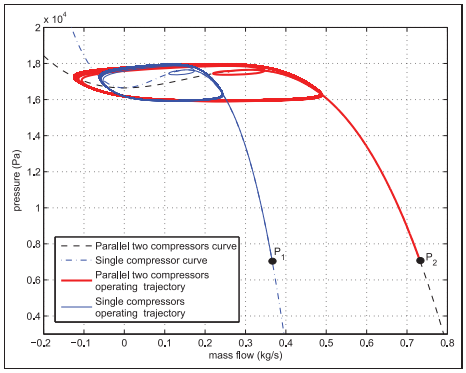

Figure 24. Operating trajectory of two identical compressors in parallel configuration during the surge condition.

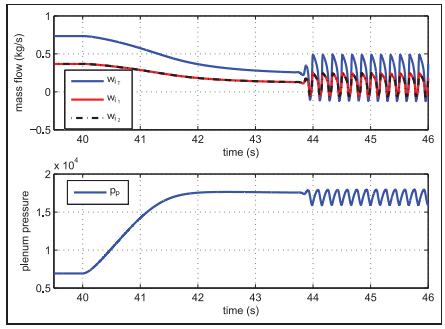

Figure 25. Mass flow and pressure of two identical compressors in parallel configuration during the surge condition.

compressor networks were demonstrated by combining two bond graph models of a single compressor. Simulations of the parallel and serial configurations during surge have illustrated the complex behavior of these systems.

9. Further work

The developed models are quite simple as the modeling was purpose designed for control system development. Experiments are necessary to validate the models. The bond graph model is open to be modified such that modeling more complex systems can be done directly based on the presented model, for example including surge control in the compressor networks.

Funding

This work was supported by Siemens Oil and Gas Solutions Offshore through the Siemens–NTNU research collaboration project.

References

1. Epstein AH, Williams JEF and Greitzer EM. Active suppression of compressor instabilities. In *Proceedings of the AIAA 10th aeroacoustic conference*, Seattle, WA, 1986, paper 86–1994.
2. Willems F and de Jager B. Modeling and control of compressor flow instabilities. *IEEE Control Syst* 1999; 19(5): 8–18. DOI:10.1109/37.793434 .
3. Gravdahl JT, Egeland O and Vatland SO. Drive torque actuation in active surge control of centrifugal compressor. *Automatica* 2002; 38: 1881–1893.
4. Uddin N and Gravdahl JT. Active compressor surge control using piston actuation. In *ASME 2011 dynamic systems and control conference and BATH/ASME symposium on fluid power and motion control*. Virginia: American Society of Mechanical Engineers, 2011, pp. 69–76.
5. Yoon SY, Lin Z and Allaire PE. *Control of Surge in Centrifugal Compressors by Active Magnetic Bearings: Theory and Implementation*. Springer Science & Business Media, 2012.
6. Uddin N and Gravdahl JT. Introducing back-up to active compressor surge control system. In *Proceedings of the 2012 IFAC workshop on automatic control in offshore oil and gas production*, 2012, pp. 263–268.
7. Botros K, Campbell P and Mah D. Dynamic simulation of compressor station operation including centrifugal compressor and gas turbine. *J Eng Gas Turbines Power* 1991; 113: 300–311.
8. Botros K. Transient phenomena in compressor stations during surge. *J Eng Gas Turbines Power* 1994; 116: 133–142.
9. Chapman K and Abbaspour M. Non-isothermal compressor station transient modeling. In *PSIG annual meeting*. Pipeline Simulation Interest Group, 2003.
10. Osiadacz AJ. Different transient models-limitations, advantages and disadvantages. In *28th PSIG annual meeting*. Pipeline Simulation Interest Group, 1996, pp. 23–25.
11. Mohitpour M, Thompson W and Asante B. The importance of dynamic simulation on the design and optimization of pipeline transmission systems. In *ASME international pipeline conference*, 1996.
12. dos Santos SP, et al. Transient analysis a must in gas pipeline design. In *PSIG annual meeting*. Pipeline Simulation Interest Group, 1997.
13. Tao W and Ti H. Transient analysis of gas pipeline network. *Chem Eng J* 1998; 69: 47–52.
14. Abbaspour M, Chapman KS and Keshavarz A. Dynamic modeling of non-isothermal gas pipeline systems. In *2004 international pipeline conference*. American Society of Mechanical Engineers, 2004, pp. 2155–2163.
15. Greitzer EM. Surge and rotating stall in axial flow compressor, part I: Theoritical compression system model. *J Eng Power* 1976; 98: 190–198.
16. Uddin N and Gravdahl JT. Bond graph modeling of centrifugal compressor system. In *Proceedings of the international conference on bond graph modeling*, Genoa, Italy, 2012.
17. Borutzky W. *Bond Graph Methodology: Development and analysis of multidisciplinary dynamic system models*. New York: Springer, 2010.
18. Karnopp D, Margolis D and Rosenberg R. *System Dynamics: A Unified Approach*. New York: John Wiley & Sons, 1990.
19. Fink D, Cumpsty N and Greitzer E. Surge dynamics in a free-spool centrifugal compressor system. *J Turbomach* 1992; 114: 321–331.
20. Gravdahl JT and Egeland O. Centrifugal compressor surge and speed control. *IEEE Trans Control Syst Technol* 1999; 7: 567–579.
21. Moore FK and Greitzer EM. A theory of post stall transients in an axial compressors system: Part I-Development of equation. *J Eng Gas Turbine Power* 1986; 108: 68–76.
22. Borutzky W. Bond graph modelling and simulation of multidisciplinary systems–an introduction. *Sim Modell Practice Theory* 2009; 17: 3–21.
23. Nisenfeld A. *Centrifugal Compressors: Principles of Operation and Control* (Monograph Series). Instrument Society of America, 1982. ISBN 9780876645642.
24. Forsthoffer WEB. *Forsthoffer's Rotating Equipment Handbooks Vol. 5: Compressors*. Amsterdam: Elsevier, 2005.
25. Gravdahl JT and Egeland O. *Compressor Surge and Rotating Stall: Model and control*. London: Springer, 1999.
26. Kurz R and White R. Surge avoidance in gas compression systems. *J Turbomach* 2004; 126: 501–506.
27. Williams JEF, Harper MFL and Allwright DJ. Active stabilization of compressor instability and surge in a working engine. *ASME J Turbomach* 1993; 115: 68–75.
28. Simon JS and Valavani L. A Lyapunov based nonlinear control scheme for stabilizing a basic compression system using a close-coupled control valve. In *Proceedings of the American control conference*, 1991, pp. 2398–2406.
29. Bøhagen B and Gravdahl JT. Active surge control of compression system using drive torque. *Automatica* 2008; 44: 1135–1140.
30. Williams JEF and Huang XY. Active stabilization for compressor surge. *J Fluid Mech* 1989; 204: 245–262.
31. Gysling D, Dugundji D, Greitzer EM, et al. Dynamic control of centrifugal compressor surge using tailored structures. *ASME J Turbomach* 1991; 113: 710–722.
32. Willems F and de Jager B. Active compressor surge control using a one-side controlled bleed/recycle valve. In *Proceedings of the 37th IEEE conference on decission and control*, 1998, pp. 2546–2551.
33. Menon ES. *Gas Pipeline Hydraulics*. Bocan Raton, FL: CRC Press, 2005.

Author biographies

Nur Uddin received the B.Sc. degree in Aerospace Engineering from Bandung Institute of Technology, Indonesia in 2002 and M.Eng. in Mechanical Engineering from Gyeongsang National University, South Korea in 2009. He is currently a Ph.D. student at the Department of Engineering Cybernetics NTNU and is researching modeling and control of turbo machinery. His research interests include modeling and control of dynamical systems.

Jan Tommy Gravdahl received the Siv.ing. and Dr.ing. degrees in engineering cybernetics from the Norwegian

University of Science and Technology (NTNU), Trondheim, Norway, in 1994 and 1998, respectively. He is currently a professor at the Department of Engineering Cybernetics, Norwegian University of Science and Technology (NTNU), Trondheim, Norway. He was a visiting professor at the Centre for Complex Dynamic Systems and Control, The University of Newcastle, Newcastle, Australia in 2007–2008. He has published more than 200 international conference and journal papers. He is the author of *Compressor Surge and Rotating Stall: Modeling and Control* (Springer, 1999), coauthor of *Modeling and Simulation for Automatic Control* (Marine Cybernetics, 2002), coeditor of *Group Coordination and Cooperative Control* (Springer, 2006), and coauthor of *Snake Robots: Modelling, Mechatronics, and Control* (Springer, 2013), coauthor of *Modeling and Control of Vehicle–Manipulator Systems* (Springer, 2013), and coauthor of *Vehicle–Manipulator Systems: Modeling for Simulation, Analysis, and Control* (Springer, 2014). His current research interests include mathematical modeling and nonlinear control in general, modeling and control of turbomachinery, control of vehicles, spacecraft, robots, and nanopositioning devices. He received the *IEEE Transactions on Control System Technology* Outstanding Paper Award in 2000.

Paper E A Compressor Surge Control System: Combination Active Surge Control and Surge Avoidance.

Published in the *Proceedings of the 13th International Symposium on Unsteady Aerodynamics, Aeroacoustics and Aeroelasticity of Turbomachines* (ISUAAAT13) in Tokyo, Japan, September 11-14, 2012.

ISUAAAT13-S5-2

A COMPRESSOR SURGE CONTROL SYSTEM: COMBINATION ACTIVE SURGE CONTROL SYSTEM AND SURGE AVOIDANCE SYSTEM

Nur Uddin *
Engineering Cybernetics
Norwegian University of Science and Technology
Trondheim, Norway 7491
Email: nur.uddin@itk.ntnu.no

Jan Tommy Gravdahl
Engineering Cybernetics
Norwegian University of Science and Technology
Trondheim, Norway 7491
Email: Jan.Tommy.Gravdahl@itk.ntnu.no

ABSTRACT

A novel method for combining active surge control system (ASCS) and surge avoidance system (SAS) for a centrifugal compressor is presented. ASCS is a promising method to improve compressor operating area by stabilizing surge. However, this method is not applied yet in industrial compressors. Safety issue is considered in implementing the ASCS. A failure in ASCS may endanger the compressor by entering deep surge as the compressor is allowed to operate in the stabilized surge area. Combination of ASCS and SAS is proposed to improve the safety by utilizing the SAS as a back-up system. SAS is a reliable method in surge control and widely applied in industrial compressors. However, the compressor operating area is reduced by applying the SAS. An ASCS by using piston actuation is used as a case study and performance evaluations of the combined system are done by simulations.

1 INTRODUCTION

Compressor operating area can be described by plotting compressor pressure rise against flow for varying compressor speed and called a compressor map. The stable compressor operating area is limited for low mass flows by the so-called surge line and for high mass flows by the stone wall or choke line. Operating the compressor at mass flows below the surge line will drive the compression system into an instability known as surge. This is an axisymmetric oscillation of mass flow and pressure rise and is followed by severe vibrations in the compression system. The vibrations may reduce the reliability of the system and large amplitude vibrations may lead to compressor damage, especially to compressor blades and bearings.

The compressor surge phenomenon can be solved by preventing the compressor operating point from entering the surge area. This solution is known as a surge avoidance system (SAS). The SAS usually works by recycling flow from downstream to upstream when the operating point reaches a surge control line (SCL). The SCL is located to the right of the surge line and becomes the minimum allowed mass flow for the compressor equipped with SAS. Such surge avoidance schemes successfully ensure safe operation, but the introduction of the SCL reduces the usable size of compressor map, thereby restricting the compressor operational envelope.

Another surge solution is to stabilize the surge phenomenon by using an active control system. This method is known as active surge control system (ASCS) and was proposed by Epstein et al. in [1]. Since then a number of theoretical and experimental results have been published. A number of different actuators and control methods have been applied, as summarized by [2]. Recent developments in this field include the work by [3] on hydraulic actuators as well as [4] on drive torque actuation.

Active surge control systems have mainly been implemented in laboratories and have not yet found wide spread use in industrial compression systems. To our best knowledge, an industrial compressor equipped with ASCS has not been reported yet and it is believed that concerns about safety is the main reason. Since ASCS works by stabilizing surge to enlarge the operating area, the enlarged area is open loop unstable such that a failure in the active system may cause the compressor to go unstable by entering surge. A back-up system can be a solution to improve the safe operating of the compressor equipped with ASCS. We have introduced blow-off surge control as the back-up of a main ASCS using piston actuation [5]. The PAASCS as the main system is working by default and the back-up system is working only if the PAASCS should fail. The changing operation from the main system to the back-up system is carried out by a switch. The result shows the back-up system was able to keep the compressor in a safe operation when the ASCS is fail. The ASCS with piston actuation or known as piston actuated active surge control system (PAASCS) was proposed in [6]. A piston is applied to absorb plenum energy during compressor surge. An improvement in control design to minimize the required piston stroke was done by including integral action as

*Address all correspondence to this author.

TABLE 1. Dimensional and non-dimensional variables

Variable	Dim.	Non-Dim.
Pressure	p	$\psi = \frac{p}{\frac{1}{2}\rho U^2}$
Compressor pressure rise	p_c	ψ_c
Throttle pressure drop	p_t	ψ_t
Mass flow	w	$\phi = \frac{w}{\rho U A_c}$
Effective duct length	L	
Sound velocity	a_0	
Duct cross section area	A	
Piston stroke	L_s	$\lambda = \frac{L_s}{L_c}$
Piston cross section area	A_s	
Mean rotor velocity	U	
Fluid density	ρ	
Volume	V	

Subscripts

f	feed line	b	buffer	s	piston
c	compressor	d	discharge	p	plenum
1	inlet	t	throttle	r	recycle line

presented in [7]. Active surge control using a blow off valve was presented in [8].

Considering the application of blow-off surge control is limited and not applicable in several industrial process, for example in natural gas, petrochemical or toxic gas, then recycling surge control (SAS) should be applied. A model of a compressor equipped by SAS including the effect of the recycling flow to the upstream states was studied in [9]. It was also presented an example of PI controller for the SAS. This paper builds on the work in [5] by combining ASCS and SAS where the SAS is used as the back-up of the ASCS to improve the safe operation of ASCS. Since the SAS is widely applied in industrial compressors, it also is proposed as a bridge to make the ASCS closer to the industrial implementation. A case study using piston actuated active surge control system and a failure due to piston saturation is presented. Stability of the switching operating of the both system is shown by the system trajectories.

This work is carried out by using non-dimensional equation. The paper consists of five sections as started by introduction in section I. Section II is describing compressor dynamics including surge phenomenon. Section III is presenting compressor surge and control. Active surge control using piston actuation and surge avoidance system are described. Section IV presents an active surge control with a back-up system by combining PAASCS and SAS.

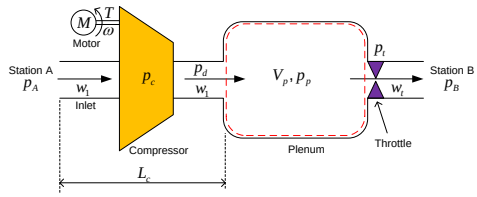

FIGURE 1. Model of basic compression system.

2 Compressor Dynamics

A model of a compression system was introduced by Greitzer in [10] and shown in Fig. 1. It is assumed that the pressure at station A and B are same at a constant value and all pressures in the system are measured relative to the pressure at the both stations. Dynamics of the compression system are given as follows:

$$\dot{w}_1 = \frac{A_c}{L_c}[p_c - p_p] \tag{1}$$

$$\dot{p}_p = \frac{a_0^2}{V_p}[w_1 - w_t] \tag{2}$$

and the non-dimensional form are:

$$\dot{\phi}_1 = B(\psi_c - \psi_p) \tag{3}$$

$$\dot{\psi}_p = \frac{1}{B}(\phi_1 - \phi_t) \tag{4}$$

where B is the Greitzer parameter defined by $B = \frac{U}{2\omega_H L_c}$ and ω_H is Helmholtz frequency defined by $\omega_H = a_0\sqrt{\frac{A_c}{V_p L_c}}$. The time derivative is done using non-dimensional time defined by $\tau = t\,\omega_H$.

The compressor pressure rise is given as a function of mass flow and compressor rotational speed $p_c(w_1, \omega)$ and usually presented in a compressor map provided by the compressor manufacturer. The function can also be obtained in experiments by performing engine test to collect data and approximated by a function. Moore and Greitzer introduced a cubic function to approximate compressor pressure rise for a constant rotational speed [11]:

$$\psi_c(\phi_1) = \psi_{c_0} + H\left[1 + \frac{3}{2}\left(\frac{\phi_1}{W} - 1\right) - \frac{1}{2}\left(\frac{\phi_1}{W} - 1\right)^3\right] \tag{5}$$

where ψ_{c_0} is the shut-off value of the axisymmetric characteristic, W is the semi-width of the cubic axisymetric compressor characteristic and H is the semi-hight of the cubic axisymetric compressor characteristic, consult [11] for more detailed definition. Non-dimensional throttle mass flow is defined by:

$$\phi_t = \gamma_t\sqrt{\psi_p} \tag{6}$$

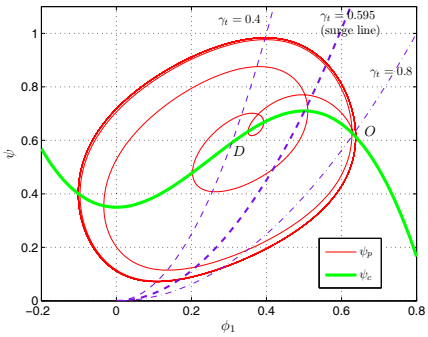

FIGURE 2. System trajectory during surge.

where γ_T is a function of the throttle setting.

3 Surge and Control

3.1 Surge

Compressor operating point is defined as an intersection between compressor characteristic curve and the load (throttle) characteristic curve. Two operating points O and D are shown in Fig. 2. The operating point O is a stable operating point as located in the right side of surge line, but the operating point D is unstable operating point (in the surge area) as located in the left side of the surge line. Figure 2 is showing the system trajectory when the compressor operating point moves from O to D by reducing the throttle setting from $\gamma_t = 0.8$ to $\gamma_t = 0.4$. Surge as defined by an axisymmetric oscillation of mass flow and pressure rise is shown by a limit cycle in that figure.

Compressor surge can be stabilized either by increasing upstream energy or decreasing downstream energy [9]. Flowing out fluid from the plenum will decrease the downstream energy such that it can be applied in surge control. Compressor dynamics including surge control by plenum flow-out is given by:

$$\dot{\phi}_1 = B(\psi_c - \psi_p) \tag{7}$$

$$\dot{\psi}_p = \frac{1}{B}(\phi_1 - \phi_t - \phi_u) \tag{8}$$

where ϕ_u is plenum flow-out as the control flow. Surge avoidance system (SAS) and piston-actuated active surge control (PAASCS) are the examples of surge control based on the plenum flow-out control. PAASCS is not only able to remove fluid from the plenum, but also to inject fluid back into the plenum such that the value of ϕ_u can be positive and/or negative.

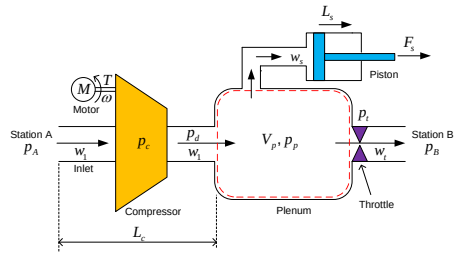

FIGURE 3. Model of compressor with PAASCS.

3.2 Piston Actuated Active Surge Control System

A model of a compression system equipped with piston for active surge control is shown in Fig. 3 and the non-dimensional dynamics equations are given as follows [6]:

$$\dot{\phi}_1 = B[\psi_c - \psi_p] \tag{9}$$

$$\dot{\psi}_p = \frac{1}{B}\left[\phi_1 - \phi_t - \frac{k_a}{2B}\dot{\lambda}\right] \tag{10}$$

$$\ddot{\lambda} = \frac{2B^2}{M_s}(k_a\psi_p + u_s). \tag{11}$$

The control flow in PAASCS is a function of the piston velocity as given by:

$$\phi_s = \frac{k_a}{2B}\dot{\lambda} \tag{12}$$

where $k_a = \frac{A_s}{A_c}$. The control force to drive the piston can be designed by using the available control methods. An example design by using linear quadratic control including integral action was presented in [7] and the control law was given as follows:

$$u_s = \tilde{u}_s - k_a\psi_{p_O} \tag{13}$$

where $\tilde{u}_s = -K_1\tilde{x}_1$ and $\tilde{x}_1$ is states deviation from operating point O given by $\tilde{x}_1 = [(\phi_1 - \phi_{1_O}), (\psi_p - \psi_{p_O}), \dot{\lambda}, \lambda, \int \lambda dt]^T$. It is assumed that the piston is idle at zero position at operating point O. A control design using the method results in $K_1 = \begin{bmatrix}5867.2 & -476.4 & 260.9 & 1328.8 & 316.2\end{bmatrix}$ and the closed loop eigenvalues at $s_{1,2} = -4.9292 \pm 5.5060i$, $s_3 = -6.7789$ and $s_{4,5} = -0.2117 \pm 0.2037i$. All eigenvalues are located in the left half plane (LHP) such that the system locally asymptotically stable.

Figure 4 shows the system trajectory of compressor equipped by PAASCS. It is shown the system is stable even though the operating point moves in the left side of surge control line. Figure 5 shows the piston displacement during the surge stabilization.

An alternative control law using feedback from plenum pressure and piston displacement only can be found in [6].

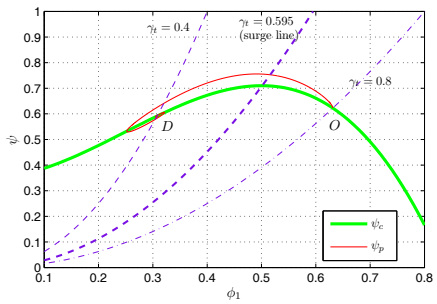

FIGURE 4. System trajectory of compressor with PAASCS when the operating point changed from O to D.

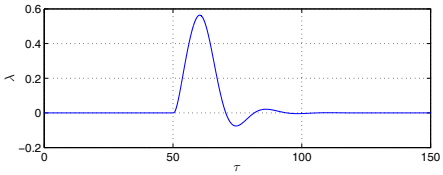

FIGURE 5. Piston displacement during the surge stabilization.

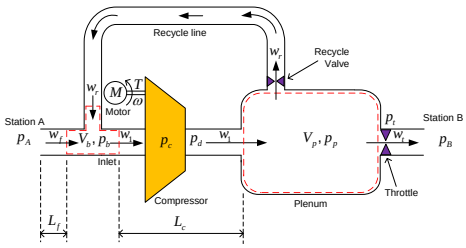

FIGURE 6. Model of compressor with SAS.

3.3 Surge Avoidance System

A compression system equipped with SAS is shown Fig. 6. The effect of the recycling flow to the inlet flow is shown by a control volume in the inlet called buffer. The non-dimensional dynamic equations are given as follows [9]:

$$\dot{\phi}_f = -B_I \psi_b \tag{14}$$

$$\dot{\psi}_b = \frac{1}{B_C}\left[\phi_f + \phi_r - \phi_1\right] \tag{15}$$

$$\dot{\phi}_1 = B\left[\psi_b + \psi_c - \psi_p\right] \tag{16}$$

$$\psi_p = \frac{1}{B}\left[\phi_1 - \phi_t - \phi_r\right] \tag{17}$$

where $B_I = \frac{A_I L_c}{A_c L_f} B$, $B_C = \frac{V_b}{V_p} B$ and ϕ_r is recycled mass flow as the plenum flow-out control. The recycled mass flow is a function of plenum pressure as described by:

$$\phi_r = k_{\gamma_r} u_r \sqrt{(\psi_p - \psi_b)} \tag{18}$$

where k_{γ_r} is recycle-valve constant and u_r is the valve control signal signal. The range value of u_r is from 0 to 100 %.

A control design using proportional and integral (PI) control was presented in [9] as follows:

$$u_r = K_p \phi_e + K_i \int \phi_e dt \tag{19}$$

where K_p is proportional gain, K_i is integrator gain, and ϕ_e is mass flow error defined by:

$$\phi_e = \phi_{SCL} - \phi_1 \tag{20}$$

where ϕ_{SCL} is mass flow at the surge control line. Only the non-negative mass flow error is used to generate the valve control signal, such that:

$$\phi_e = \begin{cases} \phi_e & \text{for } \phi_e \geq 0 \\ 0 & \text{for } \phi_e < 0. \end{cases} \tag{21}$$

We choose $\psi_{SCL} = 0.55$ in the case study. Figure 7 shows the system trajectory of a compressor equipped by SAS when the operating point moves from O to D. It shows the operating point is not able to reach the point D and goes to point E located at the SCL.

4 Active Surge Control with a Back-up System

4.1 Combining PAASCS and SAS

It has been shown that both PAASCS and SAS are able to maintain the stable compressor operation. However, it should be noted that PAASCS is stabilizing surge by moving the piston such that the surge control performance depends on the piston performance. The piston performance has some limitations and one is the maximum stroke. In a condition when the required stroke is more than the maximum stroke then the piston is saturated. It has been shown in Fig. 5 that the system stabilization for the changing operation from point O to D requires piston stroke up to 0.56. In the case the available piston has maximum stroke ± 0.40, the piston will be saturated during the stabilizing surge. Figure 8 shows the system trajectory of surge stabilization by using a piston with maximum stroke ± 0.40. The piston saturation makes the PAASCS fail to stabilize the system and the compressor is entering surge.

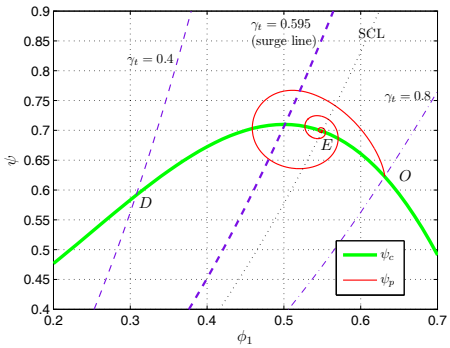

FIGURE 7. System trajectory of compressor with SAS when the operating point changed from O to D.

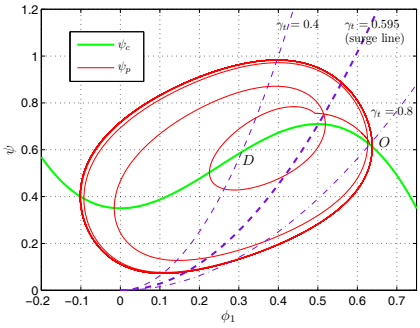

FIGURE 8. System trajectory of compressor with PAASCS when the piston saturates during changing operation from O to D.

A back-up system is then necessary for the active surge control system to recover the compressor when the active system should fail. For that purpose, we use SAS as the back-up of PAASCS as shown in Fig. 9. A switch is used to change the operation from the PAASCS to SAS and works only if the PAASCS should fail. We only consider the failures of the PAASCS due to piston saturation. The failure is detected by observing the piston velocity $\dot{\lambda}$ and the piston control law output $\bar{u}_s$. Since both PAASCS and SAS use plenum flow-out (ϕ_u) for surge control then switching algorithm can be defined as follows:

$$\phi_u = \begin{cases} \phi_s \\ \phi_r \quad \text{for } \bar{u}_s \neq 0 \wedge \dot{\lambda} = 0 \end{cases} \tag{22}$$

where $\wedge$ is AND logic operator. The switching is only one-way from the main system to the back-up system and not in the reverse way. Figure 10 shows the control loop of

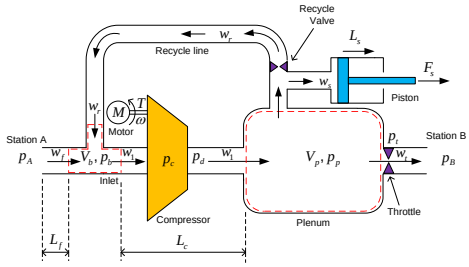

FIGURE 9. A model of compressor with PAASCS and SAS as the back-up.

PAASCS including SAS as the back-up system.

Figure 11 shows the trajectories of the compressor system with PAASCS and SAS as the back-up. The SAS recovers the compressor system from entering surge by moving the operating point to point E when the piston is fail. The system trajectories shows the switching system is locally asymptotic stable.

Figure 12 shows the SAS is recycling the flow when the piston saturates for recovery the compressor from entering surge. The compressor mass flow and plenum pressure during the recovery are shown in Fig. 13. The compressor is recovered and operates steady at mass flow 0.55 which is value of the chosen ϕ_{SCL}.

5 Conclusions

An active surge control system using piston actuation combined with SAS as the back-up system was presented. A failure in ASCS may make a disaster to the compressor system by occurring surge. Applying a back-up for the ASCS is necessary to improve the system safety as shown by the simulation result. The back-up system is only used to recover the compressor system from entering surge when the active system should fail by using one-way switching mechanism.

6 Future Works

This study is remaining an analytic proof for the switching stability and is taken in account as a future work. By using the analytic proof, the case study could be extended to a possibility of using two-way switching and a failure case due to jamming piston. A test rig in laboratory scale is prepared to do experiment for evaluating this concept.

ACKNOWLEDGMENT

This work was supported Siemens Oil and Gas Solutions Offshore through the Siemens-NTNU collaboration project.

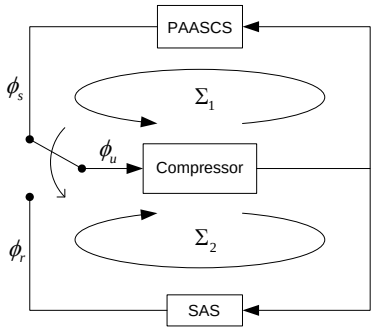

FIGURE 10. Control loop of compressor with PAASCS and SAS as the back-up.

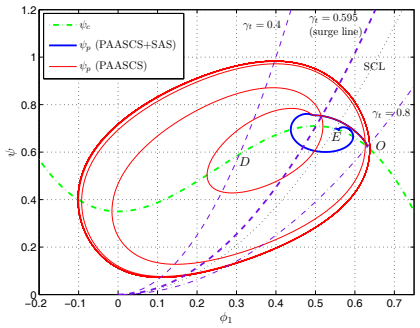

FIGURE 11. System trajectory of compressor with PAASCS and SAS as the back-up compared to the compressor with PAASCS only when the piston saturates during changing operation from O to D.

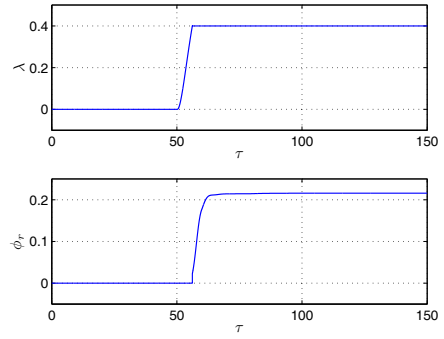

FIGURE 12. SAS is recycling flow when the piston saturates.

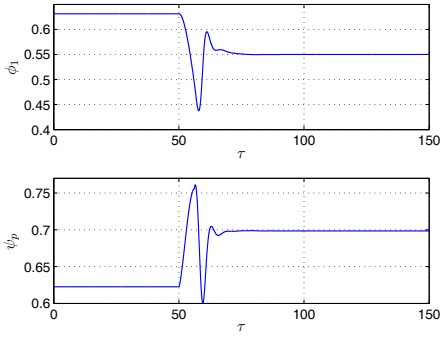

FIGURE 13. Compressor mass flow and plenum pressure of compressor equipped with PAASC and SAS as the back-upwhen the PAASC is fail.

REFERENCES

[1] Epstein, A. H., Williams, J. E. F., and Greitzer, E. M., 1989. "Active suppression of aerodynamics instability in turbo machines". *J. Propulsion and Power,* ***5***, pp. 204–211.

[2] Willems, F., and de Jager, B., 1999. "Modeling and control of compressor flow instabilities". *Control System Magazine,* ***19***, pp. 8–18.

[3] Arnulfi, G. L., Giannattasio, P., Micheli, D., and Pinamonti, P., 2001. "An innovative device for passive control of surge in industrial compression system". *J. Turbomachinery,* ***123***, pp. 473–782.

[4] Bøhagen, B., and Gravdahl, J. T., 2008. "Active surge control of compression system using drive torque". *Automatica,* ***44***, pp. 1135–1140.

[5] Uddin, N., and Gravdahl, J. T., 2012. "Introducing back-up to active compressor surge control system". In Proc. of the 2012 IFAC Workshop on Automatic Control in Offshore Oil and Gas Production.

[6] Uddin, N., and Gravdahl, J. T., 2011. "Active compressor surge control using piston actuation". *ASME Conference Proceedings,* ***2011***(54754), pp. 69–76.

[7] Uddin, N., and Gravdahl, J. T., 2011. "Piston-actuated active surge control of centrifugal compressor including integral action". In Proc. of the 11th International Conf. on Control Automation and System, pp. 991–996.

[8] Willems, F., and de Jager, B., 1998. "Active compressor surge control using a one-sided controlled bleed/recycle valve". In Decision and Control, 1998. Proceedings of the 37th IEEE Conference on, Vol. 3, pp. 2546 –2551.

[9] Uddin, N., and Gravdahl, J. T., 2012. "Bond graph modeling of centrifugal compressor system". In Proc. of The 10th International Conference on Bond Graph

TABLE 2. SIMULATION PARAMETERS

Variable	Value	Variable	Value	Variable	Value
$\frac{V_b}{V_p}$	0.005	$\frac{L_f}{L_c}$	0.1	$\frac{A_f}{A_c}$	1
$\frac{A_s}{A_c}$	1	ψ_{c_0}	0.352	W	0.25
ϕ_{fO}	0.6312	ϕ_{SCL}	0.55	K_i	15
ϕ_{1_O}	0.6312	H	0.18	ψ_{b_O}	0
ψ_{p_O}	0.6226	K_p	20	k_{γ_r}	0.05
M_s	21.85	k_a	1	B	0.8

Modeling and Simulation (ICBGM 2012).

[10] Greitzer, E. M., 1976. "Surge and rotating stall in axial flow compressor, part I: Theoritical compression system model". *J. Engineering for Power,* ***98***, pp. 190–198.

[11] Moore, F. K., and Greitzer, E. M., 1986. "A theory of post stall transients in an axial compressors system: Part I-Development of equation". *J. Engineering for Gas Turbine and Power,* ***108***, pp. 68–76.

Paper F Two General State Feedback Control Laws for Compressor Surge Stabilization

Submitted to *The 24th Mediterranean Conference on Control and Automation in Athens, Greece, June 21-24, 2016.*

Two General State Feedback Control Laws for Compressor Surge Stabilization*

Nur Uddin and Jan Tommy Gravdahl

***Abstract*— Active surge control system (ASCS) can be classified into two types: upstream energy injection and downstream energy dissipation [1]. Two novel state feedback control laws termed ϕ-control for the upstream energy injection and ψ-control the downstream energy dissipation are presented. Both state feedback control laws are derived by using the Lyapunov based control method such that the closed loop systems are global asymptotic stable (GAS). The ϕ-control applies feedback from the compressor mass flow sensor to generate extra pressure to the compressor upstream line, while the ψ-control generates an extra flow out of the plenum using feedback from the compressor discharged pressure and the plenum pressure. Both state feedback control laws offer a minimum number of sensors requirement. Moreover, the ψ-control requires feedback from pressure sensors only which are readily available and make real-time implementation of the system to be easier.**

I. INTRODUCTION

The operating area of a compressor is commonly shown by a compressor map. The map shows curves of compressor produced pressure versus compressor mass flow. Figure 1 shows an example of compressor map for a constant compressor speed. The compressor operating area at lower mass flow is limited by a surge line and stone wall at the hight mass flow. Surge line is a limit of stability where the right side area of the line is stable while the left side area is unstable. Operating the compressor in the unstable area result in compressor surge. Operating a compressor beyond the stonewall result in compressor choke.

Compressor choke is a condition when the gas velocity relative to the blade is equal to the speed of sound such that the compressor cannot pump any more gas [2]. According to [3], a compressor can only operate in stonewall if the head (energy) required by the process system is low enough such that the compressor operates in the high-flow-rate region of the compressor map. The high flow rate requires a larger pipe diameter, which is more costly. For economic reasons, this is a rare case because the process pipe is designed to minimize the pipe diameter and therefore increase the head required at high flow rates. Stonewall is also not a destructive phenomenon. Therefore, surge receives more attention in compressor studies. Moreover, the high-efficiency compressor operating points are located close to the surge line.

*This work was supported by Siemens Oil and Gas Solutions Offshore through the Siemens-NTNU research collaboration project.

Nur Uddin and Jan Tommy Gravdahl are with Department of Engineering Cybernetics, Norwegian University of Science and Technology, O.S. Bragstads plass 2D, Trondheim, Norway N-7491 nur.uddin@itk.ntnu.no, Jan.Tommy.Gravdahl@itk.ntnu.no

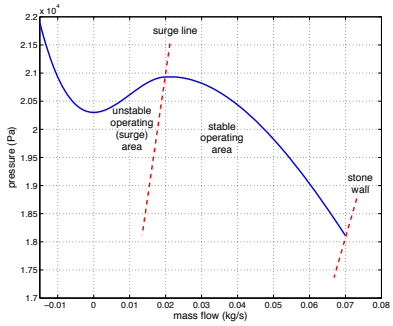

Fig. 1. A compressor map with surge line.

Compressor surge is an aerodynamic instability in the compression system and results in an axisymmetric oscillation of the compressor flow and the compressor produced pressure. It is also defined as a condition where the pressure developed by a compressor (upstream pressure) is less than the system pressure (downstream pressure) [2]. It occurs due to inability of the impeller to produce the amount of required energy for the process system [3]. Surge is physically indicated by pressure fluctuation, reversal of flow, temperature fluctuation and followed by severe vibration. Surge leads to compressor damage especially at the rotating parts, for examples: compressor blades, shaft and bearing, and also pipeline connections and structure. Therefore, a compressor is always prevented to enter surge during the operation. There are two methods to prevent a compressor from experiencing surge: surge avoidance system (SAS) and active surge control system (ASCS).

SAS is the traditional method to prevent a compressor entering surge. SAS works by defining a surge control line which is located on the right side of the surge line as a limit of the minimum compressor flow. It makes the compressor operating point not reach the surge line. The margin between surge control line and surge line is known as surge margin. The surge margin is defined by a compressor operator and 10 % is commonly used. The SAS method is implemented through a recycling flow mechanism by using a recycle valve and recycle line or blowing-off flow mechanism by using a blow-off valve. When the compressor operating point is crossing the surge control line, the recycle valve or the

blow-off valve will open to discharge the downstream fluid and result in increasing the flow such that the compressor operating point will stay at the surge control line. This method works well to prevent a compressor from entering surge and is commonly applied in industrial compressors. However, applying SAS reduces the compressor operating envelope as the limit of minimum compressor flow is surge control line instead of surge line. Moreover, the compressor operating points with high efficiency are commonly located closed to the surge line such that a compressor equipped with SAS may not be able to reach the highest efficiency.

As opposed to the SAS which limits the compressor operating area by a surge control line, ASCS is stabilizing surge by an active element such that the compressor operating point is allowed to cross the surge line into the stabilized surge area such that the operating envelope is enlarged. The active element, or actuator, is driven by a controller based on a state feedback control law. The ASCS method was introduced by [4]. ASCS is offering an enlargement of the compressor operating envelope towards lower flows and an opportunity to reach higher compressor efficiency. Several studies by applying different control methods and different actuators have been presented. Nonlinearity in the compressor dynamics gives a challenge in designing the surge control. Several studies by applying linear and nonlinear control methods to design ASCS controller have been presented. The linear control design is done by linearizing the compressor dynamics at an operating point to get a linear compressor model such that linear control methods can be applied. Examples of ASCS designed by using linear control theory have been presented in [5]–[7]. The linear control design is able to stabilize compressor surge, but it only achieves local asymptotic stability with limited region of attraction (operating area). On the other hand, nonlinear control methods are promising global asymptotic stability (GAS). The GAS is proved by the Lyapunov stability method which is requiring a Lyapunov function. Backstepping is a systematic non-linear control method to find a state feedback and Lyapunov function such that GAS of the closed loop system is guaranteed. Several works on applying Lyapunov-based or backstepping methods for active surge control were presented in [8]–[10]. However, the method may result in a complicated and impractical state feedback [10].

A compressor model is required in surge control design. Greitzer compression model [11] is one of the most applied models in surge control studies. The Greitzer model is able to predict the transient response subsequent to a perturbation from steady operating condition.

Several actuators have been applied in active surge control and example includes: moveable plenum wall [5], close coupled valve [8], drive torque [12], magnetic bearing [13] and piston actuation [10]. Consult [14] for more actuators applied in ASCS. Considering the working principle of the actuators in stabilizing surge, ASCS can be classified into two types: upstream energy injection and downstream energy dissipation [1]. The upstream energy injection is increasing the pressure at compressor upstream line while

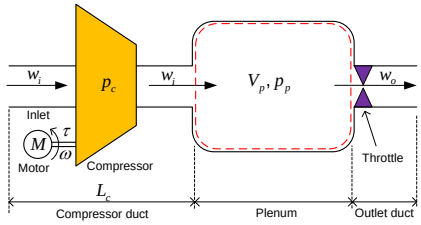

Fig. 2. Model of single compression system.

the downstream energy dissipation is decreasing the pressure at the compressor downstream line (plenum) by flowing out more fluid from the plenum.

This paper presents two new general state feedback controls called ϕ-control and ψ-control for compressor surge stabilization by using ASCS in the types of upstream energy injection and downstream energy dissipation, respectively. Both state feedback controls are derived by using Lyapunov based control method such that the GAS of the closed loop system is guaranteed.

II. Compression System

The Greitzer compression model is shown in Figure 2 and the dynamic equations are given as follows [11]:

$$\dot{w}_i = \frac{A_c}{L_c}(p_c - p_p) \quad (1)$$

$$\dot{p}_p = \frac{a_0^2}{V_p}(w_i - w_o), \quad (2)$$

where w_i is the inlet mass flow, A_c is the compressor duct cross-sectional area, L_c is the effective length of the equivalent compressor duct, p_c is the compressor pressure rise, p_p is the plenum pressure, a_0 is the speed of sound, V_p is the plenum volume, and w_o is the outlet mass flow. It is assumed that the pressures are measured relative to the ambient pressure.

The outlet mass flow is the set point which represents the desired mass flow of a compressor operation. The inlet mass flow will be equal to the outlet mass flow at steady state. The compressor operating point is changing by adjusting the outlet mass flow, where it is physically done by adjusting a throttle. The outlet mass flow is defined by:

$$w_o = k_T u_T \sqrt{p_p} \quad (3)$$

where k_T is the throttle constant and u_T is the throttle opening with range value from 0 to 100 %.

Defining constants $B_1 = \frac{A_c}{L_c}$ and $B_2 = \frac{a_0^2}{V_p}$, the dynamic equations can be expressed as:

$$\dot{w}_i = B_1(p_c - p_p) \quad (4)$$

$$\dot{p}_p = B_2(w_i - w_o). \quad (5)$$

The compressor pressure rise is plotted as a function of the flow for several compressor speeds in a compressor map and

is commonly provided by the compressor manufacturer. The map can be obtained by collecting data in a compressor performance test and approximated by a mathematical function. Approximation by a cubic function for constant compressor speed was introduced by [15] as follows:

$$p_c(w_i) = p_{c_0} + H\left[1 + \frac{3}{2}\left(\frac{w_i}{W} - 1\right) - \frac{1}{2}\left(\frac{w_i}{W} - 1\right)^3\right], \quad (6)$$

where p_{c_0} is the shut-off value of the axisymmetric characteristic, W is the semi-width of the cubic axisymetric compressor characteristic, and H is the semi-height of the cubic axisymetric compressor characteristic; consult [15] for more detailed definitions.

III. Principal Work of Active Surge Control

Modeling a compressor system by using bond graph was presented in [1]. Analysis of the bond graph model results in two basic surge solutions for stabilizing compressor surge: upstream energy injection and downstream energy dissipation. Several presented actuators for ASCS are basically working based on one of the two approaches. Based on the Greitzer model, the upstream energy injection results in additional upstream pressure and the downstream energy dissipation results in additional flow out from the plenum in order to stabilize compressor surge. Derivations of state feedback control law for the both basic surge solutions by using Lyapunov control method are presented as follow.

A. Upstream energy injection

A bond graph model of a compression system with active surge control system in the class of upstream energy injection is shown Figure 3. Dynamic equations of the system based on the bond graph model are given as follows[1]:

$$I\dot{q}_i = p_c - p_p + e_{19} \quad (7)$$
$$C\dot{p}_p = q_i - q_o, \quad (8)$$

where $I = \frac{\rho L_c}{A_c}$, $C = \frac{V_p}{\rho a_0^2}$, e_{19} is an effort (pressure p_u) generated by an active element S_u, and q is volumetric flow. The relation with mass flow is $w = \rho q$. By assuming the flow is incompressible and using the defined constants B_1 and B_2, the dynamic equations (7) and (8) can be expressed as follows:

$$\dot{w}_i = B_1(p_c - p_p + p_u) \quad (9)$$
$$\dot{p}_p = B_2(w_i - w_o). \quad (10)$$

Theorem 1: A ϕ-control with a state feedback $p_u = -k_1(w_i - w_{i_{ref}})$ where $k_1 > k_m$ and $k_m = \left.\frac{\partial p_c}{\partial w_i}\right|_{\max}$, makes the operating point of a compressor system in (9) and (10) at mass flow $w_{i_{ref}}$ to be GAS.

Proof: Define new variables $z_1 = p_c - p_p + p_u$ and $z_2 = w_i - w_o$, and a Lyapunov function candidate

$$V_1 = \frac{B_1}{2}z_1^2 + \frac{B_2}{2}z_2^2. \quad (11)$$

[1]Notation according to [1]

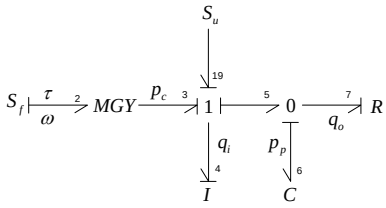

Fig. 3. Bond graph model of active surge control in a class of upstream energy injection [1].

The time derivative of V_1 is given as follows:

$$\begin{aligned}
\dot{V}_1 &= B_1 z_1 \dot{z}_1 + B_2 z_2 \dot{z}_2 \\
&= B_1(p_c - p_p + p_u)(\dot{p}_c - \dot{p}_p + \dot{p}_u) + B_2(w_i - w_o)(\dot{w}_i - \dot{w}_o) \\
&= \dot{w}_i(\dot{p}_c - \dot{p}_p + \dot{p}_u) + \dot{p}_p\dot{w}_i - \dot{p}_p\dot{w}_o \\
&= \dot{w}_i\dot{p}_c - \dot{w}_i\dot{p}_p + \dot{w}_i\dot{p}_u + \dot{p}_p\dot{w}_i - \dot{p}_p\dot{w}_o \\
&= \frac{\partial p_c}{\partial w_i}\dot{w}_i^2 + \dot{w}_i\dot{p}_u - \frac{\partial w_o}{\partial p_p}\dot{p}_p^2
\end{aligned}$$

Let $\dot{p}_u = -k_1\dot{w}_i$,

$$\begin{aligned}
\dot{V}_1 &= \left(\frac{\partial p_c}{\partial w_i} - k_1\right)\dot{w}_i^2 - \frac{\partial w_o}{\partial p_p}\dot{p}_p^2 \\
&= \left(\frac{\partial p_c}{\partial w_i} - k_1\right)B_1^2(p_c - p_p + p_u)^2 - \frac{\partial w_o}{\partial p_p}B_2^2(w_i - w_o)^2 \\
&= \left(\frac{\partial p_c}{\partial w_i} - k_1\right)B_1^2 z_1^2 - \frac{\partial w_o}{\partial p_p}B_2^2 z_2^2, \quad (12)
\end{aligned}$$

where $\frac{\partial w_o}{\partial p_p} = \frac{w_o}{2p_p} > 0$, see the Appendix for the derivation of $\frac{\partial w_o}{\partial p_p}$. Selecting $k_1 > k_m$ where $k_m = \left.\frac{\partial p_c}{\partial w_i}\right|_{\max}$ results in $\dot{V}_2 < 0$ such that the closed loop system of (9) and (10) is GAS. The state feedback control is given as

$$p_u = -k_1\int \dot{w}_i dt = -k_1(w_i - w_{i_{ref}}), \quad (13)$$

where $w_{i_{ref}}$ is the desired compressor mass flow which is the desired throttle mass flow w_o. ■

The value of k_m can be obtain by using (6) and it is resulted in $k_m = \frac{3H}{2W}$. Equation (13) is the state feedback control to stabilize surge by maintaining the compressor to operate at the desired mass flow and called as ϕ-control.

B. Downstream energy dissipation

A bond graph model of a compression system with active surge control system in the class of downstream energy dissipation is shown in Figure 4. Dynamic equation of the system based on the bond graph model is given as follows[2]:

$$I\dot{q}_i = p_c - p_p \quad (14)$$
$$C\dot{p}_p = q_i - q_o - f_{20}, \quad (15)$$

where f_{20} is a flow out from the plenum generated by an active element R_u and it is defined as the volumetric flow

[2]Notation according to [1]

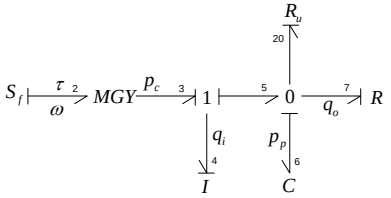

Fig. 4. Bond graph model of active surge control in a class of downstream energy dissipation [1].

q_u. By assuming the flow is incompressible and using the defined constants B_1 and B_2, the dynamic equations (14) and (15) can be expressed as:

$$\dot{w}_i = B_1(p_c - p_p) \quad (16)$$
$$\dot{p}_p = B_2(w_i - w_o - w_u). \quad (17)$$

Theorem 2: A ψ-control with a state feedback $w_u = -\frac{k_2 B_1}{B_2}(p_c - p_p)$, where $k_m < k_2 < k_n$ with $k_m = \frac{\partial p_c}{\partial w_i}\Big|_{\max}$ and $k_n = \frac{\partial p_p}{\partial w_o}\Big|_{\min}$, makes the operating point of a compression system in (16) and (17) at a desired mass flow w_o to be GAS.

Proof: Recall the defined variables $\theta_1 = p_c - p_p$ and $\theta_2 = w_i - w_o$, and define a Lyapunov function candidate:

$$V_2 = \frac{B_1}{2}\theta_1^2 + \frac{B_2}{2}\theta_2^2. \quad (18)$$

Time derivative of V_2 is given as follows:

$$\begin{aligned}
\dot{V}_2 &= B_1\theta_1\dot{\theta}_1 + B_2\theta_2\dot{\theta}_2 \\
&= B_1(p_c - p_p)(\dot{p}_c - \dot{p}_p) + B_2(w_i - w_o)(\dot{w}_i - \dot{w}_o) \\
&= \dot{w}_i(\dot{p}_c - \dot{p}_p) + B_2(w_i - w_o - w_u + w_u)(\dot{w}_i - \dot{w}_o) \\
&= \dot{w}_i\dot{p}_c - \dot{w}_i\dot{p}_p + B_2(w_i - w_o - w_u)(\dot{w}_i - \dot{w}_o) \\
&\quad + B_2 w_u(\dot{w}_i - \dot{w}_o) \\
&= \dot{w}_i\dot{p}_c - \dot{w}_i\dot{p}_p + \dot{p}_p(\dot{w}_i - \dot{w}_o) + B_2 w_u(\dot{w}_i - \dot{w}_o) \\
&= \dot{w}_i\dot{p}_c - \dot{w}_i\dot{p}_p + \dot{p}_p\dot{w}_i - \dot{p}_p\dot{w}_o + B_2 w_u(\dot{w}_i - \dot{w}_o) \\
&= \dot{w}_i\dot{p}_c - \dot{p}_p\dot{w}_o + B_2 w_u\dot{w}_i - B_2 w_u\dot{w}_o \\
&= \frac{\partial p_c}{\partial w_i}\dot{w}_i^2 + B_2 w_u\dot{w}_i - B_2 w_u\dot{w}_o - \dot{p}_p\dot{w}_o. \quad (19)
\end{aligned}$$

Let $w_u = -\frac{k_2}{B_2}\dot{w}_i$ such that

$$\dot{V}_2 = \left(\frac{\partial p_c}{\partial w_i} - k_2\right)\dot{w}_i^2 + k_2\dot{w}_i\dot{w}_o - \dot{p}_p\dot{w}_o,$$

and by applying Young's inequality:

$$\begin{aligned}
\dot{V}_2 &\leq \left(\frac{\partial p_c}{\partial w_i} - k_2\right)\dot{w}_i^2 + k_2\left(\frac{\dot{w}_i^2}{2} + \frac{\dot{w}_o^2}{2}\right) - \dot{p}_p\dot{w}_o \\
&= \left(\frac{\partial p_c}{\partial w_i} - \frac{k_2}{2}\right)\dot{w}_i^2 + \frac{k_2}{2}\dot{w}_o^2 - \dot{p}_p\dot{w}_o \\
&= \left(\frac{\partial p_c}{\partial w_i} - \frac{k_2}{2}\right)\dot{w}_i^2 + \frac{k_2}{2}\left(\frac{\partial w_o}{\partial p_p}\dot{p}_p\right)^2 - \dot{p}_p\left(\frac{\partial w_o}{\partial p_p}\dot{p}_p\right) \\
&= \left(\frac{\partial p_c}{\partial w_i} - \frac{k_2}{2}\right)\dot{w}_i^2 + \left[\frac{k_2}{2}\left(\frac{\partial w_o}{\partial p_p}\right)^2 - \frac{\partial w_o}{\partial p_p}\right]\dot{p}_p^2 \\
&= \left(\frac{\partial p_c}{\partial w_i} - \frac{k_2}{2}\right)\dot{w}_i^2 + \left[\frac{k_2}{2}\left(\frac{\partial w_o}{\partial p_p}\right)^2 - \frac{\left(\frac{\partial w_o}{\partial p_p}\right)^2}{\frac{\partial w_o}{\partial p_p}}\right]\dot{p}_p^2 \\
&= \left(\frac{\partial p_c}{\partial w_i} - \frac{k_2}{2}\right)\dot{w}_i^2 + \left(\frac{k_2}{2} - \frac{\partial p_p}{\partial w_o}\right)\left(\frac{\partial w_o}{\partial p_p}\right)^2\dot{p}_p^2 \\
&= \left(\frac{\partial p_c}{\partial w_i} - \frac{k_2}{2}\right)B_1^2(p_c - p_p)^2 \\
&\quad + \left(\frac{k_2}{2} - \frac{\partial p_p}{\partial w_o}\right)\left(\frac{\partial w_o}{\partial p_p}\right)^2 B_2^2(w_i - w_o - w_u)^2 \\
&= \left(\frac{\partial p_c}{\partial w_i} - \frac{k_2}{2}\right)B_1^2\theta_1^2 \\
&\quad + \left(\frac{k_2}{2} - \frac{\partial p_p}{\partial w_o}\right)\left[\frac{\partial w_o}{\partial p_p}B_2\left(\theta_2 + \frac{k_2}{B_2}B_1\theta_1\right)\right]^2. \quad (20)
\end{aligned}$$

Selecting $k_m < k_2 < k_n$, where $k_m = \frac{\partial p_c}{\partial w_i}\Big|_{\max}$ and $k_n = \frac{\partial p_p}{\partial w_o}\Big|_{\min}$, results in $\dot{V}_2 < 0$ such that the closed loop system in (16) and (17) is GAS by a state feedback control

$$w_u = -\frac{k_2 B_1}{B_2}(p_c - p_p). \quad (21)$$

■

It is shown in Appendix that $\frac{\partial p_p}{\partial w_o} = \frac{2p_p}{w_o}$ and therefore $k_n = \frac{2p_p}{w_o}\Big|_{\min}$. The value of k_n can be obtained by finding the operating point at the maximum mass flow in the compressor map for the corresponding compressor speed. Equation (21) is the state feedback control to stabilize surge by maintaining the compressor discharged pressure to be equal to the plenum pressure and we call it as ψ-control. Note that the (21) requires feedback from pressure only, a quantity that is more readily available for measurement than mass flow. It makes real-time implementation of the system to be easier.

C. Actuator

Block diagrams of ASCS in the class of upstream energy injection and downstream energy dissipation are shown in Figures 5 and 6, respectively. Actuator is the mean to execute the state feedback control into physical action. The type of actuator is not limited as long as it can generate mass flow w_u or pressure p_u. The actuator should have fast response and accurate value. However, an ideal actuator may not available such that it will be a trade-off between actuator and the surge control performance.

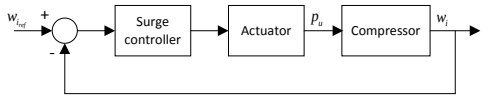

Fig. 5. Block diagram of active surge control with upstream energy injection (ϕ-control).

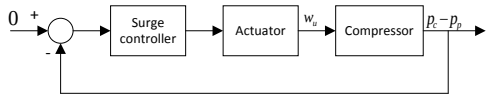

Fig. 6. Block diagram of active surge control with downstream energy dissipation (ψ-control).

IV. Simulation

Simulations are presented to demonstrate the performance of the ASCS in the class of upstream energy injection and downstream energy dissipation for stabilizing compressor surge. The simulations use parameters given in Table I and a compressor map in Figure 1. The compressor map shows that the surge point, which is the minimum stable compressor mass flow, is located at mass flow 0.02 kg/s and pressure 20.93 kPa, while the choke point, which is the maximum compressor mass flow, is located at mass flow 0.07 kg/s and pressure 18.1 kPa. Based on the available data, we obtain $k_m = 4.725 \times 10^4$ kPa.s/kg, $k_n = 5.17 \times 10^5$ kPa.s/kg, $B_1 = 9.3 \times 10^{-3}$ m, and $B_2 = 1.156 \times 10^6$ m^{-1}s^{-2}. Therefore, the control parameters for the upstream energy injection (ϕ-control) is $k_1 > 4.725 \times 10^4$ and the downstream energy dissipation (ψ-control) is $4.725 \times 10^4 < \frac{k_2}{2} < 5.17 \times 10^5$. In this simulation, we choose $k_1 = 6.24 \times 10^4$ and $k_2 = 10^5$.

Two simulations will be carried out to show the performance of the the ϕ-control and the ψ-control in stabilizing surge and the simulation scenario is give as follows. Both simulations will be done by operating the compressor at point A where the mass flow is 0.06 kg/s as the initial point and at $t = 40$ seconds the operating point is shifted to B where the mass flow is 0.01 kg/s by closing the throttle. The operating points A is located in the stable operating area while B is in the surge area. The compressor will enter surge and the surge control will be activated a few second after the compressor surge. The simulation results are given as follows.

The performance of the upstream energy injection (ϕ-control) ASCS is shown in Figure 7 for the time response of the system and Figure 8 for the system trajectory. The compressor operating point is shifted from point A to B by reducing the mass flow from 0.06 to 0.01 kg/s at $t = 40$. The compressor enters surge after the the operating point passed the surge point as shown in compressor operating trajectory in Figure 8.The surge is shown by oscillations at compressor mass flow oscilation (w_i) and plenum pressure (p_p) in Figure 7 and limit cycle in Figure 8. The surge is stabilized after the surge control is activated at $t = 43$ seconds and the system is finally operating stable at point B where the mass flow is 0.01 kg/s.

TABLE I
Simulation Parameters

Parameter	Value	Unit	Parameter	Value	Unit
a_0	340	m/s	V_p	0.1	m^3
L_c	0.41	m	A_c	0.0038	m^2
p_{c_0}	20.3	kPa	H	0.315	kPa
W	0.01	kg/s			

The performance of the downstream energy dissipation (ψ-control) ASCS is shown in Figure 9 for the time responses and Figure 10 for the system trajectory. Figure 9 is shown that the compressor enters to surge at $t = 40$ seconds after the operating point is shifted to point B. The surge is stabilized after the surge control is activated at $t = 43.6$ seconds and the system is operating stable at point B where the mass flow is 0.01 kg/s. The reason of activating the surge control at $t = 43.6$ seconds and not at $t = 43$ seconds as in previous simulation is solely to give more clear visualization of the compressor operating trajectory in Figure 10.

Figure 9 also shows that the control mass flow w_u instantaneously jumped when the surge control was activated. It requires the actuator to generated a high mass flow instantaneously and is not practical. The jump of w_u is the effect of derivative control where the w_u is proportional to $\dot{w}_i$ and it can be eliminated by limiting w_u in a reasonable value. The w_u should not more than w_i. Figure 12 shows simulation result of applying limiter to the w_u with limitation range $-0.02 \leq w_u \leq 0.02$ kg/s. The surge is stabilized although the w_u is limited. A limiter is not necessary for the upstream energy injection as it is not a derivative control. The p_u is proportional to the deviation of w_i to $w_{i_{ref}}$.

V. Conclusion

Two state feedback controls called ϕ-control for ASCS with upstream energy injection and ψ-control for ASCS with downstream energy dissipation were presented including the GAS proof of the closed loop systems. Both state feedback controls stabilize surge and the closed loop system is GAS. An advantage of the proposed schemes is the reduced sensor requirements, ϕ-control is only requiring a mass flow sensor and the ψ-control is only requiring two pressure sensors to measure compressor discharge pressure and the plenum pressure. The ϕ-control can be directly implemented in real-time system as the pressure sensor is readily available. However, it is not the same for the $\psi - control$ due to the available mass flow sensor has slow response and not able to capture compressor surge. As an alternative mass flow observer introduced in [16] can be used to get an estimated mass flow. Application of the both feedback controls depends on the actuator type for ASCS, whether it is in the class of upstream energy injection or downstream energy dissipation.

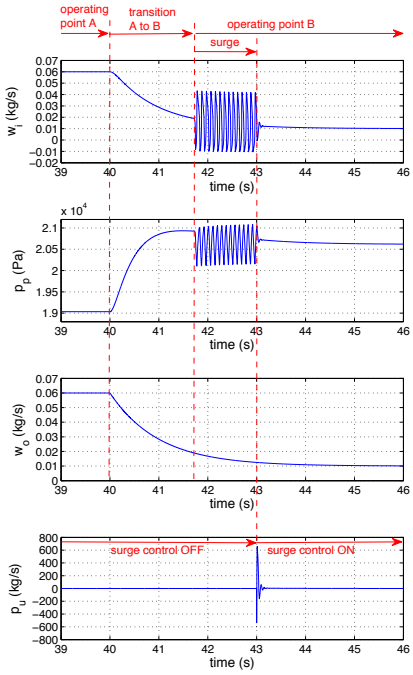

Fig. 7. Time responses of a compression system equipped by an active surge control using upstream energy injection.

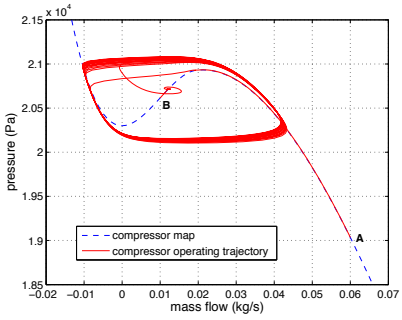

Fig. 8. Operating trajectory of a compression system equipped by an active surge control using upstream energy injection.

Appendix

The value of $\frac{\partial p_p}{\partial w_o}$ is given as follows:

$$\begin{aligned} w_o &= k_T u_T \sqrt{p_p} \\ \frac{dw_o}{dp_p} &= \frac{k_T u_T}{2\sqrt{p_p}} = \frac{w_o}{2p_p} \end{aligned}$$

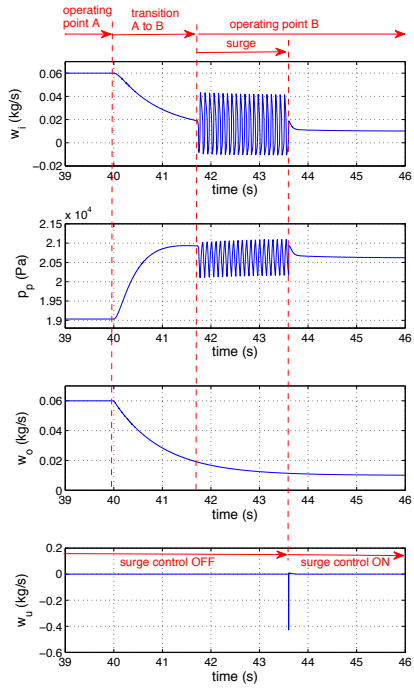

Fig. 9. Time responses of a compression system equipped by an active surge control using downstream energy dissipation.

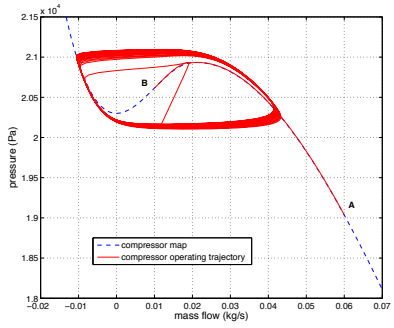

Fig. 10. Operating trajectory of a compression system equipped by an active surge control using downstream energy dissipation.

$$\begin{aligned} p_p &= \frac{1}{(k_T u_T)^2} w_o^2 \\ \frac{dp_p}{dw_o} &= \frac{2}{(k_T u_T)^2} w_o = \frac{2p_p}{w_o}. \end{aligned}$$

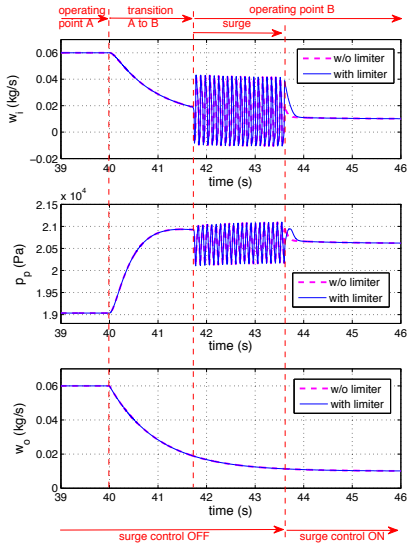

Fig. 11. Time responses of a compression system equipped by an active surge control using downstream energy dissipation including limiter for the actuator.

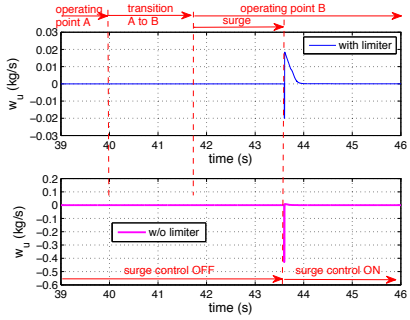

Fig. 12. Comparison of control mass flow used in downstream energy dissipation with limiter and without limiter.

Acknowledgements

The authors acknowledge the financial support of Siemens Oil and Gas Solutions Offshore through the Siemens-NTNU research collaboration project.

References

[1] N. Uddin and J. T. Gravdahl, "Bond graph modeling of centrifugal compression systems," *SIMULATION*, vol. 91, no. 11, pp. 998–1013, 2015.

[2] A. Nisenfeld, *Centrifugal Compressors: Principles of Operation and Control*, ser. Monograph series / Instrument Society of America. Instrument Society of America, 1982.

[3] W. E. B. Forsthoffer, *Forsthoffer's rotating equipment handbooks vol.5: Compressors*. Oxford: Elsevier Science, 2005.

[4] A. H. Epstein, J. E. F. Williams, and E. M. Greitzer, "Active suppression of compressor instabilities," in *Proc. of AIAA 10th Aeroacoustic Conference*, no. 86-1994, Seattle, 1986.

[5] J. E. F. Williams and X. Y. Huang, "Active stabilization for compressor surge," *J. Fluid Mechanics*, vol. 204, pp. 245–262, 1989.

[6] D. Gysling, D. Dugundji, E. M. Greitzer, and A. H. Epstein, "Dynamic control of centrifugal compressor surge using tailored structures," *ASME J. Turbomachinery*, vol. 113, pp. 710–722, 1991.

[7] N. Uddin and J. T. Gravdahl, "Piston-actuated active surge control of centrifugal compressor including integral action," in *Proc. of the 11th International Conference on Control Automation and System*, Gyeonggi-do, South Korea, 2011.

[8] J. S. Simon and L. Valavani, "A lyapunov based nonlinear control scheme for stabilizing a basic compression system using a close-coupled control valve," in *Proc. of the American Control Conference*, Massachusetts, US, 1991, pp. 2398–2406.

[9] J. T. Gravdahl and O. Egeland, "Compressor surge control using a close-coupled valve and backsteeping," in *Proc. of the American Control Conference*, New Mexico, US, June 1997.

[10] N. Uddin and J. T. Gravdahl, "Active compressor surge control using piston actuation," in *ASME 2011 Dynamic Systems and Control Conference and Bath/ASME Symposium on Fluid Power and Motion Control*. Virginia, US: American Society of Mechanical Engineers, 2011, pp. 69–76.

[11] E. M. Greitzer, "Surge and rotating stall in axial flow compressor, part I: Theoritical compression system model," *J. Engineering for Power*, vol. 98, pp. 190–198, 1976.

[12] J. T. Gravdahl, O. Egeland, and S. O. Vatland, "Drive torque actuation in active surge control of centrifugal compressor," *Automatica*, vol. 38, pp. 1881–1893, 2002.

[13] S. Y. Yoon, Z. Lin, and P. E. Allaire, *Control of Surge in Centrifugal Compressors by Active Magnetic Bearings: Theory and Implementation*. London: Springer Verlag, 2012.

[14] F. Willems and B. de Jager, "Active compressor surge control using a one-side controlled bleed/recycle valve," in *Proc. of the 37th IEEE Conf. on Decission and Control*, Florida, US, 1998, pp. 2546–2551.

[15] F. K. Moore and E. M. Greitzer, "A theory of post stall transients in an axial compressors system: Part I-Development of equation," *J. Engineering for Gas Turbine and Power*, vol. 108, pp. 68–76, 1986.

[16] B. Bøhagen and J. T. Gravdahl, "On active surge control of compressors using a mass flow observer," in *Proceedings of the 41st IEEE Conference on Decision and Control*, vol. 4. IEEE, 2002, pp. 3684–3689.

Paper G Active Compressor Surge Control System by Using Piston Actuation: Implementation and Experimental Results

Accepted in *The 11th IFAC Symposium on Dynamics and Control of Process Systems, including Biosystems (DYCOPS-CAB 2016) in Trondheim, Norway, June 6-8, 2016.*

Active Compressor Surge Control System by Using Piston Actuation: Implementation and Experimental Results ⋆

Nur Uddin, **Jan Tommy Gravdahl**

Dept. of Engineering Cybernetics
Norwegian University of Science and Technology (NTNU),
O.S. Bragstads plass 2D, Trondheim, Norway N-7491
(e-mail: nur.uddin@itk.ntnu.no, Jan.Tommy.Gravdahl@itk.ntnu.no)

Abstract: A novel implementation and experimental test results of a piston actuated active surge control system (PAASCS) on a laboratory scale pipeline-compressor system are presented. The experimental test is done to prove the concept of stabilizing compressor surge by dissipating the plenum energy using a piston actuation. The PAASCS's controller is applying ψ-control introduced in (Uddin and Gravdahl, 2016), which only uses feedback from pressure measurements at the compressor discharge and in the plenum. Practical aspects of implementing the PAASCS are presented including: flow measurement, generating a compressor map based on a compressor performance test, piston design, and the test setup. The experimental test results show that the PAASCS is able to stabilize surge and prove the concept of PAASCS with the advantage of ψ-control which stabilizes compressor surge by using feedback from pressure measurements only.

Keywords: Compressor, active surge control, pitot tube flow measurement, linear actuator, hardware in the loop test, experimental.

1. INTRODUCTION

A centrifugal compressor operating area is commonly shown by a compressor map, where the compressor operation at low mass flows is limited by a surge line. The operating area on the left side of the surge line is unstable and will lead to surge, while it is stable operating area on the right side of the line. Compressor surge is an aerodynamic instability in the compression system and results in an axisymmetric oscillation of the compressor mass flow and the compressor pressure. The instability is physically indicated by pressure fluctuation, reversal flow, temperature fluctuation and followed by severe vibration. Compressor surge leads to compressor damage especially at the rotating parts, for examples: compressor blades, shaft and bearing, and also pipeline and structure (Gravdahl and Egeland, 1999).

A method to stabilize surge by using a state feedback control was introduced by Epstein et al. (1986). The method is known as active surge control system (ASCS). Several actuators have been applied in the ASCS as summarized in (Willems and de Jager, 1999; Uddin and Gravdahl, 2015), for examples: movable plenum wall, close couple valve, drive torque, active magnetic bearing, and piston actuation. Based on how the actuators work to stabilize surge, the ASCS can be classified in two types: upstream energy injection and downstream energy dissipation (Uddin and Gravdahl, 2015). The upstream energy injection ASCS is stabilizing surge by increasing the upstream pressure to increase the upstream energy, while the downstream energy dissipation ASCS is stabilizing surge by flowing extra fluid out from the plenum to decrease the downstream energy. Two general state feedback control law for the both ASCS types were introduced by Uddin and Gravdahl (2016), and named ϕ-control for the upstream energy injection and ψ-control for the down stream energy dissipation. Both control laws make the closed loop system globally asymptotically stable (GAS) and the advantage of them are the minimum sensor requirement. The ϕ-control requires feedback from the compressor mass flow measurement only, while the ψ-control requires feedback from pressure measurements at the compressor discharge and in the plenum only.

Piston actuated active surge control system (PAASCS) was in introduced by Uddin and Gravdahl (2011b). It is in the class of ASCS with downstream energy dissipation. Theoretical works to improve the PAASCS performance have been done by: introducing integral action to eliminate piston drift (Uddin and Gravdahl, 2011a), and introducing a back-up system by using blow-off mechanisms (Uddin and Gravdahl, 2012b) and by using surge avoidance system (SAS) (Uddin and Gravdahl, 2012a) for fail-safe operation.

This paper presents the implementation and the experimental test results of a PAASCS on a laboratory scale pipeline-compressor system running at a constant compressor speed. An experimental test setup is built in Compressor laboratory at Departement of Engineering Cybernetics, NTNU. The PAASCS control law is applying

⋆ The authors acknowledge the financial support of Siemens Oil and Gas Solutions Offshore through the Siemens-NTNU research collaboration project.

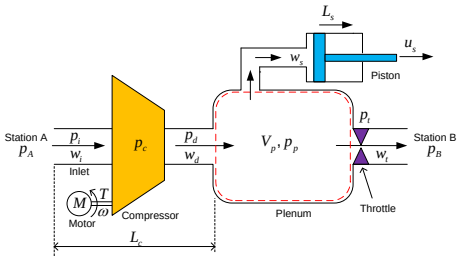

Fig. 1. Piston actuated active surge control system.

the ψ-control. The control gain is determined by using the test setup parameters and a compressor map. The compressor map is obtained through a compressor performance test. The control law algorithm is written in Matlab and Simulink and embedded in a dSpace board to build a hardware in loop simulation. The PAASCS is tested experimentally to see the performance of the system in stabilizing surge. The test is started by running the compressor at a constant speed and reducing the flow by closing an outlet valve (throttle) such that the compressor is entering surge while the PAASCS is inactive. The PAASCS is then activated after the compressor is in surge. The surge is shown by pressures oscillation sensed by pressure sensors at the compressor discharge and in the plenum. This is the first experimental confirmation of actively stabilizing compressor surge by using piston actuation.

2. SYSTEM DYNAMICS AND CONTROL

A model of PAASCS is shown in Figure 1. The PAASCS model is a modification of the Greitzer compressor model (Greitzer, 1976) by adding a piston. The assumptions in the Greitzer model are applied in the PAASCS model. The p_A and p_B are the ambient pressures and assumed to be equal, and fluid pressures in the system are measured relative to the ambient pressure. It is assumed that pressure drop along the ducts in the system are neglected. Therefore, the compressor discharge pressure (p_d) is equal to the compressor pressure rise (p_c), and the compressor discharge mass flow (w_d) is equal to the inlet mass flow (w_i). Dynamic equations of the PAASCS model are given as follows (Uddin and Gravdahl, 2011b):

$$\dot{w}_i = \frac{A_c}{L_c}(p_c - p_p) \tag{1}$$

$$\dot{p}_p = \frac{a_0^2}{V_p}(w_i - w_o - w_s), \tag{2}$$

where A_c is the compressor duct cross-sectional area, L_c is the effective length of the equivalent compressor duct, p_p is the plenum pressure, a_0 is the speed of sound, V_p is the plenum volume, w_o is the outlet mass flow, and w_s is the piston mass flow. The outlet mass flow is the set point of the desired compressor operating mass flow. A compressor operating point is an equilibrium point where $\dot{w}_i = 0$ and $\dot{p}_p = 0$. The piston mass flow is defined by:

$$w_s = \rho A_s \frac{dL_s}{dt}, \tag{3}$$

Table 1. Major components of test setup.

Component	Detail
Compressor	Supercharger Vortech V-1 S-Trim Race M
Pressure sensor	Druck PTX 610
Mass flow sensor	Endress+Hauser t-mass 65F80
Valve	Siemens PN 10
Pipeline	Polypropylene pipe with diameter 75mm
Plenum	Cylindrical vessel
Control board	dSpace DS1103
Piston	See Section 3.3

where ρ is the fluid density, A_s is the piston cross-sectional area, and L_s is the piston position. To simplify the surge control design, we ignore the piston dynamic and assume that the piston will generate a mass flow w_s following a reference signal. Define constants $B_1 = \frac{A_c}{L_c}$ and $B_2 = \frac{a_0^2}{V_p}$, and substitute them into (1) and (2) such that results in:

$$\dot{w}_i = B_1(p_c - p_p) \tag{4}$$

$$\dot{p}_p = B_2(w_i - w_o - w_s). \tag{5}$$

The PAASCS is in the class of downstream energy dissipation ASCS (Uddin and Gravdahl, 2011b) such that the ψ-control introduced in (Uddin and Gravdahl, 2016) is applicable.

Theorem 1. The ψ-control states that an equilibrium point of (4) and (5) is globally asymptotically stable (GAS) if $w_s = w_u$, where $w_u = -k_u(p_c - p_p)$ with $\frac{2B_1}{B_2}k_m < k_u < \frac{2B_1}{B_2}k_n$, $k_m = \left.\frac{\partial p_c}{\partial w_i}\right|_{\max}$ and $k_n = \left.\frac{\partial p_p}{\partial w_o}\right|_{\min}$.

The stability proof can be found in (Uddin and Gravdahl, 2016). The surge control requires w_s to behave as w_u, and it is the task of a piston as the actuator of PAASCS.

3. LABORATORY TEST SETUP

The concept of PAASCS is implemented and tested on a laboratory scale pipeline-compressor system at Compressor Laboratory in Department of Engineering Cybernetics, NTNU. A PAASCS test setup is built as shown in Figure 2. Major components in the setup are listed in Table 1 and most of the components have been used in an experimental work on compressor surge control using torque drive (Bøhagen, 2007). Fluid pressures in the setup are measured relative to the ambient pressure.

3.1 Mass flow measurement

The mass flow sensor used in the setup is Endress+Hauser t-mass 65F80-AE2AG1AAAAAA. It is a high performance mass flow sensor for industrial gases and compressed air. The sensor is configured to measure mass flow at a range of 0 to 0.26 kg/s. The sensor has high accuracy with measurement error 2% of the measured value (Endress+Hauser, 2015). However, the sensor response is quite slow such that it is only applicable for measuring steady flow and not for measuring unsteady flow. Because surge is unsteady flow, we measure mass flow using a pitot tube as an alternative solution. The pitot tube is installed at the compressor inlet duct and equipped with two pressure sensors to measure the total pressure (p_t) and the static pressure (p_s). The mass flow is calculated by following equation:

$$\bar{w} = A_c\sqrt{2\rho(p_t - p_s)}, \tag{6}$$

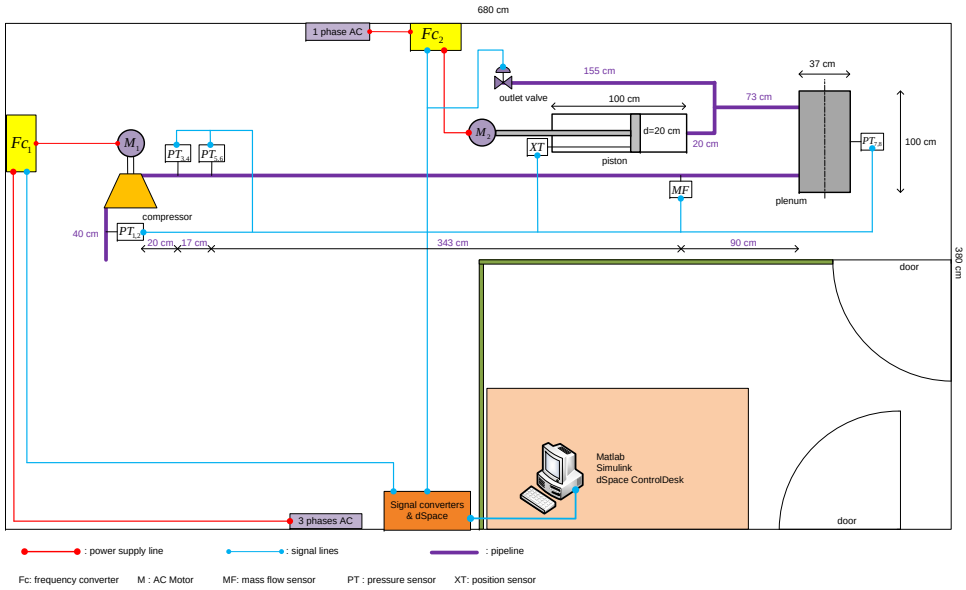

Fig. 2. Compression system with PAASCS test setup at Compressor Laboratory, Dept. of Engineering Cybernetics, NTNU.

where $\bar{w}$ is the calculated mass flow and A_c is the inlet pipe cross-sectional area. The fluid density (ρ) is assumed to be constant and equal to the ambient air density. The calculated mass flow is corrected by calibrating the mass flow measurement using pitot tube with the mass flow measurement using the mass flow sensor. The corrected mass flow is given as follows:

$$w = 0.45\bar{w} - 0.0035, \tag{7}$$

where w is the corrected mass flow. The main reasons for this correction are misalignment of pitot tube and incorrect air density. The pitot tube mass flow measurement provides a much faster response than the mass flow sensor.

3.2 Compressor Performance Test

A compressor map of the test setup is obtained through a compressor performance test. The performance test is done by running the compressor at a constant speed for several operating points and recording data of the compressor mass flow and the compressor discharged pressure for each operating points. The compressor mass flow is measured using the pitot tube and calculated using (7). The operating point is changed by adjusting the throttle opening.

A test was done by running the compressor at 23978 RPM for eight operating points. The initial operating point is at throttle opening 40% and reduced gradually at 5% for the other seven operating points. The operating points are labelled sequentially by alphabet A to H. The test results show that the compressor is operating stable at the operating points A to G (throttle opening 40% to 10%), but not at the operating point H (throttle opening 5%). Figure 3 shows the compressor states for operating points A to G. The compressor entered surge at operating point H as shown in Figure 4. The compressor surge is shown by oscillations of the compressor mass flow, the compressor discharge pressure, and the plenum pressure. The mass flow measurement is not accurate because reversal flows (negative flows) were physically observed during surge in the performance test, but the measurement output is not negative. The surge phenomenon is therefore presented by pressure oscillations in this study. A further study on flow measurement during surge using a pitot tube is suggested.

A compressor map for stable compressor operating points are obtained by approximating the compressor states of the seven operating points (A to G) by a cubic function as shown by "*Approximation 1*" in the Figure 3. The peak point of curve "Approximation 1" is the surge point. The compressor map for unstable compressor operating points are estimated by a cubical function introduced in (Moore and Greitzer, 1986) and given as follows:

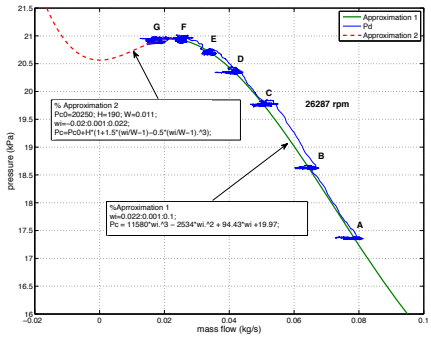

Fig. 3. Compressor map obtained by a performance test.

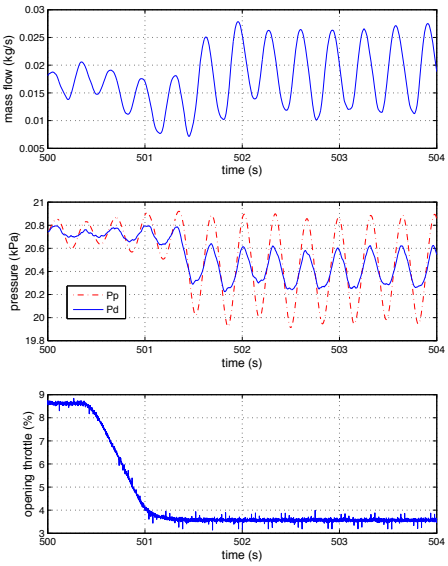

Fig. 4. Compressor is surge at operating point H with throttle setting 5%.

$$p_c(w_i) = p_{c_0} + H\left[1 + \frac{3}{2}\left(\frac{w_i}{W} - 1\right) - \frac{1}{2}\left(\frac{w_i}{W} - 1\right)^3\right] \quad (8)$$

where p_{c_0} is the shut-off value of the axisymmetric characteristic, W is the semi-width of the cubic axisymetric compressor characteristic, and H is the semi-height of the cubic axisymetric compressor characteristic; consult (Moore and Greitzer, 1986) for more detailed definitions. The value of H is approximated by the amplitude of the compressor discharged pressure oscillation during compressor surge as shown in Figure 4. The mass flow of the surge point is equal to $2W$. The value of p_{c_0} is approximated by subtracting $2H$ from the pressure of the surge point. The estimated compressor performance curve at unstable operating area is shown by "Approximation 2" in Figure 3.

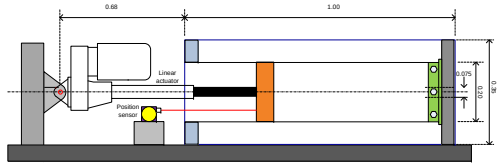

Fig. 5. Piston design.

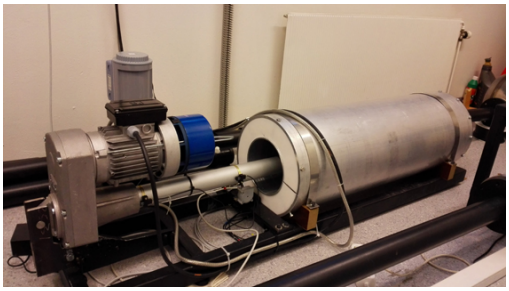

Fig. 6. Piston unit.

3.3 Piston

A piston as the actuator of PAASCS is required to have sufficient power and speed to generate mass flow w_s to stabilize compressor surge. Based on the compressor map, the piston must be able to work at pressure 21 kPa. The piston mass flow is determined by the piston cross-sectional area and the piston speed. To minimize the length of the piston, the piston should have a larger cross-sectional area. By considering further applications of the piston, we decided to have a piston with diameter 0.2 m. The piston was designed as shown in Figure 5. The piston is driven by a linear actuator Servomech UAL4RV2C500 which has maximum speed 0.44 m/s, maximum displacement 0.5 m, and maximum force 1700 N (Servomech, 2015). The piston displacement is sensed by a spring loaded potentiometer Multicomp SP1-50 Transducer. The piston displacement is set up in the range of $\pm$ 0.25 m. The piston was manufactured by the workshop staff at Engineering Cybernetics, NTNU as shown in Figure 6.

The piston dynamics is obtained through a closed loop system identification using the data of the piston displacement and the input signal. Figure 7 shows a block diagram of the closed loop system identification where $L_{s_{ref}}$ is the position input as the reference signal, L_s is the piston displacement, k_{s_1} is a proportional control gain, k_{s_2} is the position sensor gain which is a conversion factor from meter to volt, and G_s is the piston transfer function. An initial test by exciting the piston using a step function reference signal showed that the piston movement is very

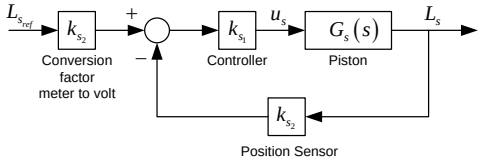

Fig. 7. Block diagram of piston system identification.

slow. Therefore, a proportional controller, $k_{s_1} = 10$, is applied to get a faster response. The value of k_{s_2} is 6.17 volt/m, which was obtained through a calibration of the piston position sensor. Processing the data of the piston input and the piston displacement using Matlab Toolbox for System Identification results in a model with transfer function:

$$G_s(s) = \frac{L_s(s)}{u_s(s)} = \frac{0.251}{s(s + 5.405)} \tag{9}$$

where L_s is the piston displacement in meters and u_s is the piston input voltage in volts.

4. PAASCS IMPLEMENTATION

Figure 8 shows block diagram of PAASCS implementation and the values of parameters in the test setup are given in Table 2. The algorithms in the block diagram are

Table 2. PAASCS Test Setup Parameters

Parameter	Value	Unit	Parameter	Value	Unit
a_0	340	m/s	V_p	0.12	m^3
L_c	0.8	m	A_c	0.0038	m^2
ρ	1.2041	kg/m^3	A_s	0.0314	m^2

implemented in a Simulink model and embedded into a dSpace board DS1103 to build a hardware in the loop (HIL) simulation. The dSpace board has a 20-channels digital to analog converter (DAC) and an 8-channels analog to digital converter (ADC) as the interfaces to connect with actuators and sensors, respectively.

The surge control gain k_u is calculated by using Theorem 1 where $\frac{2B_1}{B_2}k_m < k_u < \frac{2B_1}{B_2}k_n$. By using (8), compressor map in Figure 3, and the test setup parameters, it can be obtained $k_m = \frac{3H}{2W} = 2.5909 \times 10^4$ Pa.s/kg, $k_n = \frac{2p_p}{w_o}\Big|_{\min} = 3.3684 \times 10^5$ Pa.s/kg, $B_1 = 0.0047$, and $B_2 = 963330$. The calculation results in $2.555 \times 10^{-4} < k_u < 3.3 \times 10^{-3}$. We choose $k_u = 4 \times 10^{-4}$ for the experimental test. The output of the surge controller is w_u which is a reference mass flow for the piston. Since we only have a position sensor in the piston, the reference mass flow is converted to velocity with a conversion factor $\frac{1}{\rho A_s}$. The velocity is a reference velocity for the piston. An inner closed loop with a piston controller is required to assure that the piston movement follows the reference velocity. The piston controller is a PID controller with $k_p = 120$, $k_i = 5$, and $k_d = 1$. The Filter 1 is a first-order low-pass Butterworth filter with passband frequency 20π rad/s and the Filter 2 is a first-order low-pass Butterworth filter with passband frequency 60π rad/s.

5. EXPERIMENTAL RESULTS

An experimental test is performed to test the PAASCS performance. The compressor is running at 24335 RPM and the throttle opening is reduced to 5% such that the compressor enters surge as shown by the pressure oscillations since $t = 475$ seconds in Figure 9. The PAASCS controller is then turned on at $t = 482$ seconds and is suppressing the pressure oscillations. It results in stabilizing the compressor surge. The PAASCS controller is then turned off at $t = 513$ seconds and as can be seen the compressor is driven back to surge.

The experimental results in Figure 9 show that the piston velocity is not following the reference signal given by the surge controller. An investigation of the piston using the closed loop system identification data shows that piston bandwidth is about 1.2 Hz. The piston bandwidth is quite low compared to the surge frequency which is 3.5 Hz. This indicates that the piston response is quite slow to follow the reference signal.

The piston was also experience with some drift. Integral control was recommended by (Uddin and Gravdahl, 2011a) to eliminate the piston drift. It has been applied in this experimental test but it does not give to much improvement in this experiment. The slow response of the piston is the main reason of it.

It is expected that a faster linear actuator for the piston would lead to better performance. Nevertheless, surge was stabilized with the current actuator.

6. CONCLUSION AND FURTHER WORKS

An implementation and experimental test of PAASCS were done and the results were presented. The PAASCS is able to stabilize compressor surge and prove the concept of PAASCS. The PAASCS by using ψ-control makes the implementation simple as only requiring feedback from pressure measurements.

Recommendation of further works to improve the PAASSC are given as follows. The performance of PAASCS can be improved by using a better linear actuator with higher bandwidth. The measurement of piston velocity can be improved by using velocity sensor instead of using the time derivative of the position sensor output. The mass flow measurement by using pitot tube can be improved by considering that the air density is varying instead of assuming it as a constant. The air density can be approximated as a function of temperature. Another solution for the mass flow measurement is by using an observer as introduced in (Bøhagen and Gravdahl, 2002).

ACKNOWLEDGEMENTS

The authors would like to thank to Per Inge Snildal and Terje Haugen for constructing the piston, and Rune Mellingseter for the electrical installation.

REFERENCES

Bøhagen, B. (2007). *Active surge control of centrifugal compression systems: Theoretical and experimental results of drive actuation.* Ph.D. thesis, Norwegian University of Science and Technology.

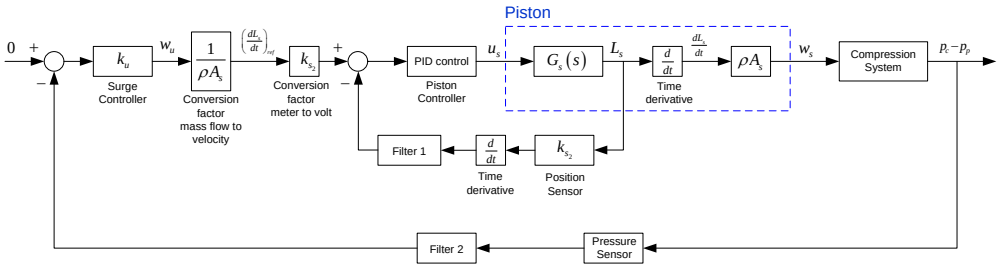

Fig. 8. PAASCS block diagram.

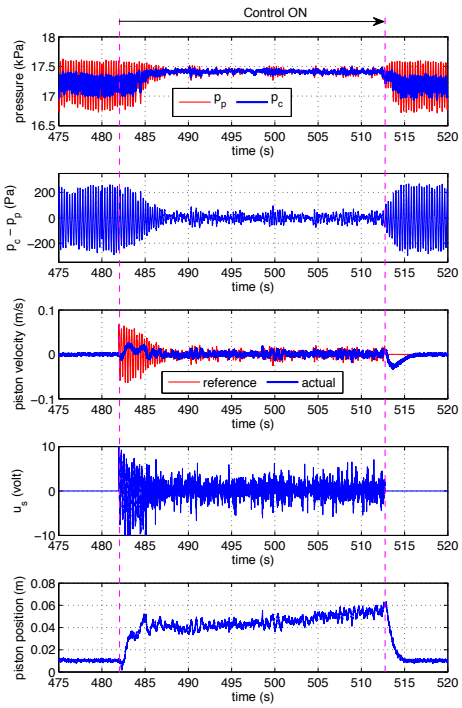

Fig. 9. Experimental result of PAASCS.

Bøhagen, B. and Gravdahl, J.T. (2002). On active surge control of compressors using a mass flow observer. In *Proceedings of the 41st IEEE Conference on Decision and Control*, volume 4, 3684–3689. IEEE.

Endress+Hauser (2015). Technical information proline t-mass 65f, 65i thermal mass flowmeter. URL `https://portal.endress.com/wa001/dla/5000009/2467/000/03/TI00069DEN_1314.pdf`. [Online; accessed 20-October-2015].

Epstein, A.H., Williams, J.E.F., and Greitzer, E.M. (1986). Active suppression of compressor instabilities. In *Proc. of AIAA 10th Aeroacoustic Conference*, 86-1994. Seattle.

Gravdahl, J.T. and Egeland, O. (1999). *Compressor surge and rotating stall: Model and control*. Springer Verlag, London.

Greitzer, E.M. (1976). Surge and rotating stall in axial flow compressor, part I: Theoritical compression system model. *J. Engineering for Power*, 98, 190–198.

Moore, F.K. and Greitzer, E.M. (1986). A theory of post stall transients in an axial compressors system: Part I-Development of equation. *J. Engineering for Gas Turbine and Power*, 108, 68–76.

Servomech (2015). Mechanical linear actuators catalogue. URL `http://www.servomech.com`. [Online; accessed 20-October-2015].

Uddin, N. and Gravdahl, J.T. (2011a). Piston-actuated active surge control of centrifugal compressor including integral action. In *Proc. of the 11th International Conference on Control Automation and System*. Gyeonggi-do, South Korea.

Uddin, N. and Gravdahl, J.T. (2012a). A compressor surge control system: Combination active surge control and surge avoidance. In *Proc. of the 13th International Symposium on Unsteady Aerodynamics, Aeroacoustics, and Aeroelasticity of Turbomachinery (ISUAAAT)*. Tokyo, Japan.

Uddin, N. and Gravdahl, J.T. (2012b). Introducing back-up to active compressor surge control system. In *Proc. of the 2012 IFAC Workshop on Automatic Control in Offshore Oil and Gas Production*, 263–268. Trondheim, Norway.

Uddin, N. and Gravdahl, J.T. (2011b). Active compressor surge control using piston actuation. In *ASME 2011 Dynamic Systems and Control Conference and Bath/ASME Symposium on Fluid Power and Motion Control*, 69–76. Virginia, US.

Uddin, N. and Gravdahl, J.T. (2015). Bond graph modeling of centrifugal compression systems. *SIMULATION*, 91(11), 998–1013.

Uddin, N. and Gravdahl, J.T. (2016). Two general state feedback control laws for compressor surge stabilization. *submitted to The 24th Mediterranean Conference on Control and Automation*.

Willems, F. and de Jager, B. (1999). Modeling and control of compressor flow instabilities. *Control Systems, IEEE*, 19(5), 8 –18.

References

G. L. Arnulfi, P. Giannattasio, D. Micheli, and P. Pinamonti. An innovative device for passive control of surge in industrial compression system. *Journal of Turbomachinery*, 123:473–782, 2001.

C. Backi, J. Gravdahl, and E. Grotli. Nonlinear observer design for a greitzer compressor model. In *2013 21st Mediterranean Conference on Control Automation (MED)*, pages 1457–1463. IEEE, Jun. 2013. doi: 10.1109/MED.2013.6608913.

H. P. Bloch. *A Practical Guide to Compressor Technology*. Wiley-Interscience, New York, 2006.

B. Bøhagen. *Active surge control of centrifugal compression systems: Theoretical and experimental results of drive actuation*. PhD thesis, Norwegian University of Science and Technology, 2007.

B. Bøhagen and J. T. Gravdahl. On active surge control of compressors using a mass flow observer. In *Proceedings of the 41st IEEE Conference on Decision and Control*, volume 4, pages 3684–3689. IEEE, 2002.

M. P. Boyce. *Centrifugal Compressors: A Basic Guide*. PennWell Books, Tulsa, OK, 2003.

R. N. Brown. *Compressors Selection and Sizing (3rd Edition)*. Gulf Professional Publishing, Burlington, MA, 2005.

O. Egeland and J. T. Gravdahl. *Modeling and Simulation for Automatic Control*. Marine Cybernetics, Trondheim, Norway, 2002.

A. H. Epstein, J. E. F. Williams, and E. M. Greitzer. Active suppression of compressor instabilities. In *Proceedings of the AIAA 10th Aeroacoustic Conference*, number 86-1994, Seattle, 1986.

A. H. Epstein, J. E. F. Williams, and E. M. Greitzer. Active suppression of aerodynamics instability in turbo machines. *Journal of Propulsion and Power*, 5:204–211, 1989.

W. E. B. Forsthoffer. *Forsthoffer's Rotating Equipment Handbooks Vol. 3: Compressors*. Elsevier, Oxford, UK, 2005.

J. Gravdahl and N. Uddin. Industrial compressor system, Feb. 29 2012. URL https://www.google.com/patents/EP2423515A1?cl=un. EP Patent App. EP20,100,173,999.

J. T. Gravdahl and O. Egeland. *Compressor Surge and Rotating Stall: Modeling and Control*. Springer Verlag, London, 1999.

J. T. Gravdahl, O. Egeland, and S. O. Vatland. Drive torque actuation in active surge control of centrifugal compressors. *Automatica*, 38:1881–1893, 2002.

E. M. Greitzer. Surge and rotating stall in axial flow compressor, part I: Theoretical compression system model. *Journal of Engineering for Gas Turbines and Power*, 98:190–198, 1976.

D. Gysling, D. Dugundji, E. M. Greitzer, and A. H. Epstein. Dynamic control of centrifugal compressor surge using tailored structures. *ASME Journal of Turbomachinery*, 113:710–722, 1991.

F. K. Moore and E. M. Greitzer. A theory of post stall transients in an axial compressors system: Part I-Development of equation. *Journal of Engineering for Gas Turbine and Power*, 108:68–76, 1986.

A. Nisenfeld. *Centrifugal Compressors: Principles of Operation and Control*. Monograph series. Instrument Society of America, 1982. ISBN 9780876645642.

J. Pinsley, G. Guenette, A. H. Epstein, and E. M. Greitzer. Active stabilization of centrifugal compressor surge. *ASME Journal of Turbomachinery*, 113:723–732, 1991.

J. S. Simon and L. Valavani. A lyapunov based nonlinear control scheme for stabilizing a basic compression system using a close-coupled control valve. In *Proceedings of the American Control Conference*, pages 2398–2406, 1991.

N. Uddin. Stochastic optimal preview control for active suspension system of a full tracked vehicle model. Master's thesis, Gyeongsang National University, South Korea, 2009.

N. Uddin and J. T. Gravdahl. Active compressor surge control using piston actuation. In *ASME 2011 Dynamic Systems and Control Conference and BATH/ASME Symposium on Fluid Power and Motion Control*, pages 69–76, Virginia, USA, 2011a.

N. Uddin and J. T. Gravdahl. Piston-actuated active surge control of centrifugal compressor including integral action. In *Proceedings of the 11th International Conference on Control Automation and System*, pages 991–996, 2011b.

N. Uddin and J. T. Gravdahl. Introducing back-up to active compressor surge control system. In *Proceedings of the 2012 IFAC Workshop on Automatic Control in Offshore Oil and Gas Production*, pages 263–268, Trondheim, Norway, 2012a.

N. Uddin and J. T. Gravdahl. Bond graph modeling of centrifugal compressor system. In *Proceedings of the International Conference on Bond Graph Modeling*, Genoa, Italy, 2012b.

N. Uddin and J. T. Gravdahl. A compressor surge control system: Combination active surge control and surge avoidance. In *Proceedings of the 13th International Symposium on Unsteady Aerodynamics, Aeroacoustics and Aeroelasticity of Turbomachines (ISUAAAT 13)*, pages 263–268, Tokyo, Japan, Sep. 11-14 2012c.

N. Uddin and J. T. Gravdahl. Bond graph modeling of centrifugal compression system. *SIMULATION*, 91(11):998–1013, 2015.

N. Uddin and J. T. Gravdahl. Two general state feedback control laws for compressor surge stabilization. *submitted to The 24th Mediterranean Conference on Control and Automation*, 2016a.

N. Uddin and J. T. Gravdahl. Active compressor surge control system by using piston actuation: Implementation and experimental results. *Accepted in the 11th IFAC Symposium on Dynamics and Control of Process Systems, including Biosystems (DYCOPS-CAB 2016), to be held in Trondheim, Norway, June 6-8, 2016*, 2016b.

Vortech. Vortech v s-trim compressor map, 2015. URL http://www.vortechsuperchargers.com/maps/s-trim_map.gif. Accessed Nov. 28 2015.

F. Willems and B. de Jager. Modeling and control of compressor flow instabilities. *IEEE Control Systems*, 19(5):8–18, Oct 1999.

J. E. F. Williams and X. Y. Huang. Active stabilization for compressor surge. *Journal of Fluid Mechanics*, 204:245–262, 1989.

S. Y. Yoon, Z. Lin, and P. E. Allaire. *Control of Surge in Centrifugal Compressors by Active Magnetic Bearings: Theory and Implementation*. Springer Science & Business Media, London, 2012.

I. Youn, R. Tchamna, S. Lee, N. Uddin, S. Lyu, and M. Tomizuka. Preview suspension control for a full tracked vehicle. *International Journal of Automotive Technology*, 15(3):399–410, 2014.